2011

Hurricane Induced Land and Vegetation Changes in the Breton Sound Estuary and Chandeleur Islands Using Landsat 5 TM

Vandana Varshini Raghunathan
Louisiana State University and Agricultural and Mechanical College

HURRICANE INDUCED LAND AND VEGETATION CHANGES IN THE BRETON SOUND ESTUARY AND CHANDELEUR ISLANDS USING LANDSAT 5 TM

A Thesis

Submitted to the Graduate Faculty of the
Louisiana State University and
Agricultural and Mechanical College
in partial fulfillment of the
requirements for the degree of
Master of Science
in

The Department of Oceanography and Coastal Science

by
Vandana Varshini Raghunathan
B.E., College of Engineering, Anna University, India, June 2008
December 2011

Dedicated to my loving mother

Valarmathi Raghunathan

ACKNOWLEGEMENTS

I am very grateful to my major professor / advisor Dr. Nan Walker, for her support, guidance, patience and encouragement throughout my graduate career. I would like to thank my committee members Mr. DeWitt Braud and Dr. John White for their time and support.

My sincere thanks to:

Dr. Lowell Urbatsch, Professor at LSU Biological Sciences for help with identifying plant species in our field trip.

Mr. DeWitt Braud for help with classification procedure, generating models, analyzing results and always being there whenever I had a question.

Mr. David Walters for help with acquiring water level data.

Mr. Eddie Weeks from WAVCIS laboratory for help with the field trip and aerial photographs of the study area using plane camera and Mr. Floyd from the field support group for help with the field trip. Dr. Baozhu Liu from WAVCIS laboratory, for accompanying us to the Chandeleur Islands, help with collecting samples and running the grain size analysis procedure.

Mr. Jack Bohannan from U.S. Wildlife and Fisheries for showing us around the Chandeleur Islands.

Ms. Mary Lee Eggart, Cartographer from Department of Geography and Anthropology for help with converting images to pretty pictures.

Mr. Chet Pilley, Mr. Alaric Haag and all my lab mates at Earth Scan Laboratory, for always being there for me when I needed help with anything and being awesome all the time. Hari Sundararajan for his help and support.

And finally, to my parents Drs. Raghunathan and Valarmathi Raghunathan and my grandparents Mr. Balakrishnan and Mrs. Kasturi Balan for loving, motivating, encouraging and believing in me. My sister, Janani Sowprnika for her support. Sanjith Venkateswaran, for sticking by my side the whole time loving and encouraging me. This research was funded by a grant from the Shell Oil Company.

TABLE OF CONTENTS

LIST OF TABLES

LIST OF FIGURES

ABSTRACT

This study focuses on hurricane-induced changes in land and vegetation primarily in two study areas, the Breton Sound Estuary and the Chandeleur Islands, southeast of New Orleans, Louisiana. Breton Sound Estuary consists of the Caernarvon Diversion, a fresh water diversion of the Mississippi River that supplies this region with managed pulses of fresh water and sediments. The Chandeleur Islands are a chain of barrier islands that are uninhabited and transgressive in nature. A sequence of hurricanes in the past two decades has greatly altered both areas significantly. Satellite data were analyzed for a period of 24 years (1987-2011) of Breton Sound Estuary region and for 14 years (1997-2010) of the Chandeleur Islands. Landsat 5 Thematic Mapper data were used to classify and analyze changes using ERDAS IMAGINE 9.3 software. Images were classified into land and water classes using a hybrid classification technique that is unlike the techniques used in the past. Quantitative spatial analyses of the extent of land loss, vegetation changes and beach loss/gain over time were performed. Three change detection techniques were used in this research, which include post-classification spatial intersection, Change Vector Analysis (CVA) and image differencing. Maximum land loss in the Breton Sound Estuary region was due to Hurricane Katrina in 2005 when 196 km^2 of land was converted to water from November 2004 to October 2005. Marsh area loss in the 24-year time series coincided with the overall land area loss. An increase in marsh area was detected in three segments of the time series i.e. 1987 to 1991, 1992 (after Hurricane Andrew) to 2003 (before Hurricane Ivan) and 2006 (after Hurricane Katrina) to 2010 indicating some recovery between hurricane years. At the Chandeleur Islands, most of the land loss over the past decade was due to four major hurricanes since 1997; Hurricane Georges in 1998, Hurricane Ivan in 2004, Hurricane Katrina in 2005 and Hurricane Gustav in 2008. The most significant hurricane that impacted

these islands was Hurricane Georges in 1998 that resulted in a land loss of 76.5% measured from 1997. The land area increase after the impact of Hurricane Gustav in 2008 to 2011 was very low ranging from 0 km^2 to 2 km^2. Shoreline change detection results indicated that the barrier islands moved westward (landward), a maximum of 1.7 km in the southern section. Seven kilometres of the linear coastline was lost in the northern tip and 15 km in the southern tip. The change detection analysis and the shoreline change analysis indicated that the southern section of these islands has undergone greater damage due to erosion than the northern section.

CHAPTER 1
INTRODUCTION

1.1. Background

Two study areas were targeted for this research project. The first was the Breton Sound Estuary, which includes the Caernarvon Diversion of the Mississippi River operated since 1991. The second was the Chandeleur Island chain, approximately 63 km to the east of the Breton Sound Estuary. The study area of Breton Sound Estuary region encompassed 2020 km^2 and the Chandeleur Islands encompassed 1286 km^2 (Figure 1.1). These regions were formed from the St. Bernard Delta lobe of the Mississippi River delta complex one thousand years ago (Penland et al, 1988; Roberts, 1997). Several processes that constitute the delta cycle resulted in the formation of this delta.

According to Roberts (1997), the main stages in delta development include "(1) Delta initiation and rapid growth which is the fluvially dominated regressive phase (2) Stream capture and Lacustrine delta development (3) Bayhead delta stage (4) Shelf-stage delta building and the (5) Delta abandonment and deterioration: Marine-dominated transgressive phase".

Penland et al (1988), describe the formation of the barrier islands from a delta in three stages called "the three stage evolutionary model". The first stage is called the "erosional headlands with flanking barriers" during which the barrier progrades seaward. The second stage is the formation of the "transgressive barrier island arc" when the islands detach themselves from the delta due to abandonment followed by submergence resulting in the formation of "inner shelf shoals". Penland et al (1988) and Koch and Penland (2001) indicate that the Chandeleur Islands are still in the second stage of the barrier islands model i.e. "transgressive barrier island arc".

1.1.1. Breton Sound Estuary

Lane et al, (1999) described Breton Sound Estuary as marsh area that consists of freshwater, brackish and saltwater marsh species extending over 1100 km^2 (Figure 1.2). This first diversion of the Mississippi River was created unintentionally during the great flood of 1927. There were intermittent pulses of fresh water from the Mississippi River to the Breton Sound naturally in the last century. After construction of the man-made levees on the Mississippi River banks, the natural sediment and freshwater supply was cut off. In order to supplement this natural process, the Caernarvon Diversion was built in 1991. It was also built with the intention of protecting the fisheries industry and increasing the wetlands of coastal Louisiana (Lane et al, 1999; Stokstad, 2005; Day et al, 2007; Howes et al, 2010).

The Caernarvon River diversion is now essential to sustain the freshwater ecosystem of the habitat in this region (Day et al, 2009). Water inflow in this region is greatly influenced by the tides, winds, sea level, rise/fall of the river stage (when the diversion is open) and several other climatic factors (Day et al, 2009). These factors also control the sediment circulation in the marshes. The opening and closing of the river diversion is operated such that it is in sync with the natural high and low stages of the Mississippi river which regulates the salinity variations across the diversion region (Day et al, 2009).

1.1.2. Chandeleur Islands

The Chandeleur Islands are a group of islands that form the eastern most point of Louisiana (Figure 1.3). They extend about 80 km in length. The importance of these barrier islands is that they form a protective barrier between the coast and the Gulf of Mexico, protecting the mainland from the impact of waves and storm surges (Stone et al, 2005). They are also known for their natural habitat, which provides home for many different species of animals and birds. Some of

the well-known species include nesting sea turtles, brown pelicans, piping plovers and least terns (Fearnley et al, 2009). These islands act as a wildlife and forest preserve.

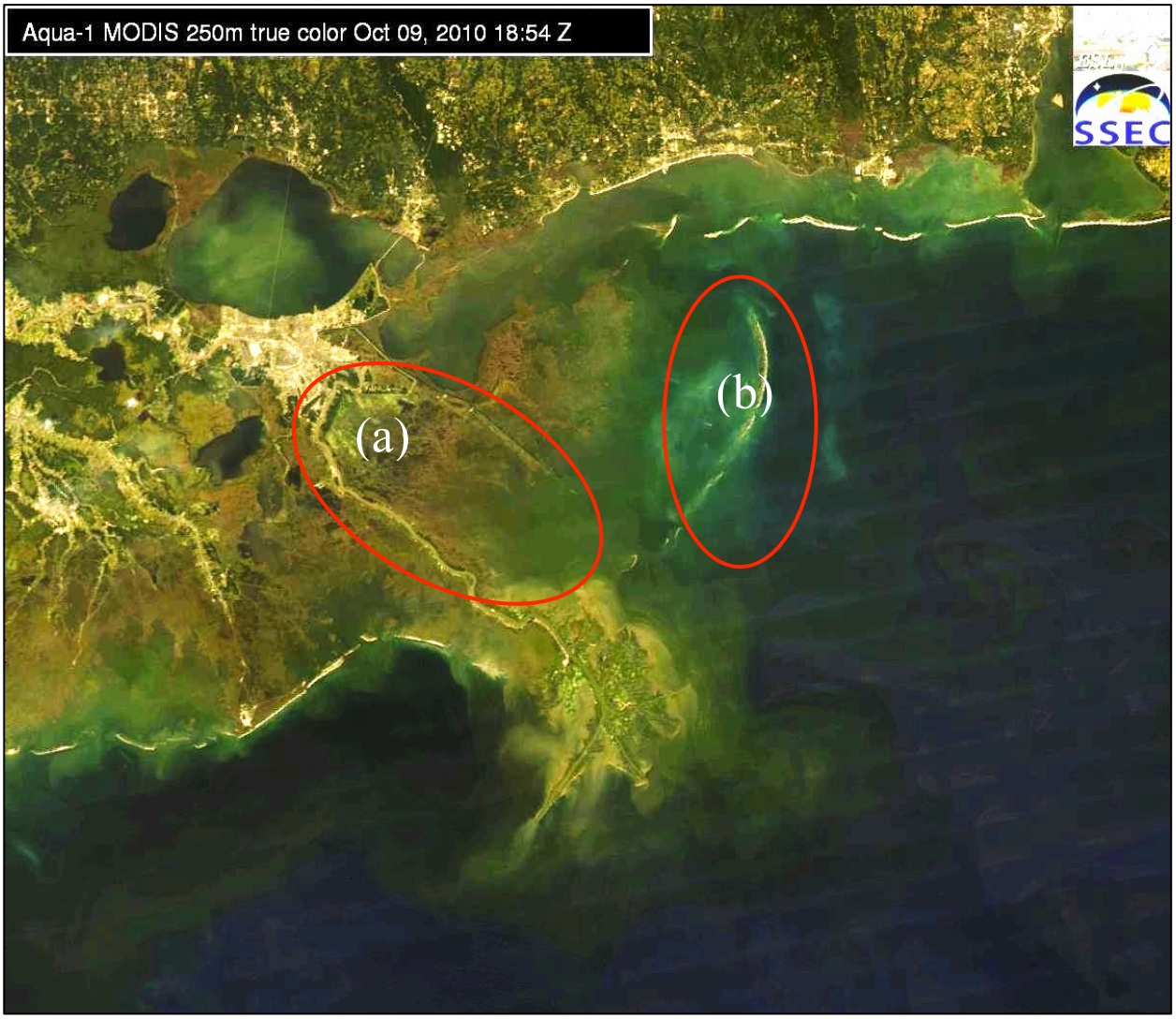

Figure 1.1 Aqua MODIS true color imagery of Mississippi River delta on 10/09/2010 showing location of the study areas (a) Breton Sound Estuary (b) Chandeleur Islands

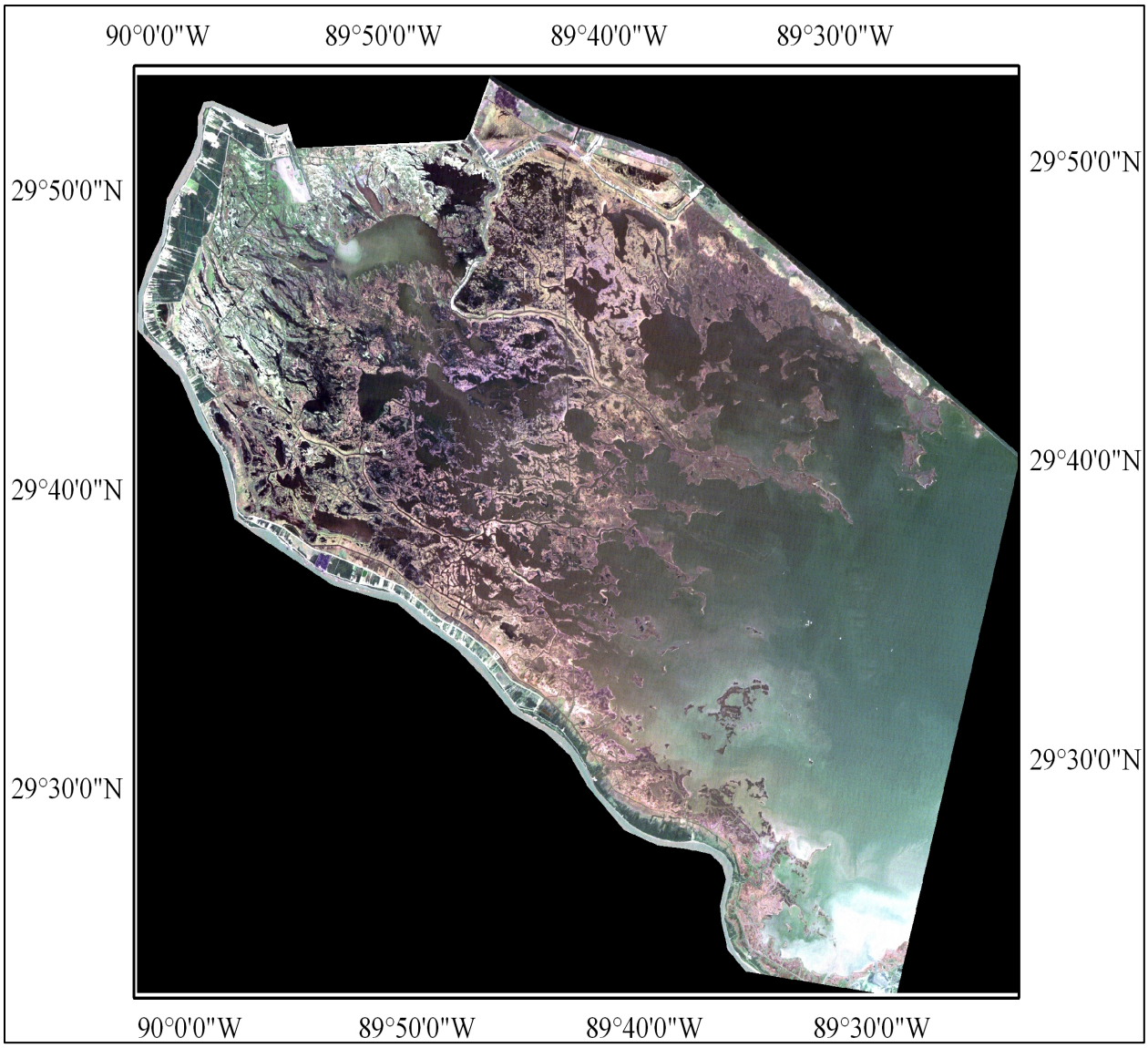

Figure 1.2 Breton Sound Estuary region study area, Landsat 5 TM image of 10/07/2010 with true color composite comprised of bands 1, 2 and 3 as 321 RGB

Hurricane and tropical storm damage has greatly affected the Chandeleur Islands causing much land loss. It is therefore essential to quantify the land losses and gains that have occurred to these islands as it may directly affect the erosion along the marshes of Breton Sound Estuary. Many modeling studies in the past have been carried out to determine the effects of these barrier islands on the mainland along with their migration towards the coast (Stone et al, 2005). Due to the low-lying nature of these islands they are likely to be greatly impacted by the global climate changes especially sea level rise (Williams, 2009).

The coastal subsidence resulting in relative sea level rise has also led to erosion of this chain of islands (Lavoie, 2009). The fact that this is a "sediment-starved environment" does not help with the rebuilding (Sallenger et al, 2009). It has been found that the sediment source for these islands in the earlier times during its evolution was mainly from the Mississippi River (Sallenger et al, 2009). The morphology of these islands is controlled by the impact and frequency of the hurricanes (Fearnley et al, 2009). The islands have evolved over time and undergone a lot of changes due to hurricane impacts along with other factors such as transgressive submergence (Kahn and Roberts, 1982). Hurricane Frederic (1979) and Hurricane Camille (1969) were considered the most devastating hurricanes before the past decade (Kahn and Roberts, 1982). These islands were affected by about 40 hurricanes in the entire century (Fearnley et al, 2009).

Four major hurricane events are considered in this research. Hurricane Georges in September 1998 was a category 4 hurricane that made landfall near Biloxi, MS (National Hurricane Center Report, 1999). Hurricane Ivan in September 2004 was a category 5 hurricane that made landfall west of Gulf Shores, AL (National Hurricane Center Report, 2005). Hurricane Katrina in August 2005 was a category 5 hurricane that made landfall in the southern

Plaquemines parish, LA (National Hurricane Center Report, 2006). Hurricane Gustav in August 2008 was a category 4 hurricane that made landfall in Cocodrie, LA (National Hurricane Center Report, 2009). The satellite images were obtained for each of these hurricanes before and after the event. The categories listed above are the maximum experienced in the Gulf of Mexico, not categories at landfall.

1.2. Land Change Analysis for Coastal Louisiana

Barras (2007) in his report on the response of the Louisiana coast to Hurricanes Katrina and Rita in 2005 measured the land loss over the entire coast of Louisiana using Landsat 5 TM data mosaics of 2004 and 2005 to generate classified images using a density-slicing technique. Classified images were then used to generate the changes in area before and after the impact of the 2005 hurricanes.

Barras et al, (2008) studied the spatial changes in coastal Louisiana from 1956 to 2006 using Landsat TM imagery. After classifying the land and water areas, they performed a regression analysis between different years to analyze their land area relationship. They found that the Breton Sound Estuary region had undergone maximum change and land loss compared to the other parts of coastal Louisiana. They also indicated that new water areas in Breton Sound Estuary region and at the Chandeleur Islands were permanent whereas it was not the case in other regions.

Barras (2009) also discussed the impacts of Hurricanes Gustav, Ike, Katrina and Rita in coastal Louisiana and observed that the land area after the impact of Hurricanes Katrina and Rita in 2005 exhibited some recovery in 2006 and 2007.

Figure 1.3 Chandeleur Island arc study area Landsat 5 TM data from 12/19/1997 with a true color composite comprised of bands 1, 2 and 3 as 321 RGB

Hurricanes Gustav and Ike in 2008 affected the western portions of coastal Louisiana much more than the eastern parts consisting of Breton Sound Estuary and Chandeleur Islands. After the passage of these hurricanes in 2008, land loss at the Chandeleur Islands was found to be 1.02 km^2 (Barras, 2009).

Barras (2009) also indicated that the land area change after Hurricane events may not be permanent for long-term analysis but could greatly affect the cumulative land loss over a period of time. Marsh area, found in the northwestern portion of the Breton Sound Estuary, was greatly affected and altered due to Hurricanes Katrina, Rita and Gustav (Barras, 2006; Barras, 2007; Barras et al, 2008; Barras, 2009)

Couvillion et al, (2011) studied the changes in coastal Louisiana from 1932 to 2010. They utilized Landsat MSS and TM data to analyze the land area changes from 1970 to 2010 and surveyed toposheets for 1932 and aerial photographs for 1956. They used density slicing primarily to classify areas using the near-infrared band and supplemented the unclassified areas with supervised and unsupervised classification. They found that the land area changes began after 1970 and the region most affected by Hurricanes Katrina and Rita was Breton Sound Estuary. They have found most of the changes to be persistent. Linear regression was used, similar to that of Barras et al, (2008), to identify the relationships between land losses from different times.

Kearney et al, (2011) analyzed the effects of the three river diversions in coastal Louisiana over a period of 19 years. They used Landsat TM data along with aerial photography to quantify marsh area with the incorporation of these data into a "spectral mixture model" that involved developing indices based on near-infrared and red bands of Landsat data. They found that maximum damage to marsh area in Breton Sound Estuary region was caused from

Hurricanes Katrina and Rita in 2005. They concluded that the diversions in coastal Louisiana did not fulfill their purpose of increasing marsh/vegetation area due to excessive nutrient load from the Mississippi River that had led to the roots being weak and susceptible to uprooting by storm events. They also attributed the Caernarvon river diversion as a cause for the increase in the "dead zone" in Gulf of Mexico.

1.3. Classification Procedure

Lillisand and Kiefer (1997), indicate classification as the process of grouping pixels of similar spectral signatures into classes. These classes could be automatically generated using unsupervised classification or could be user-defined classes known as supervised classification. The classification procedure involves creating a training signature set which consists of the classes either automatically generated by the software or user defined. Pixels that cannot be classified in any of the classes are categorized as unclassified pixels. Output from the classification is a thematic map layer with all the pixels in the image being classified into different classes. Supervised classification can be performed using one of the three classifiers such as "Minimum-Distance-to-Mean", "Gaussian-Maximum-likelihood" and "Parrellpiped".

The "Gaussian-Maximum-likelihood" classifier was used in this study to perform supervised classification. This classifier algorithm essentially assumes that the pixels in the training classes are normally distributed. Unclassified pixels are classified based on the "probability density function" i.e. the probability of the particular pixel occurring in a class. Unsupervised classification is performed using the ISODATA algorithm, which involves clustering of the pixels into classes (Lillisand and Kiefer, 1997).

Lillisand and Kiefer, (1997) used both techniques in the form of hybrid classification, which is the classification procedure used in this research. Munyati, (2000) used this hybrid

technique to classify the wetlands in Zambia. Frazier and Page (2000) utilized maximum likelihood classification to categorize water bodies using Landsat imagery. They found that it was far more accurate to utilize the three infrared bands instead of the visible bands. They also concluded that the supervised classification procedure is more accurate than density slicing technique.

1.4. Atmospheric Correction for Landsat 5 TM Imagery

Kawata et al, (1990) found that applying maximum likelihood classification techniques for image classification on both atmospherically corrected image and uncorrected images yielded the same classification accuracy. They analysed the Kanazawa area of Japan which is a mixed landuse consisting of urban areas, water, vegetation and regions of higher elevation. They concluded that atmospheric correction had little effect on results of the classification procedures. However, they found that the atmospheric correction improved the classification accuracy for water bodies such as rivers.

Fraser et al, (1997) studied the effects of atmospheric correction on image classification techniques based on a study conducted over the Atlantic Ocean on the western coast of Africa. They used the hybrid classification technique i.e. the image was first classified using "clustering" which is an unsupervised classification algorithm and the training sites obtained from this were then used to classify the image using maximum likelihood classifier. They found by comparing atmospherically corrected and uncorrected images that the effect of atmospheric correction on the classification procedure was very insignificant. Porter (1974) achieved similar results when comparing atmospherically corrected and uncorrected imagery.

Song et al, (2000) determined that the atmospheric correction procedure is not necessary for Landsat imagery when used in classification and change detection techniques. They analyzed

several atmospheric correction techniques for five different sample images for the Pearl River Delta of China. Based on their results, they concluded that atmospheric correction techniques are required when the spectral information is used. In case of classification and change detection, the spectral data is not used. It is entirely spatial. In this case, they found that the accuracy of the classification was not affected by the atmospheric correction technique. However, they suggest that consistency in the type of image used is important i.e. reflectance or radiance. Atmospheric correction played a major role when the training sites from an image of a particular time were used for another image of the same area but from a different time. In this case, the images need to be corrected for atmospheric effects. Atmospheric correction is especially essential for water environments, quantifying suspended sediments and chlorophyll a (Walker and Hammack, (2000); Walker and Rabalais, 2006)

1.5. Change Detection

Three change detection procedures were used in this research, including the post classification matrix change detection technique, principal component change analysis and image differencing. Macleod and Copgalton, (1998) analyzed these three change detection procedures on Landsat TM data. They found that the image differencing technique to be most accurate in change detection and that the post classification change detection was the next best. Post classification change detection had lesser accuracy when compared to image differencing due to the fact that the errors in post classification technique are cumulative. On the contrary, Mas, (1999) found (based on study conducted in the Terminos lagoon region of Mexico) that the post classification change detection technique had the maximum accuracy when compared to image differencing technique.

Lu et al, (2003) analyzed 31 change detection techniques for satellite imagery and discussed the pros and cons of each technique. In relation to our study, the three change detection techniques including the post classification, TCAP image differencing and Change Vector Analysis are of interest. In their discussion about the post classification, they indicate that it does not require atmospheric correction techniques and generates a change matrix, which indicates the direction of change. However, the disadvantage of this technique is that it is very time consuming and the accuracy depends on the accuracy of the classification imagery. In case of image differencing using TCAP data, it provides basic change imagery but does not contain a change matrix. Change Vector Analysis technique provides the change magnitude per pixel but the direction of change cannot be identified.

Coppin et al, (2004) discussed the use of various digital change detection technique available along with their results. They indicated that it was necessary to use more than one change detection technique simultaneously to achieve best results. Collins and Woodcock (1996) analyzed several linear change detection techniques such as "Multitemporal Kauth-Thomas Transformation", "Gramm-Schmidt Orthogonalization" and "Principal Component Analysis". They found that the Principal Component Analysis was the most accurate of the three.

1.6. Tasseled Cap Analysis

Vorovencii (2007) studied the implementation of Tasseled cap analysis on satellite data, which is a type of principal component analysis. It accumulates the information from six Landsat bands into three new bands, brightness, greenness, and wetness bands. The brightness band signifies the presence or absence of vegetation in an area. The greenness band also indicates the vegetation and their health. The wetness band is an indication of soil characteristics. Two types of TCAP transformations were developed based on the digital number (DN) and reflectance

factor. The TCAP transformation based on reflectance factor is used for atmospherically corrected images.

Crist et al (1986) defined tasseled cap transformation as “adjustment of viewing perspective”. They indicate that the TCAP transformation essentially translates the data from the six Landsat bands to the three TCAP bands based on maximum variability in information thereby effectively incorporating over 95% of the data in those three bands. The near-infrared and visible reflectance is used for generating the greenness band, which indicates the presence or absence of vegetation along with their density. The wetness band is primarily generated based on the short wave infrared band and the visible/near-infrared band.

Allen et al (2008) utilized tasseled cap transformations to classify the Atchafalaya Basin into land and water classes. They primarily utilized the wetness band to arrive at threshold values used for the classification procedure. Millward et al (2006), applied tasseled cap transformation on Landsat and Spot images for the Sanya region in China and found that the near-infrared band was ideal for discriminating vegetation.

1.7. Motivation

Bourne (2000) estimated that every 50 years Louisiana loses coastal wetlands the size of Rhode Island. This research focuses on monitoring the coastal wetlands and analyzing the pattern of land loss in the past using time series. The coastal wetlands play a major role in protecting the mainland from storm events in several ways. The wetlands brace the mainland against the impacts of waves thereby greatly reducing the storm surge (Howes et al 2010). Freshwater diversions protect from wetland loss in several ways. River water provides freshwater, nutrients and sediments. The freshwater prevents saltwater intrusion into the marshes, which would destroy the environment. The nutrients ensure healthy marsh growth and the sediment deposits

help increase the wetland areal extent. They also promote the fisheries and oyster industries (Sable and Villarrubia, 2011).

This research is a comprehensive study of two areas over time. Land classification procedures used in this research focus on the use of a hybrid technique, which greatly improves the accuracy of the classification procedure. Integration of various change detection techniques revealed the effect of tropical storm and hurricane passage on the study areas. Analyses of water levels and significant wave heights were needed to assess potential impacts on land area changes. Field trips to the study areas helped better understand the environments under study and the challenges facing remote sensing studies such as this.

1.8. Objectives

The goals of this study were to:

1) Perform a time series analysis to quantify changes of the Breton Sound Estuary and of the Chandeleur Islands using Landsat 5 Thematic Mapper satellite data using a more accurate technique than those has been used previously.
2) Assess the roles of hurricane and tropical storms to the measured changes
3) Perform shoreline change detection for the Chandeleur Islands over 14 years
4) Collect "ground truth" measurements to better understand the environment changes
5) Assess the advantages and disadvantages of the new image processing technique

Although previous studies have documented environmental changes in these areas, this research is unique because, this study is the first systematic integration of quantitative changes in both the Breton Sound Estuary and Chandeleur Islands using the same image processing technique. In addition, no other study has documented the details associated with hurricanes in the last two

decades. This study is unique due to the hybrid classification technique formulated for the image processing procedure.

1.9. Organization of Thesis

Chapter 1 of this thesis describes the previous research carried out in the Breton Sound Estuary and Chandeleur Islands regions. The need for atmospheric correction in Landsat 5 TM imagery, classification and change detection techniques in addition to various spectral analysis methods such as the tasseled cap analysis described in the past literature were further discussed. This chapter also includes the motivation and primary objectives of this research.

Chapter 2 discusses the different types of data and methodology utilized in this study. Chapter 3 focuses on the results obtained in this study. The results are categorized based on study area.

Chapter 4 is the discussion on the results obtained for the two study areas. Storm surges and water level data were compared to the results from land classification. Implications of the results were analyzed in this section. Chapter 5 is the summary and conclusion for all the findings in this research.

Appendix I illustrate the ERDAS models used for the calculation of reflectance image and eccentricity of the image. Appendix II is the model used for Tasseled cap analysis. Appendix III comprises of select satellite images used for this analysis. Appendix IV shows the grain size analysis procedure and results. Appendix V is the MATLAB code used for analyzing water levels and significant wave height data.

CHAPTER 2
DATA AND METHODOLOGY

2.1. Satellite Data

Landsat 5 Thematic Mapper (TM) data was used in this research. It was downloaded from United States Geological Survey (USGS) GLOVIS website. The TM data has seven bands that include three visible, three infrared and a thermal band.

Table 2.1 Landsat 5 Thematic Mapper bands with their wavelength and resolution (Quinn (2001) source: http://web.pdx.edu/~emch/ip1/bandcombinations.html)

Landsat 5 (TM sensor)	Wavelength(micrometers)	Resolution (meters)
Band 1 (reflective Visible Blue)	0.45 - 0.52	30
Band 2 (reflective Visible Green)	0.52 - 0.60	30
Band 3 (reflective Visible Red)	0.63 - 0.69	30
Band 4 (reflective Near-Infrared)	0.76 - 0.90	30
Band 5 (reflective Middle-Infrared)	1.55 - 1.75	30
Band 6 (emissive Thermal Infrared)	10.40 - 12.50	120
Band 7 (reflective Middle-Infrared)	2.08 - 2.35	30

Landsat imagery has a spatial resolution of 30 meters and a temporal resolution of 16 days. Imagery used for the study areas is from path 22, row 39 for the Breton Sound Estuary and path 21, row 39 for the Chandeleur Islands. The most challenging task in the process of obtaining the Landsat imagery was acquiring data that was cloud free. The Landsat imagery was collected over a period of 24 years (1987- 2011) for the Breton Sound Estuary that consisted of a total of 20 images. In case of the Chandeleur Islands, the imagery was obtained over a period of 14 years (1997-2011) with a total of 14 images.

Two different time periods were chosen for the study areas due to the following reasons; Significant change in Chandeleur Islands was from 1997 to 2005 attributed to the effect of the

sequence of hurricanes in this period, any change before this time period was in 1979 due to Hurricane Fredrick (Kahn and Roberts, 1982; Fearnley et al, 2009). In the case of Breton Sound Estuary, the construction of Caernarvon Diversion in 1991 was a significant event and the first seven band Landsat 5 Thematic Mapper data that was cloud free was available from winter of 1987.

Table 2.2 Landsat 5 TM Band Combinations used in this research
(Quinn (2001) source: http://web.pdx.edu/~emch/ip1/bandcombinations.html)

R, G, B	Potential Information Content
4,3,2	This is the "False Color Composite" where vegetation appears in shades of red, urban areas in cyan and soils in shades of brown. Dark red colors indicate healthy and thick vegetation whereas lighter colors indicate sparsely distributed or grassland areas.
3,2,1	This is called the "True Color Composite" as the features appear as visualized by human eye. Vegetation appears in shades of green. This band combination has the maximum water penetration and thereby used to identify suspended sediments.
4,5,3	This is a composite containing entirely of Infrared bands. It is best used to identify different types of vegetation in shades of brown, green and orange. It's the best indicator for land/water interfaces and used to identify soil moisture as infrared band has the maximum water absorption.

All the imagery was acquired for the fall and early winter seasons within the period from late September to early December, when the floating aquatic vegetation is minimal. This reduces the potential of false positives, as the floating vegetation could be interpreted as land area during the growing season. Anniversary or near anniversary images were obtained for both the study areas which indicates images obtained for different years but in the same season usually fall or winter.

Previous studies have demonstrated that using anniversary images is very beneficial in terms of reduction in the errors generated due to sun angle and reflectance from "phenology"

(Song and Woodcock, 2003). Errors due to reflectance from phenology are those affected by the changes in the vegetation during the different seasons of the year. This error can be greatly minimized by using images from the same season. Furthermore, these errors were found to affect processes involving spectral analysis such as principal component analysis, tasseled cap analysis and so on. In case of spatial analysis such as land classification and change detection, the results were not affected by the atmospheric errors. (Song and Woodcock, 2003; Song et al, 2006).

The cloud free Landsat imagery that was downloaded from USGS was in the form of separate bands that were projected in Universal Transverse Mercator (UTM) with WGS 1984 datum. The first step was data preparation and preprocessing. The separate Landsat bands were "Layer Stacked" using ERDAS IMAGINE 9.3. This process created a composite image of all the bands. The band combination used for this analysis was 4, 5 and 3 for the red, green and blue gun. These bands were chosen, as they were the least correlated of all the reflective Landsat TM bands (Lillisand and Kiefier 1997). In addition, the near and mid-infrared bands best distinguish the vegetation types. Band 5 is the middle infrared band, which is primarily used to delineate land from water but also has unique vegetative reflectance compared to band 4. From previous studies it is evident that band 5 has the lowest reflectance and maximum absorption in water when compared to the visible bands, which makes it ideal for land-water classification (Wu et al, 2008; Richards and Jia, 2006).

The next step was to subset the scene to the study area. The Breton Sound Estuary study area extended from 29.89°N to 29.44°N and 90.02°W to 89.43°W. The Chandeleur Islands study area extended from 30.06°N to 29.62°N and 89.04°W and 88.76°W. The area of interest (*aoi*) for the Breton Sound Estuary was created from the center of the Mississippi river to the Breton Sound and that for the Chandeleur Islands was created using a rectangle around the chain of

islands. Due to the extensive expanse of water in the Chandeleur Islands study area the images were biased by water. This was corrected by creating an *aoi* around the land area and the image statistics were recalculated for the metadata. All of the subsets were reprojected to the Universal Transverse Mercator (UTM) projection with zone 15 and WGS 1984 datum.

2.2. Digital Orthophoto Quarter Quadrangles (DOQQ)

The Digital Orthophoto Quarter Quadrangles are aerial photographs taken with an infrared camera from an aircraft. They have a spatial resolution of 1 meter. They cover a 4 by 4.5 $mile^2$ area on the ground. The imagery were available through the ATLAS website of Louisiana State University for the years 1998, 2004 and 2005. The 2010 Digital Ortho Quarter Quarter Quadrangles (DOQQQ) have a spatial resolution of 6 inches to 1 foot and were obtained from Governors Office of Homeland Security and Emergency Response (GOHSEP). These data are projected in UTM zone 15, NAD-83 datum (http://atlas.lsu.edu). The DOQQ were mostly used for accuracy assessment of the classification.

2.3. Water Level Data

Water level data were obtained from the USGS stations in the Breton Sound Estuary and the Breton Sound (Figure 2.1). The stations used were:

1. USGS 295124089542100 Caernarvon Outfall Channel at Caernarvon, LA
2. USGS 073745253 Reggio Canal near Wills Point, LA
3. USGS 07374527 Northeast Bay Gardene near Point-A-LA-Hache, LA
4. USGS 07374526 Black Bay nr Snake Island nr Pointe-A-La-Hache, LA

The data from these stations were obtained in ASCII format that had information about water level, precision, date and time of data acquisition in UTC. The water level was analyzed

using MATLAB software and the deviations from the long-term means (anomalies) were calculated for each station. Data were acquired from 1993-2011 for Northeast Bay Gardene and Black Bay near Snake Island. In case of the Caernarvon Outfall Channel and the Reggio Canal data, were available from 1999 to 2011. The water level data from the Snake island station were used for the Chandeleur Islands analysis since this was the closest station with a long-term record.

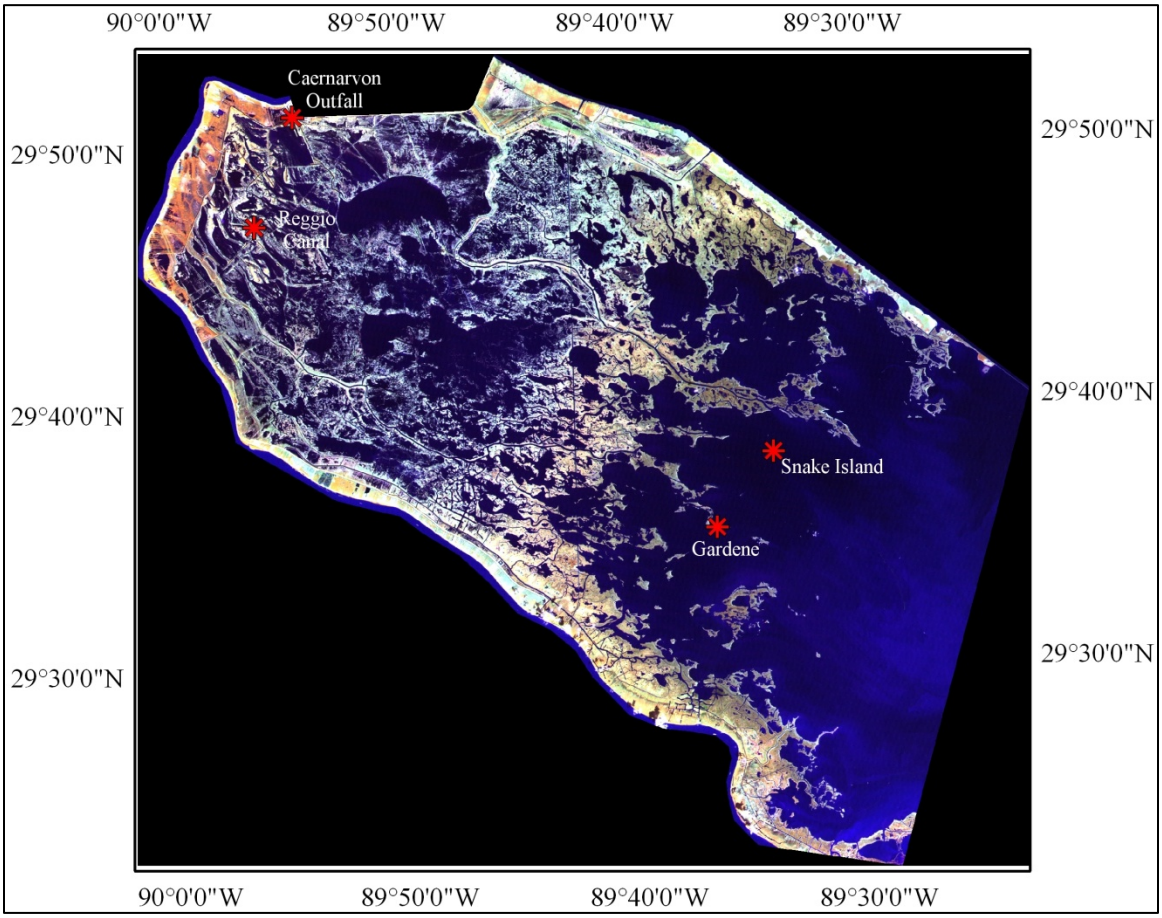

Figure 2.1 Water level stations indicated with red asterisk overlaid on Landsat 5 TM data on 10/07/2005

2.4. Wave Height Data

The wave height data were obtained from station 42007 (22 nm SSE of Biloxi, MS) operated by the National Data Buoy Center (NDBC) (Figure 2.2). This was the closest station to the Chandeleur Islands that had all the historic data for the years of image acquisition. The wave height analysis was primarily performed to analyse the potential effect of waves on the image-derived land area changes.

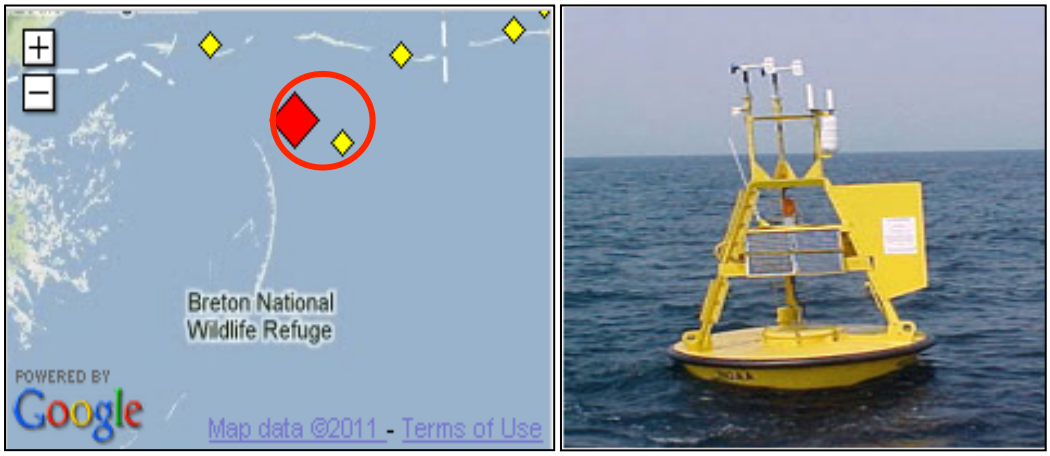

Figure 2.2 Station 42007 of NDBC; in the left panel red diamond indicates the station 42007 and the yellow diamonds are other stations nearby, right panel is a picture of the buoy at this station (source: http://www.ndbc.noaa.gov/station_page.php?station=42007)

2.5. Sediment Sample Data

The sediments from the Chandeleur Islands beach (Figure 2.3 a, b) were sampled at five places in a single transect that ran through the coordinates:

1. Sample 1: 29.95331 N, -88.82396 W
2. Sample 2: 29.95332 N, -88.82386 W
3. Sample 3: 29.95329 N, -88.82357 W
4. Sample 4: 29.95338 N, -88.82285 W
5. Sample 5: 29.95343 N, -88.82257 W

These samples were then analysed for grain size.

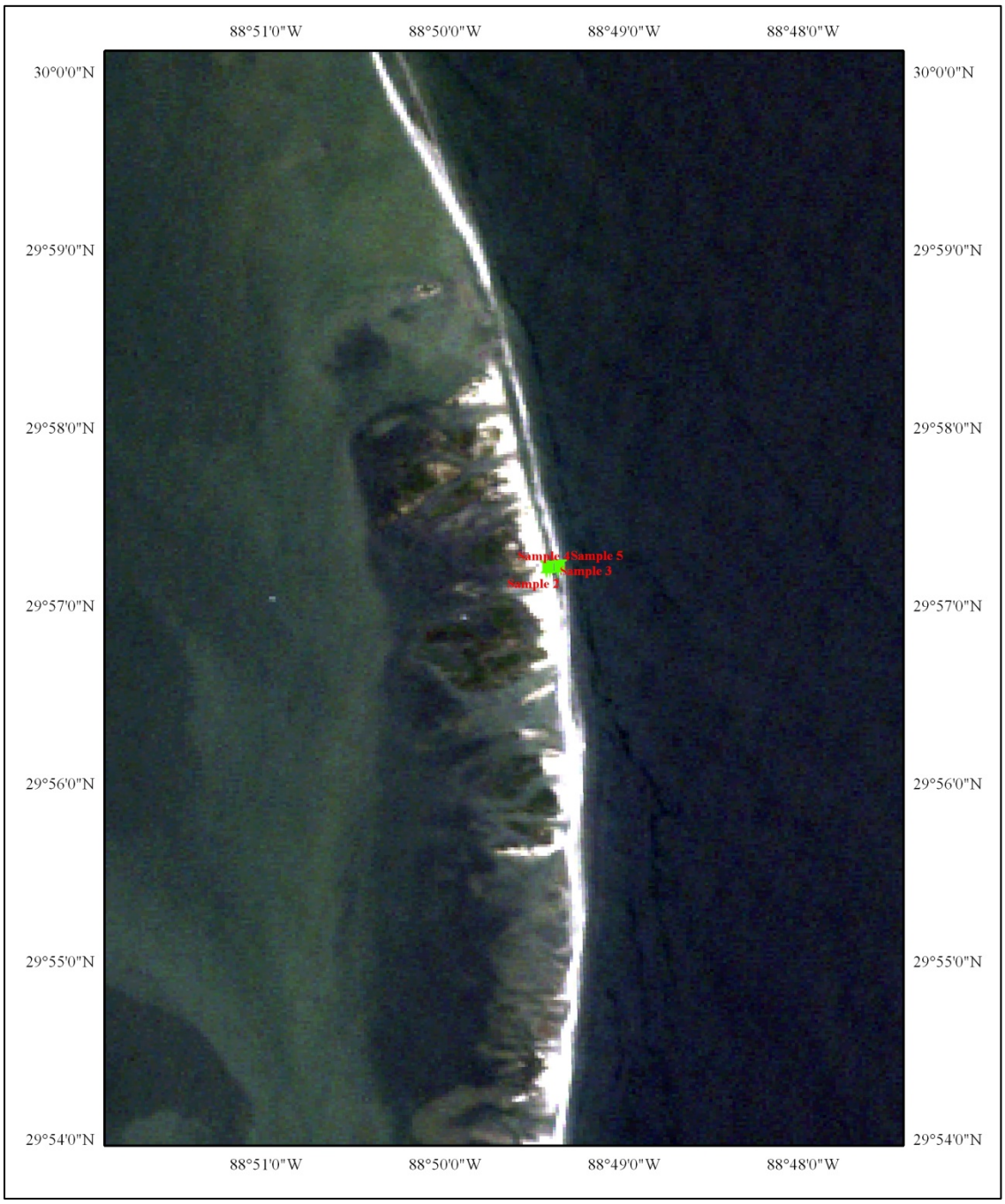

Figure 2.3 a Sites on Chandeleur Islands used for sample collection in a transect overlaid on Landsat TM data on 06/13/2011

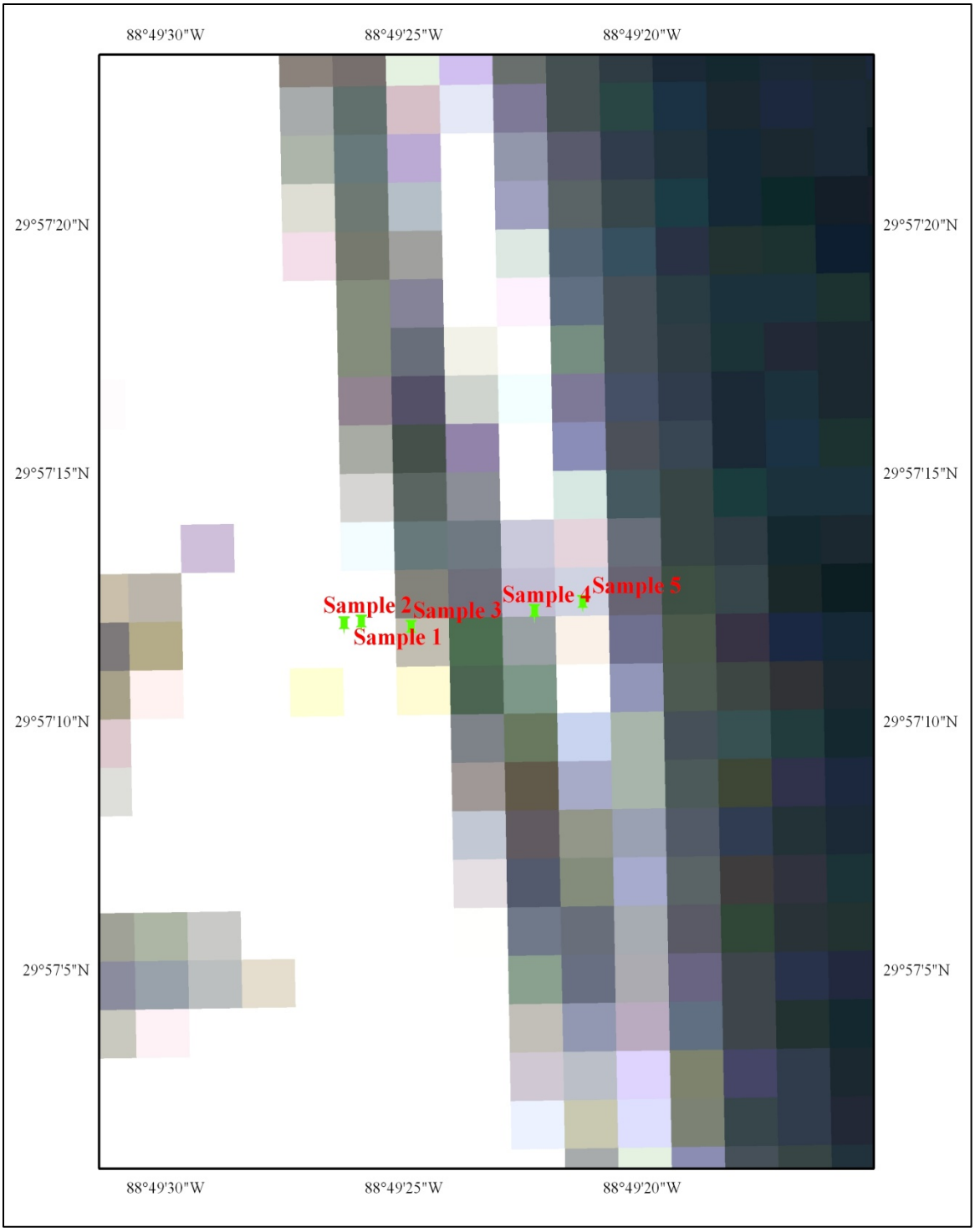

Figure 2.3 b Sites on Chandeleur Islands used for sample collection in a transect overlaid on Landsat TM data on 06/13/2011

2.6. Atmospheric Correction

In previous studies, it has been shown that atmospheric correction is not always required for Landsat 5 TM data when performing classification and image differences, as it has little effect on the accuracy of classification for land or vegetation studies (Kawata et al, 1990; Fraser et al, 1997; Song et al, 2001).

Song et al, (2001) also provide sufficient proof that this is a necessary step only when the classification of multiple images is performed using the same training sites. However, in the case of spectral analysis methods such as Tasseled cap analysis, it is essential to correct for the atmospheric effects (Song and Woodcock, 2003).

2.6.1. Reflectance Calculation

The Digital Number (DN) pixel values in the Landsat images were converted to reflectance. By converting DN to reflectance, the pixels have a meaningful value, which can be effectively used for spectral image analysis such as image differencing and comparing time series of images with one another (Edwards et al, 1999). A model was created on ERDAS IMAGINE to calculate the reflectance values, which incorporated the sun elevation and distance. The distance was calculated by using a separate model that generated the value in Astronomical Units using the Julian date of the image. The model also incorporates the exo-atmospheric solar irradiance for each band. The input for the model was the Landsat radiance values calculated from gains and offsets in each band derived from the literature on Landsat 5 TM revised recalibration table (Chander and Markham, 2007). This step is particularly necessary for the Chandeleur Islands imagery as three quarters of the imagery is covered by water area. There is a higher chance of it being affected by the atmospheric effects (Song et al, 2001).

2.7. Hybrid Classification on ERDAS IMAGINE

The classification procedure utilized in this study was a hybrid technique that incorporated both the supervised and unsupervised classification procedures. This involves a series of steps after which the image is classified to its maximum accuracy.

2.8. Supervised Classification

The first step was the creation of training sites for the subset image. For the Breton Sound Estuary region, training sites were created for three land classes (forest, marsh, developed /unvegetated) and a water class. For the Chandeleur Islands, training sites were created for three land classes (vegetation, mudflat and beach) and a water class. Multiple training sites were created for each of these classes and the signatures were analyzed for homogeneity, normality, and separability. Signatures that had a very low separability were merged and those with a very low point count were deleted.

Supervised classification was then performed based on these training sites. This is essentially a tool that is used to train the software to recognize and classify pixels within the satellite imagery based on user-defined classes. Training sites are also created such that "all the classes are represented". The classification process was performed using the maximum likelihood technique. This is an algorithm where training sites are assumed to have a normal distribution and each pixel is classified into a user specified class based on the highest probability that the pixel belongs to a particular class (Lillisand and Kiefer, 1997). The output of this step is the supervised "classified image" and a "distance image". Both were used for the next step.

Following the supervised classification, a threshold image was created using the "threshold" function of ERDAS IMAGINE 9.3. This function identifies the "incorrectly

classified pixels" in the supervised calculation by using a chi-square table. This chi-square table is automatically generated and can be altered based on the confidence interval that is entered by the user. The input for this function is the supervised classified image and the distance image. The distance file essentially contains the "Mahalanobis distance" of the initial pixel of the input raster from the signature it was assigned (ERDAS field guide). The output shows the unclassified pixels as black areas in the Breton Sound Estuary region (Figure 2.4). The unclassified pixels in the threshold image were selected in the raster attribute table and converted to an *aoi* (area of interest) file format. This *aoi* was used as a "mask" for the pixels, which were correctly classified.

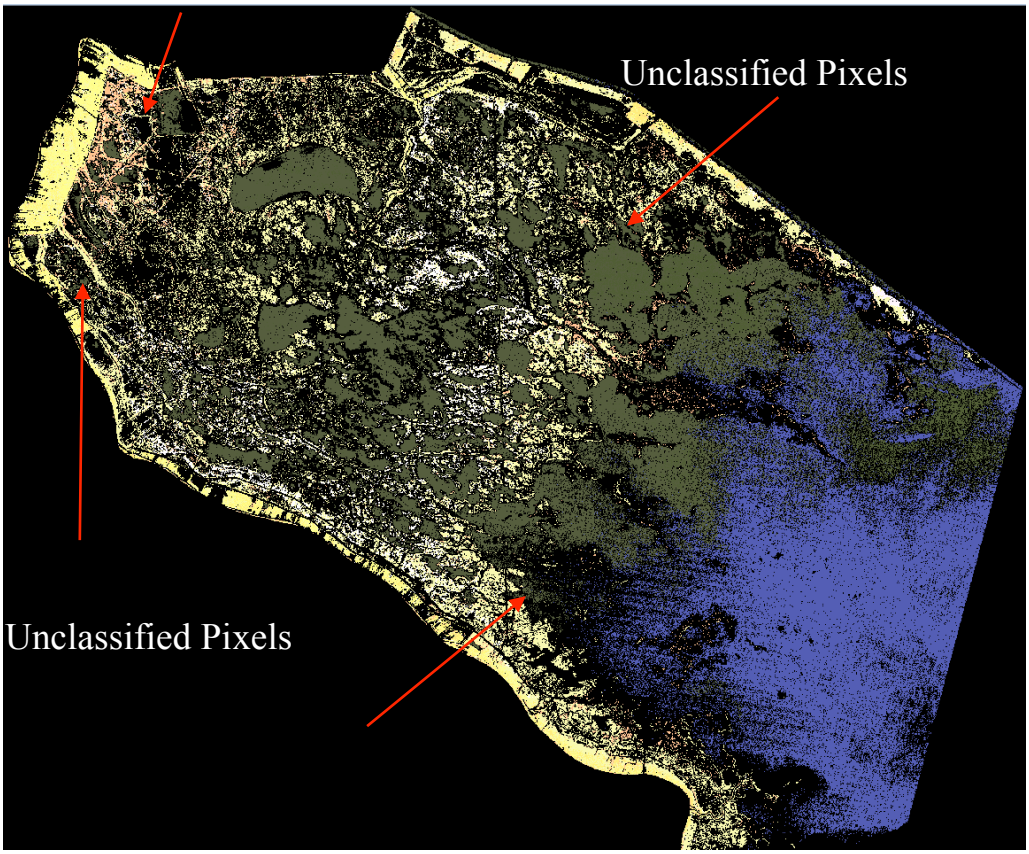

Figure 2.4 Threshold image showing the correctly classified pixels in color and the black indicates erroneously classified or unclassified pixels

2.9. ISODATA Algorithm – Unsupervised Classification

The "mask" *aoi* from the previous step was used to mask the correctly classified pixels in the unsupervised classification procedure. The TM reflectance image was used as input to create a signature set with 25 classes in 25 iterations with a threshold of 0.97. The output from this step was a signature set containing 25 classes for all the unclassified pixels from the supervised classification. A-priori probabilities were estimated based on the number of pixels in each signature, and a Maximum Likelihood decision rule was performed on the signature set using the unclassified *aoi* as mask. Since some of the signatures were non-normal due to the fact that many were outliers, a first-pass Parallelepiped decision rule was used prior to applying Maximum Likelihood (Figure 2.5). The supervised threshold and unsupervised classified images are spatial complements. These images were merged using a model to add them together, creating a final classified image of the study area (Figure 2.6). A majority filter using a 3 * 3 kernel was performed on the merged classified image. The classified images were generated for every time period to determine the temporal changes.

The advantage of the hybrid technique is that spectral variation that was not estimated using known training fields was accounted for using the ISODATA algorithm. Since both classified images complement each other a classification was produced for the complete study area.

2.10. Post-Classification Change Detection

The final classified images were used to identify changes in land area after hurricane impact. A spatial cross-tabulation (matrix algorithm) is an effective tool to analyze two multi-temporal classified images for changes. The output is a change detection image that clearly illustrates all the types of changes between the two time periods. Since the only change of interest is land

loss/gain, the land cover classes were collapsed to two categories in each image: land or water. A change detection matrix was generated with four possible outcomes: no land change, no water change, land change to water, water change to land. The result of this function produces an image with four attribute classes (Table 2.3).

Table 2.3 Matrix algorithm cross-tabulation for post classification change detection analysis

Class	Land	Water
Land	Land - no change	Land to Water
Water	Water to Land	Water – no change

2.10.1. Breton Sound Estuary

The change detection was performed for the entire time series from 1985 to 2011, along with major hurricane years (Figure 2.6) including 03-04 (Hurricane Ivan), 04-05 (Hurricane Katrina) and 07-08 (Hurricane Gustav).

2.10.2. Chandeleur Islands

The change detection was performed for the major hurricane years 97-98, 03-04, 04-05 and 07-08 for Hurricane Georges, Hurricane Ivan, Hurricane Katrina and Hurricane Gustav, respectively (Figure 2.7). Comprehensive change detection over 11 years was also calculated from 1997-2011.

2.11. Tasseled Cap Analysis

The tasseled cap analysis (TCAP) was performed on the reflectance images generated by the reflectance model. The model for generating the TCAP is shown in Appendix II. The output of the TCAP analysis consists of three bands; brightness, greenness and wetness.

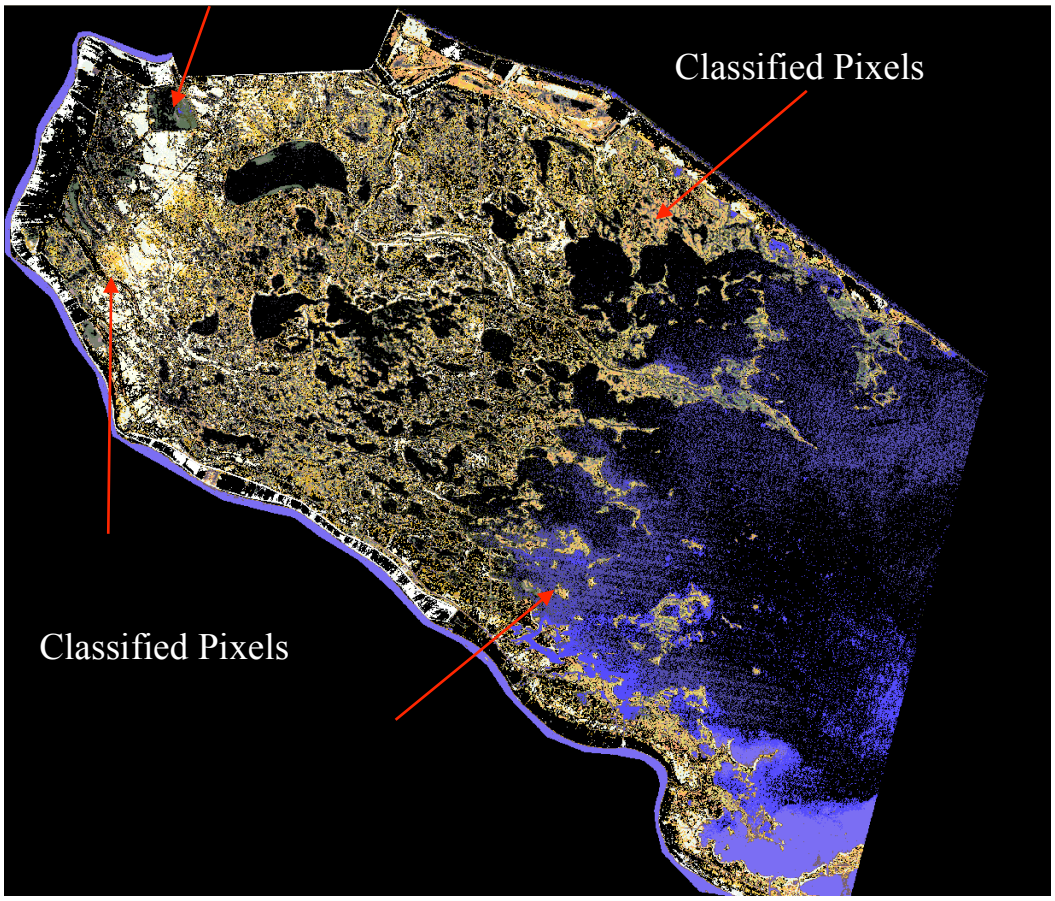

Figure 2.5 Image generated using ISODATA unsupervised signatures as input for supervised classification incorporating both parametric and non-parametric rules

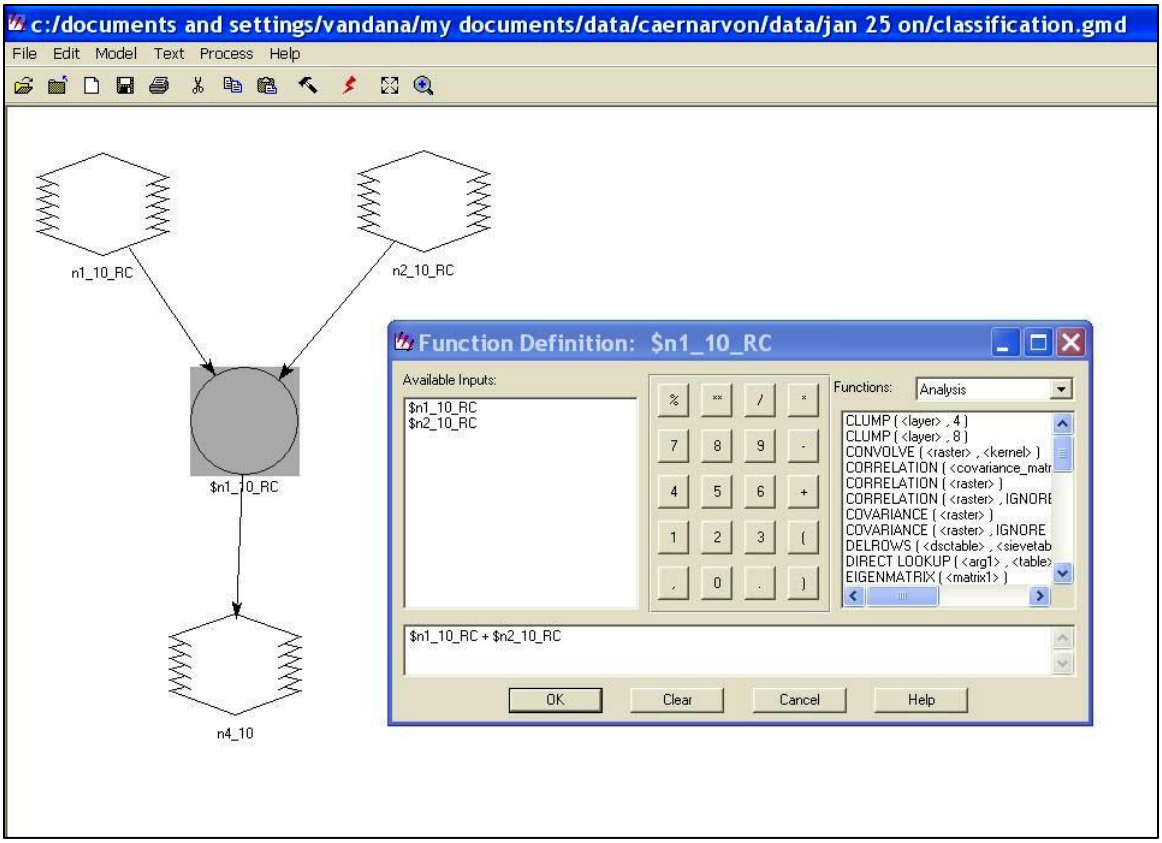

Figure 2.6 Model in ERDAS IMAGINE 9.3 model builder used for adding the threshold and ISODATA classified images

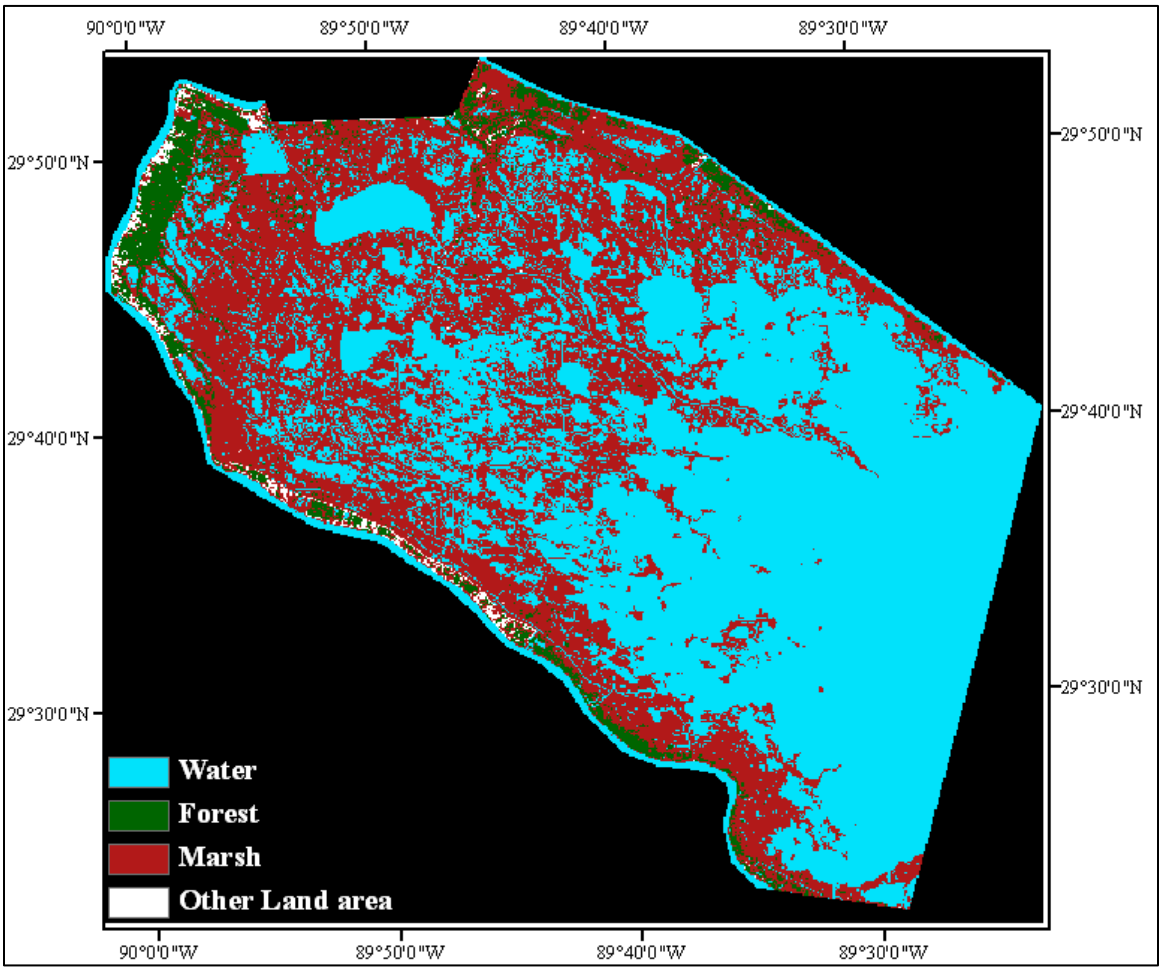

Figure 2.7 Final classified image output from the model

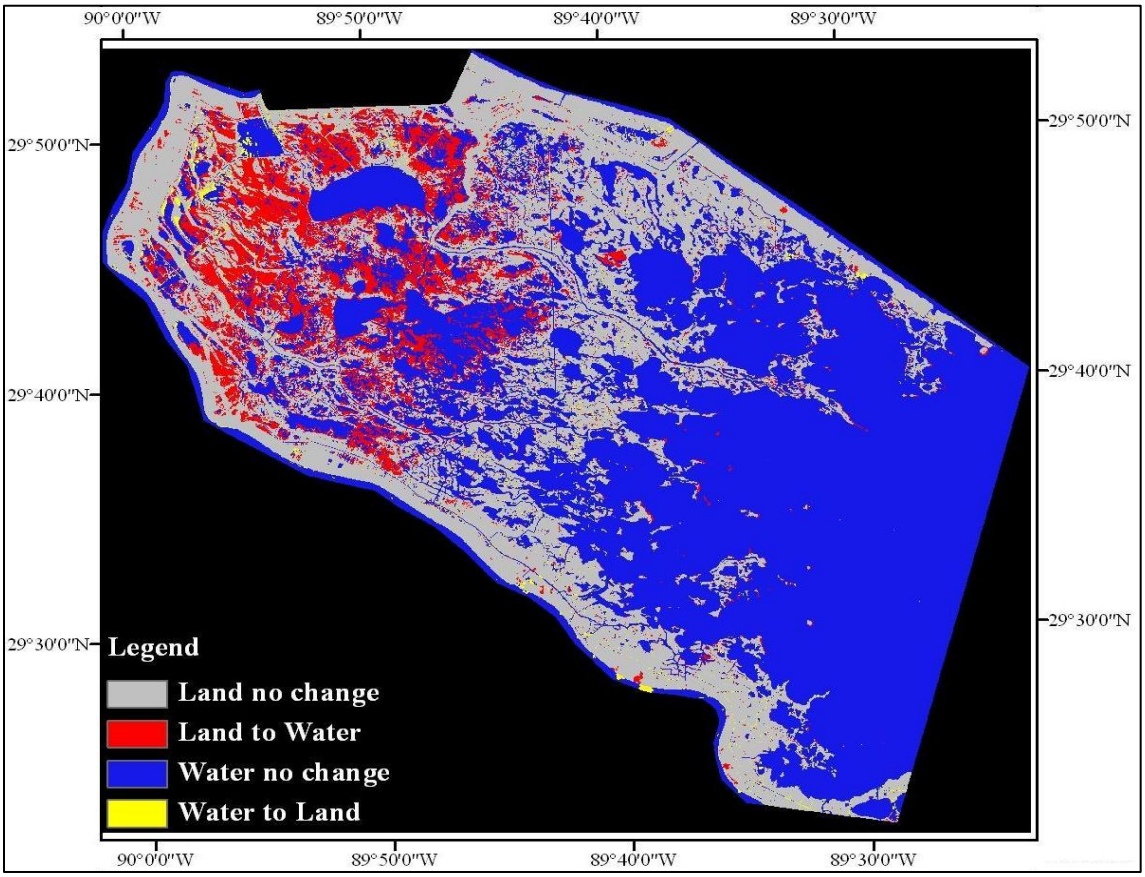

Figure 2.6 Example of change detection analysis output for Breton Sound Estuary Region for 2004-2005 (Hurricane Katrina)

The TCAP analysis is a type of Principal Component Analysis in which the information from the six bands of Landsat 5 TM was transformed to represent the three bands of the TCAP. Band 1, which is the brightness band of the TCAP, indicates the presence or absence of vegetation. Band 2, the greenness band, also signifies the amount of vegetation present. Band 3, wetness band, essentially indicates the state and moisture content of soil in the image (Vorovincii, 1998). This was performed for all the images in both study areas (Figure 2.8).

2.12. TCAP Change Detection

The TCAP change detection was performed on the greenness and the brightness bands of the TCAP results. The change detection was primarily performed for the major hurricane years along with a comprehensive change over the time period of 26 years. The change detection was performed using the KT transformation change detection technique by computing a simple difference between the TCAP greenness bands of image 2 from image 1 (Figure 2.9). A similar technique was applied to the brightness band as well (Lu et al, 2003; Han et al, 2007; Jin et al, 2004).

The Tasseled cap analysis was performed for Breton Sound Estuary region on the reflectance output (Figure 2.8). Two types of change detection were performed for the tcap of images 2004 and 2005 since maximum change was observed between these years using previous methods. The first method involved a direct subtraction of the greenness band of 2005 from greenness band of 2004 (Figure 2.9).

Another change detection analysis was performed using the "Change Vector Analysis" function. This was used to calculate the change between two images using their brightness, greenness and wetness bands. The formula used for this calculation is:

$$Change\ Magnitude = \sqrt{(brightness_1 - brightness_2)^2 + (greeness_1 - greeness_2)^2 + (wetness_1 - wetness_2)^2}$$

(Baker et al, 2007)

It is identified as "Pythagorean alteration" for the tcap change detection. The output i.e. Change Magnitude, generates an image that has areas of maximum change and change value. A threshold value is chosen to eliminate changes that are not significant thus retaining only the regions of highest change (Parmentor et al, 2003; Baker et al, 2007).

This was performed to identify the change due to the effect of Hurricane Katrina from 2004 to 2005. The individual tasseled cap images were first generated. Then the raster calculator function in ArcGIS was used to calculate the change magnitude. This output represents the regions of maximum change (Figure 3.31). This was then used to generate a mask for the unchanged pixels. The direction of change was identified using the spatial intersection change detection technique implemented earlier for both the study areas.

2.13. Water Level Data Analysis

The water level data were processed using MATLAB to generate graphs of storm surge associated with each hurricane. The water level fluctuations were studied to identify potential relationships with land area change results. A regression analysis was also performed to determine if the land area changes were related to the changes in water level. This was done using the statistical software SAS 9.2. The land area was considered as the 'y' variable and water level was considered as the 'x' variable and a 95% confidence interval was used in order to get the *p value*. Correlation coefficients were also determined for these two variables and plots generated.

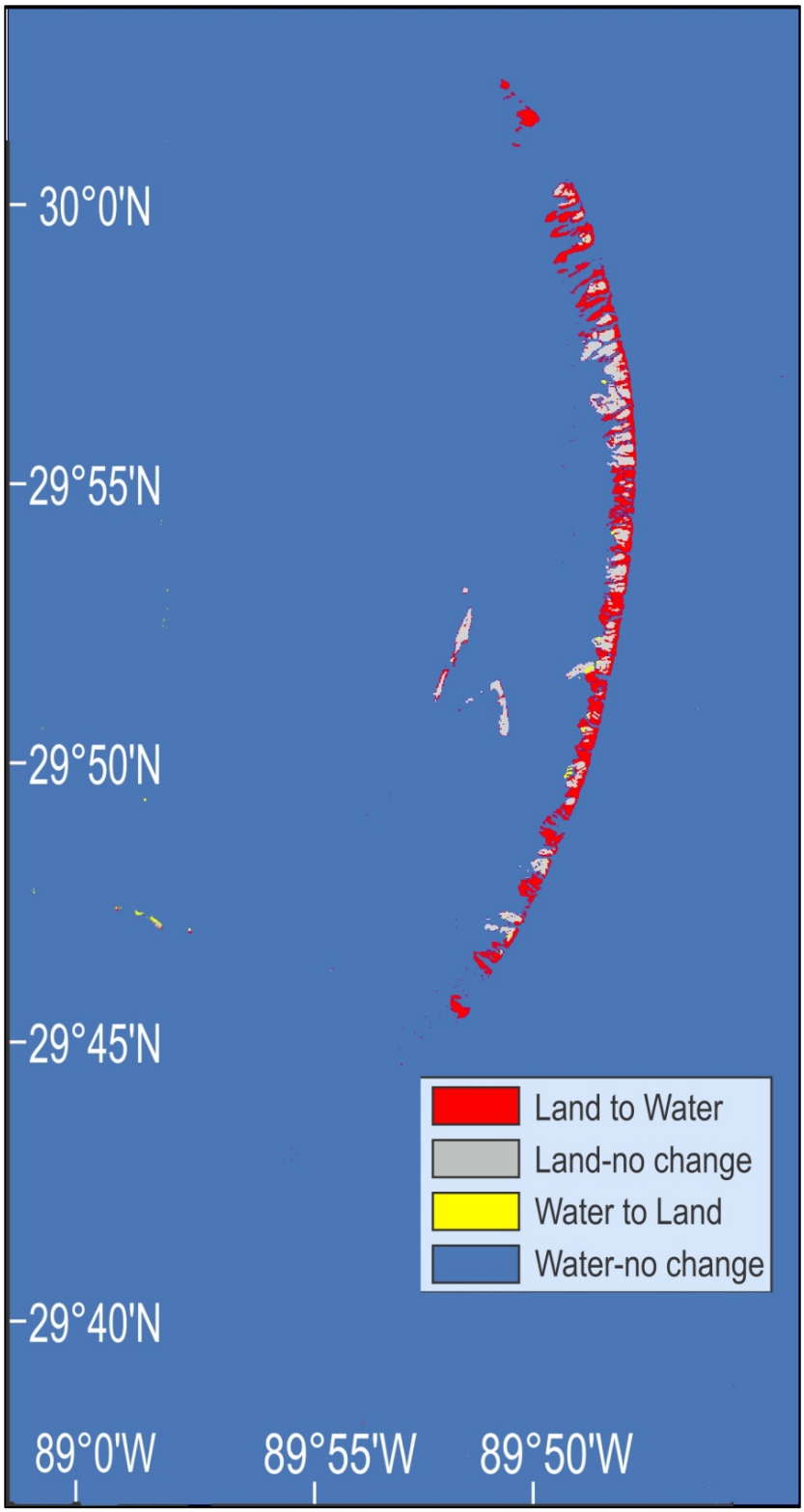

Figure 2.7 Example change detection analysis for the Chandeleur Islands for 2004-2005 (Hurricane Katrina)

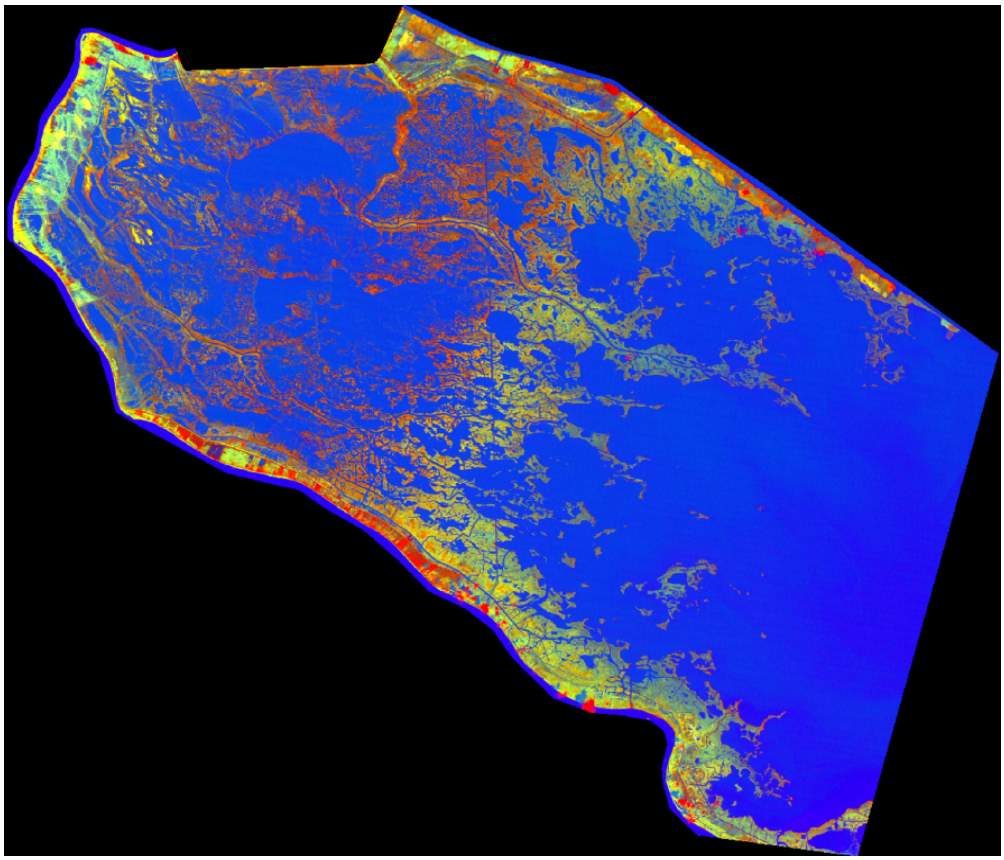

Figure 2.8 TCAP Output Image with 3 bands (brightness to Red, greenness to Green and wetness to Blue of RGB composite) for 2005 with shades of yellow and orange indicating marsh areas, blue indicating water and red indicating other land areas

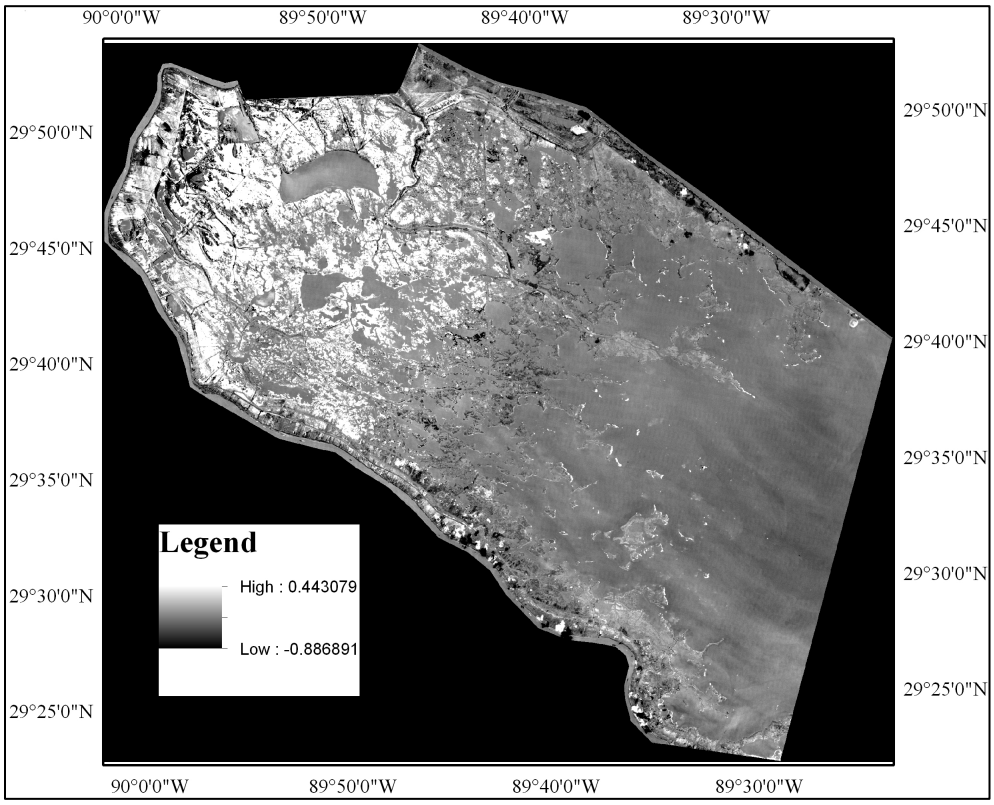

Figure 2.9 TCAP Difference Image with brighter areas showing maximum difference for 2004-2005 (Hurricane Katrina)

2.14. Wave Height Data Analysis

Regression analysis was performed on the wave height data as well with the land area as the y variable and the significant wave height as the x variable. The results were plotted and *p value* was obtained.

2.15. Field Trips to the Study Areas

Field trips play a major role in any remote sensing study as it serves to verify the information obtained from satellite data. The Breton Sound Estuary was visited twice, March 2009 and November 2009. Chandeleur Islands were visited in June 2011. The first field trip to Breton Estuary was performed in March 2009 on an airboat, to verify results from SPOT data analysis. I was a part of the other two field trips in November 2009 and June 2011. During our field trip to Breton Sound Estuary in November on a boat, we identified several species of marsh plants in varying state of senescence. Important aspect of both the field trips to Breton Sound was the large deposits of rolled up marsh debris. An aerial view of the Breton Sound Estuary was observed during our field trip in June 2011 from a seaplane. Sediment samples were collected from Chandeleur Islands during this field trip. However, we were not permitted by the USWF to take plant samples from these islands

2.15.1. Grain Size Analysis

The sediments were collected at 5 points along the transect. The sediments were then weighed on the electronic scale, which was linked to a computer to record the readings. The sieves that were used for this analysis ranged from 0.026 mm to 1 mm. The sieve sizes were first entered into the computer. The sieves were individually weighed and the values recorded by their respective sieve size. Then the sediments were run through the different sieves individually with the help of automatic sieve shaker to make sure that the sediment passes through all the sieves. The sieves

were then weighed again after the sediments were run through them. Now the new weights were recorded in a table along with the initial weight. The grain size was then calculated with MATLAB using these values based on the technique developed by Folk and Ward (1957).

CHAPTER 3
RESULTS

3.1. Breton Sound Estuary

The results from the classification of 15 images from 1987 to 2011 indicate a varying trend in land loss/gain in the Breton Sound Estuary (Figure 3.1). The blue color in this classification indicate water area, brown indicates marsh area, green indicates forest area and yellow indicates other area such as developed areas, roads and unvegetated/barren land. The marsh area in the northwestern portion of the diversion deteriorated most rapidly through the time series. This region has undergone maximum change. The most significant change was seen in the Figure 3.1 (c) classification of the October 2005 image, which was after the passages of Hurricanes Katrina and Rita. Figure 3.1 (d) is the classification of the image from October 2006 that showed an increase in unvegetated/ barren land by 39 km^2. This increase in unvegetated land was due to the rolled up marsh debris that was found in the area after the passage of the Hurricanes in 2005 (Barras, 2006). This rolled up debris was caused by the storm surge, which uprooted the marsh plants area primarily in the northwestern and central portions of the diversion. Several areas of marsh accumulation was observed on the field trip in March 2009 (Nan Walker, personal communication)

The total area considered for the Breton Sound Estuary classification was 2025 km^2. A bar graph was generated to exhibit land area changes from 1987 to 2011 (Figure 3.2). An overall land loss of 271 km^2 was observed from 1987 to 2011. In 1992, there was a decrease in land area by 21 km^2, which could be attributed to the passage of Hurricane Andrew in 1992. Decrease in land area by 41 km^2 in 2002 could be attributed to Hurricanes Isidore and Lili. In 2004, there was a decrease in land area by 20 km^2 caused by the passage of Hurricane Ivan. The biggest change

was due to Hurricane Katrina in 2005 that led to a total decrease in land area of196 km^2 from November 2004 to October 2005. This amounts to 27% of the total area lost from 1987 to 2005 image. The Mississippi River flooding in 2011 led to abnormally high water levels in this region, which gave the false impression of additional landloss totaling 90 km^2. It must also be noted that the most recent image is not from fall 2011, as the rest of the images in the time series, but it is from June 2011.

There was some recovery of the marsh in the upper portions of the diversion by October 2009, which was sustained through December 2010 (Figure 3.1 b). The June 2011 image revealed decrease in land/marsh, however this was likely due to flooding of the Mississippi River, which peaked on May 14, 2011 (US Army Corp of Engineers, 2011) (Figure 3.1 g).

Some marsh types were clearly identifiable in the images as they each had unique spectral signatures. However, due to lack of ground truth and ground control points the different types of marsh were not considered in this classification procedure. Marsh area changes were similar to the land area changes (Figure 3.2 and Figure 3.3). Over 80% of the land area was marsh. After the construction of the diversion in 1991, there was an initial loss of marsh area by 94 km^2 in 1992 attributed to the passage of Hurricane Andrew (Figure 3.3). Thereafter, there was a steady increase in marsh area until 2002, when there was a decrease in marsh area by 42 km^2 possibly due to Hurricane Lili. In 2004, Hurricane Ivan caused a decrease in marsh area by 47 km^2. As in the case of the total land area, Hurricane Katrina caused the maximum decrease in marsh area in 2005 reducing the marsh area by 173 km^2 (Figure 3.3).

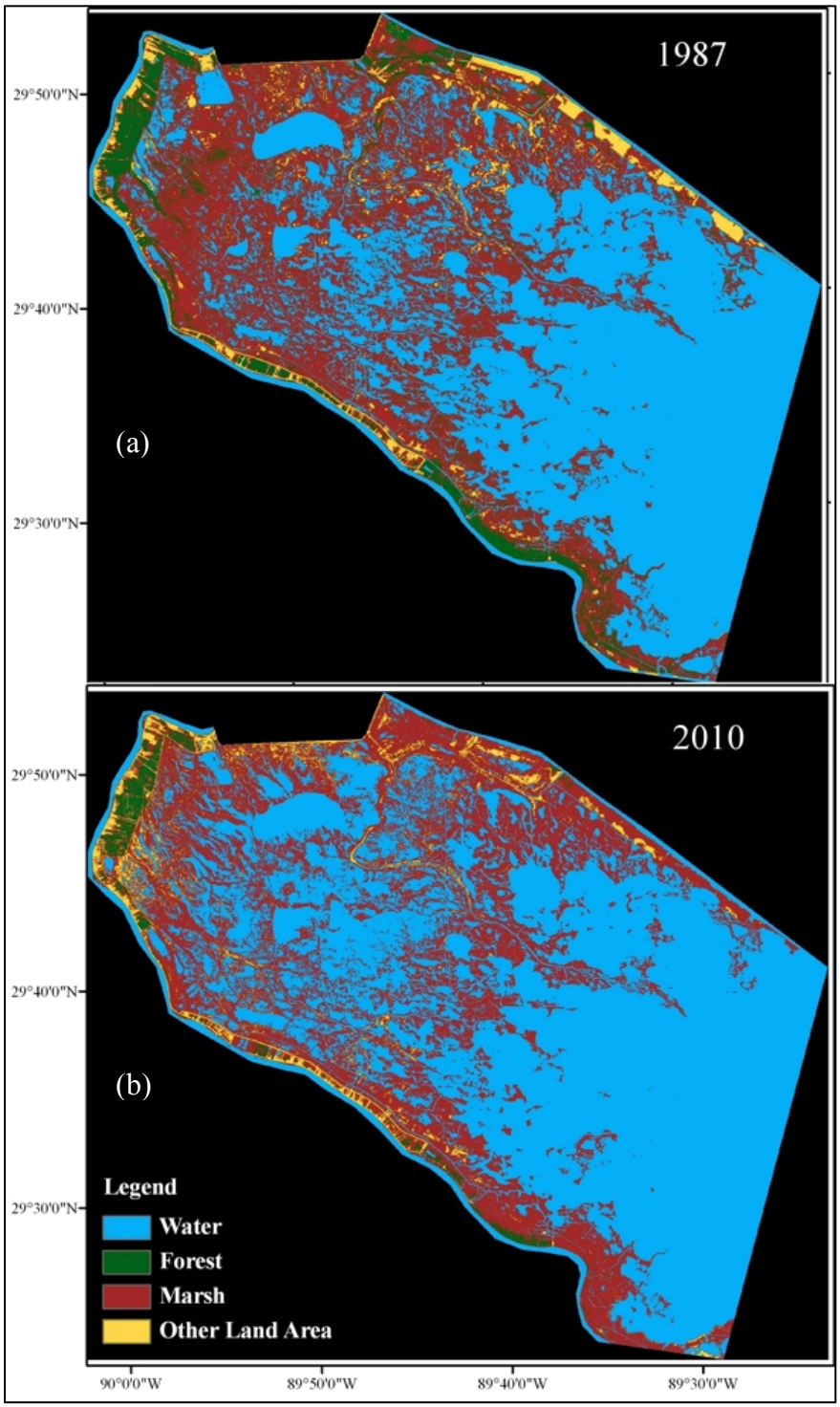

Figure 3.1 Classification of the Breton Sound Estuary (a) 10/08/1987 (b) 10/07/2010

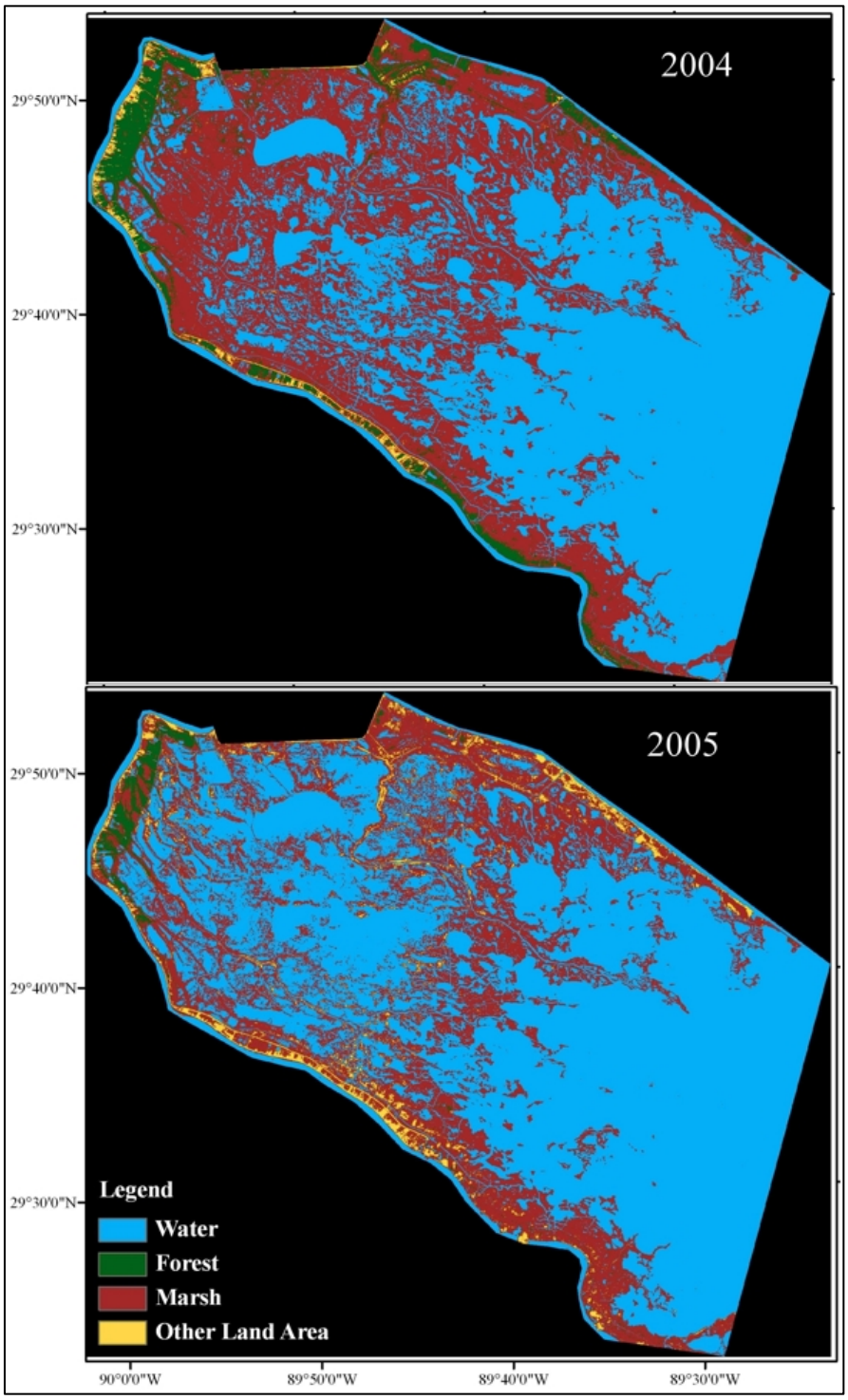

Figure 3.1 Classification of the Breton Sound Estuary (c) 11/07/2004 (d) 10/09/2005

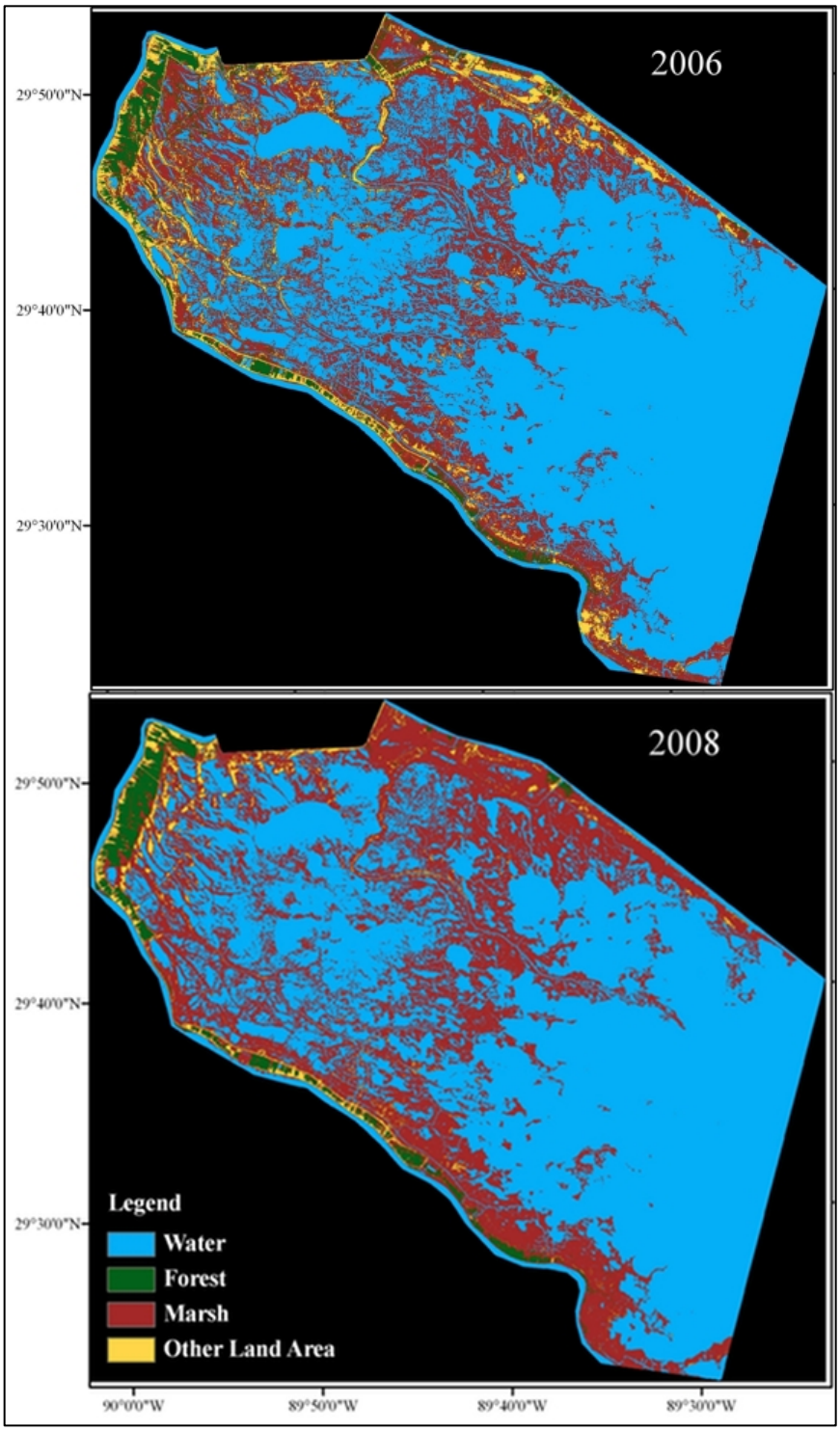

Figure 3.1 Classification of the Breton Sound Estuary (e) 09/26/2006 (f) 10/01/2008

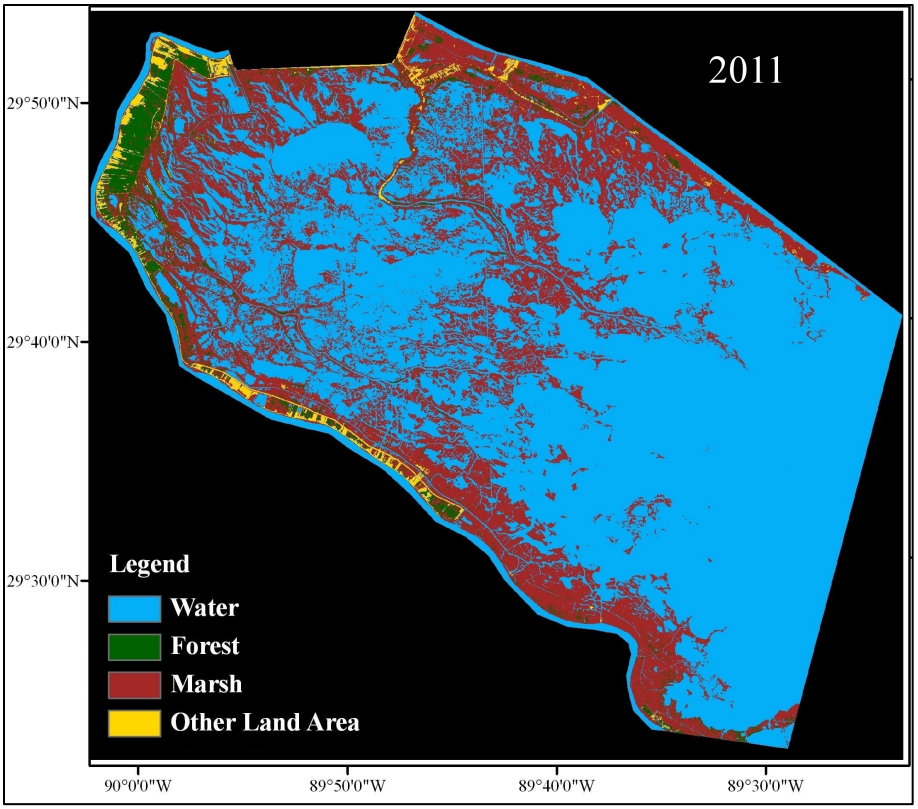

Figure 3.1 Classification of the Breton Sound Estuary (g) 06/04/2011

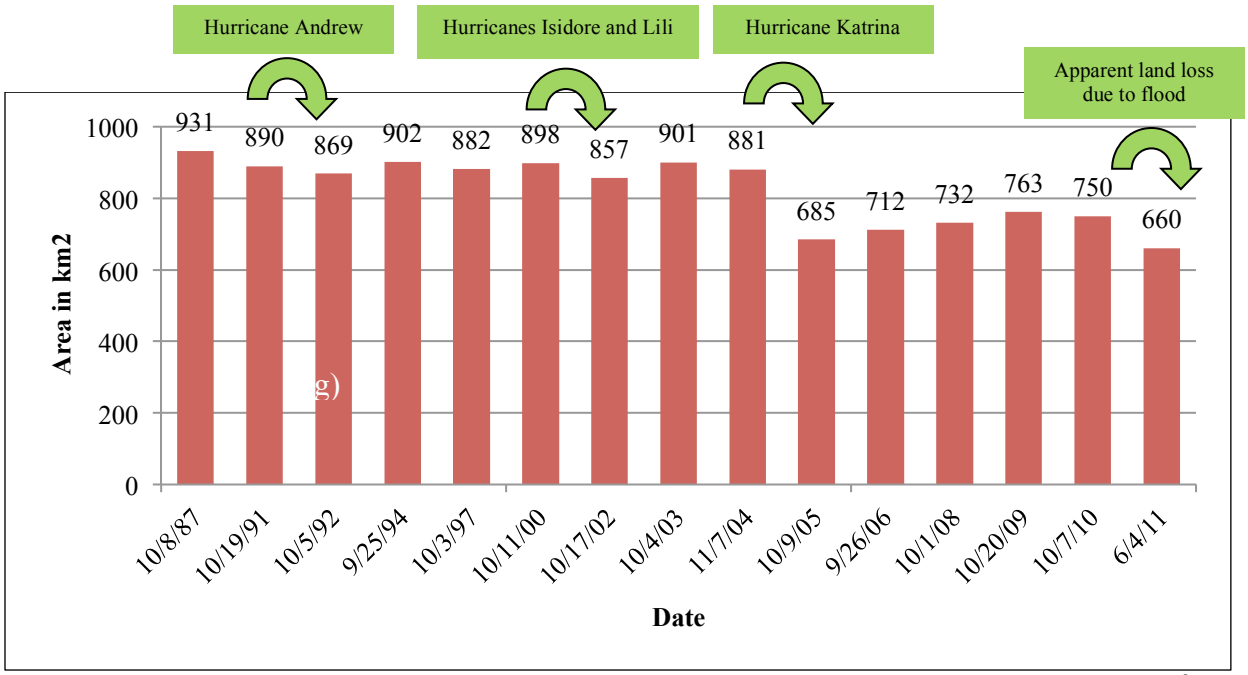

Figure 3.2 Land area changes for Breton Sound Estuary from 1987 to 2011in km^2

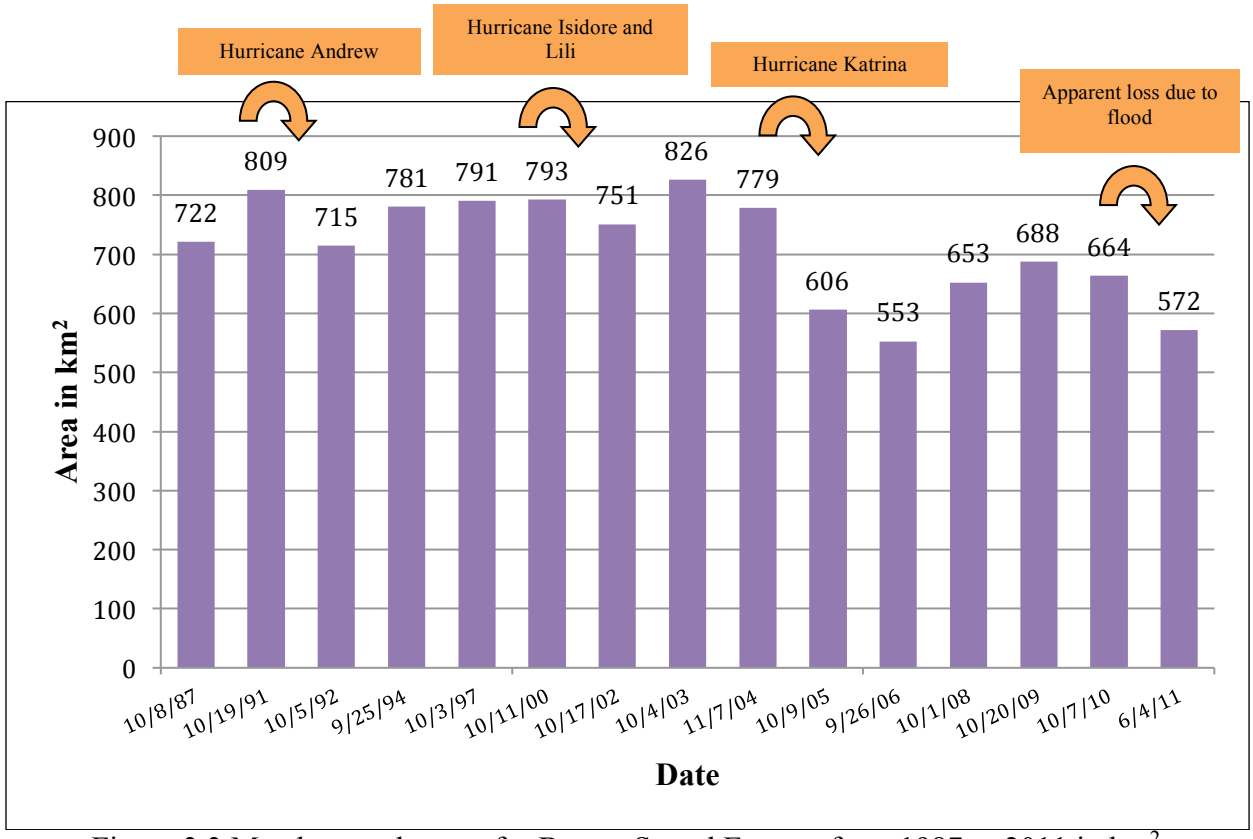

Figure 3.3 Marsh area changes for Breton Sound Estuary from 1987 to 2011 in km^2

By 2006, the marsh had not recovered. The storm surge due to these hurricanes led to rolling up of the marshes into mounds of debris that appeared as unvegetated land area in the Landsat image, therefore a decrease in marsh area on the graph (Figure 3.4). The marsh recovered somewhat in 2008 by 100 km^2 and regained another 35 km^2 in 2009. The flooding of the Mississippi river led to further decrease in the marsh area by about 92 km^2. This was obtained from the most recent image considered for the study from June 04, 2011. This image was obtained on the day of our field visit to the Chandeleur islands when we flew through the Breton Sound Estuary. It was also interesting to note that there were land/marsh losses in years with no major hurricane passage for e.g. 1987-1991, 1994-1997 and 2009-2010.

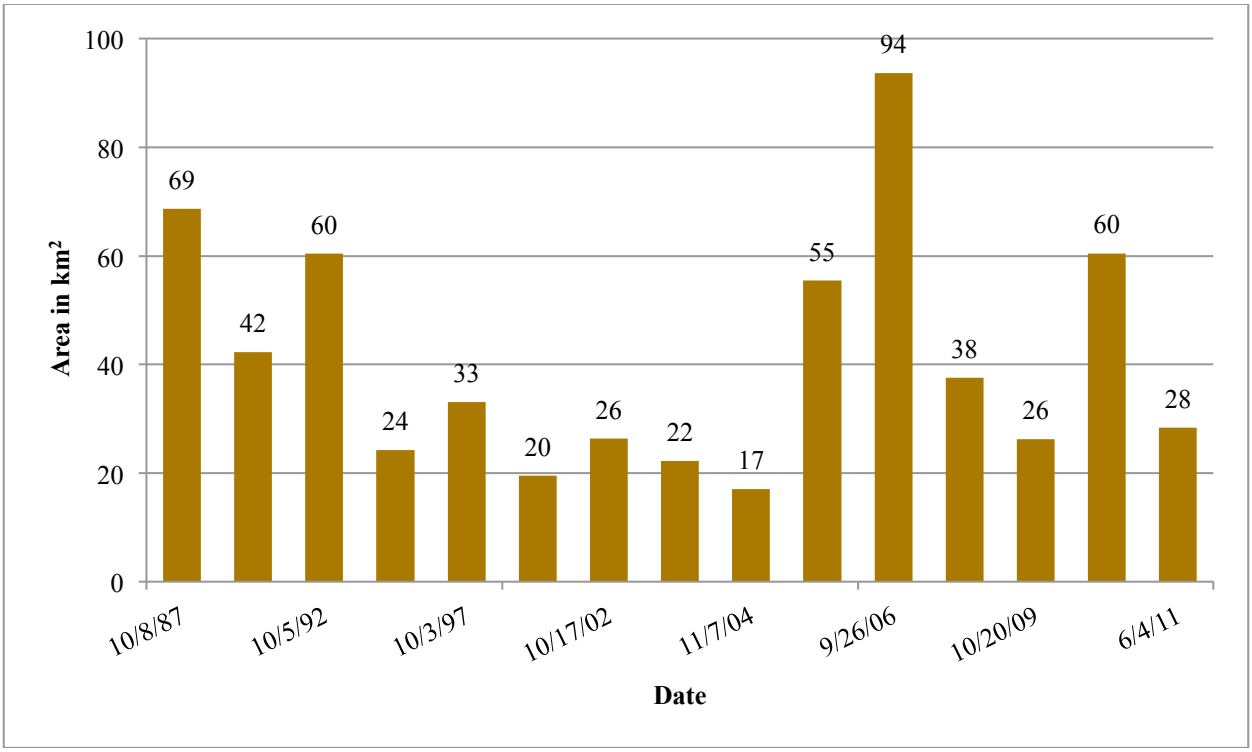

Figure 3.4 Change over the time series from 1987-2011 for other areas in the classification such as unvegetated/ barren land and developed areas

Figure 3.4 indicates the changes in other land areas such as barren/unvegetated or developed land area in Breton Sound Estuary. The graph indicates that maximum gain in area occurred in 2006, which could be due to the rolled up marsh debris. Due to this reason, there was an increase in other land area immediately after the passage of Hurricane Katrina in 2005. This is also attributable to the residual water areas after passage of Hurricane Rita in the end of September 2005, which lead to decreased area in 2005 and thereby a dramatic increase in 2006.

3.1.1. Change Detection

A 24-year change detection analysis was performed for the time series from 1987 to 2011 (Figure 3.5). The blue color indicates water areas that did not undergo any change, red color indicates the areas that were converted to water, yellow indicates areas that were water and converted to land, and gray indicates land areas. The maximum change in land area to water was

observed in 2005 due to the effect of Hurricanes Katrina and Rita, although most of the damage is attributed to Hurricane Katrina.

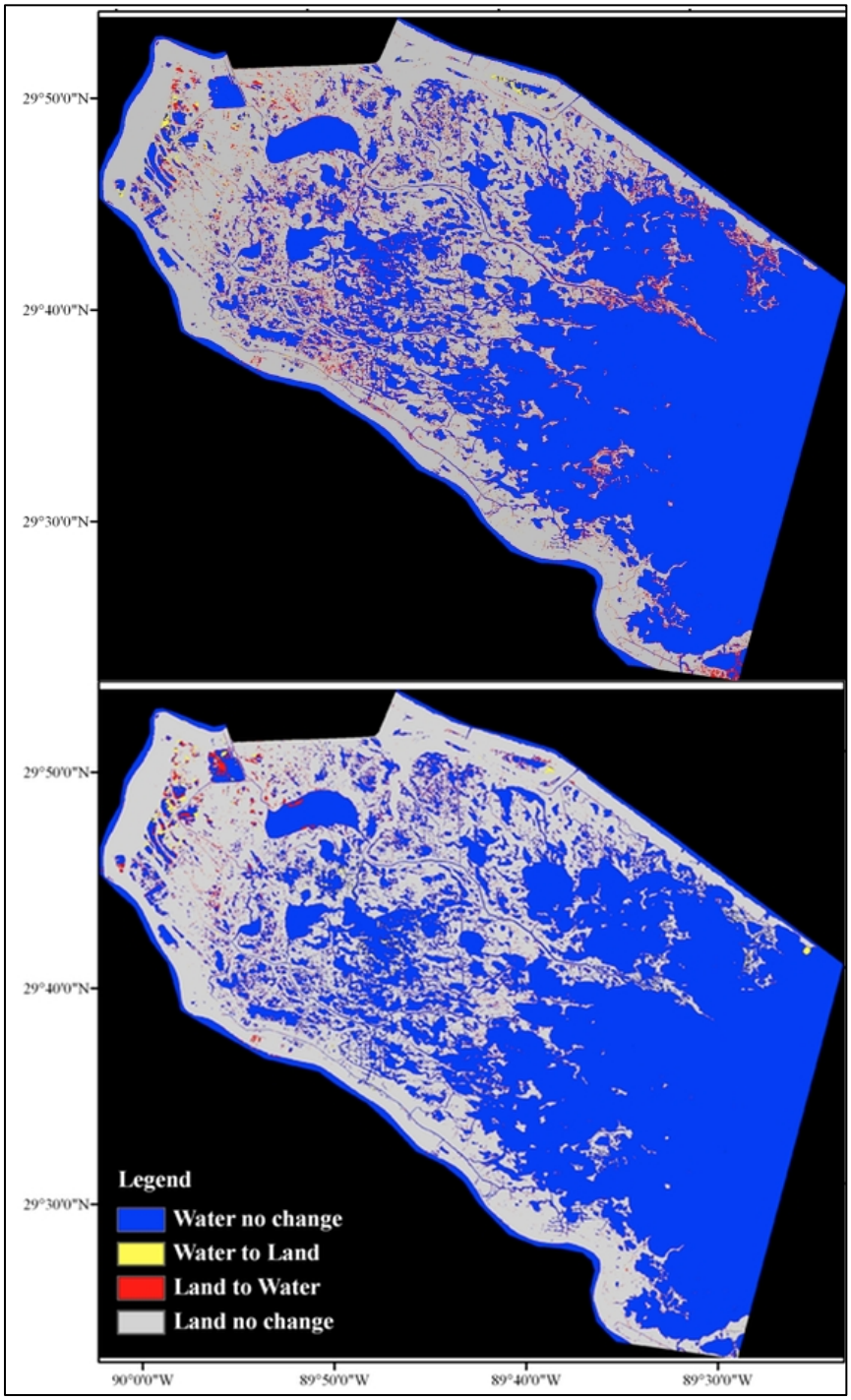

Figure 3.5 Change detection analysis for Breton Sound Estuary (a) 2000 to 2002 for Hurricanes Isidore and Lili (2002) (b) 2003-2004 for Hurricane Ivan

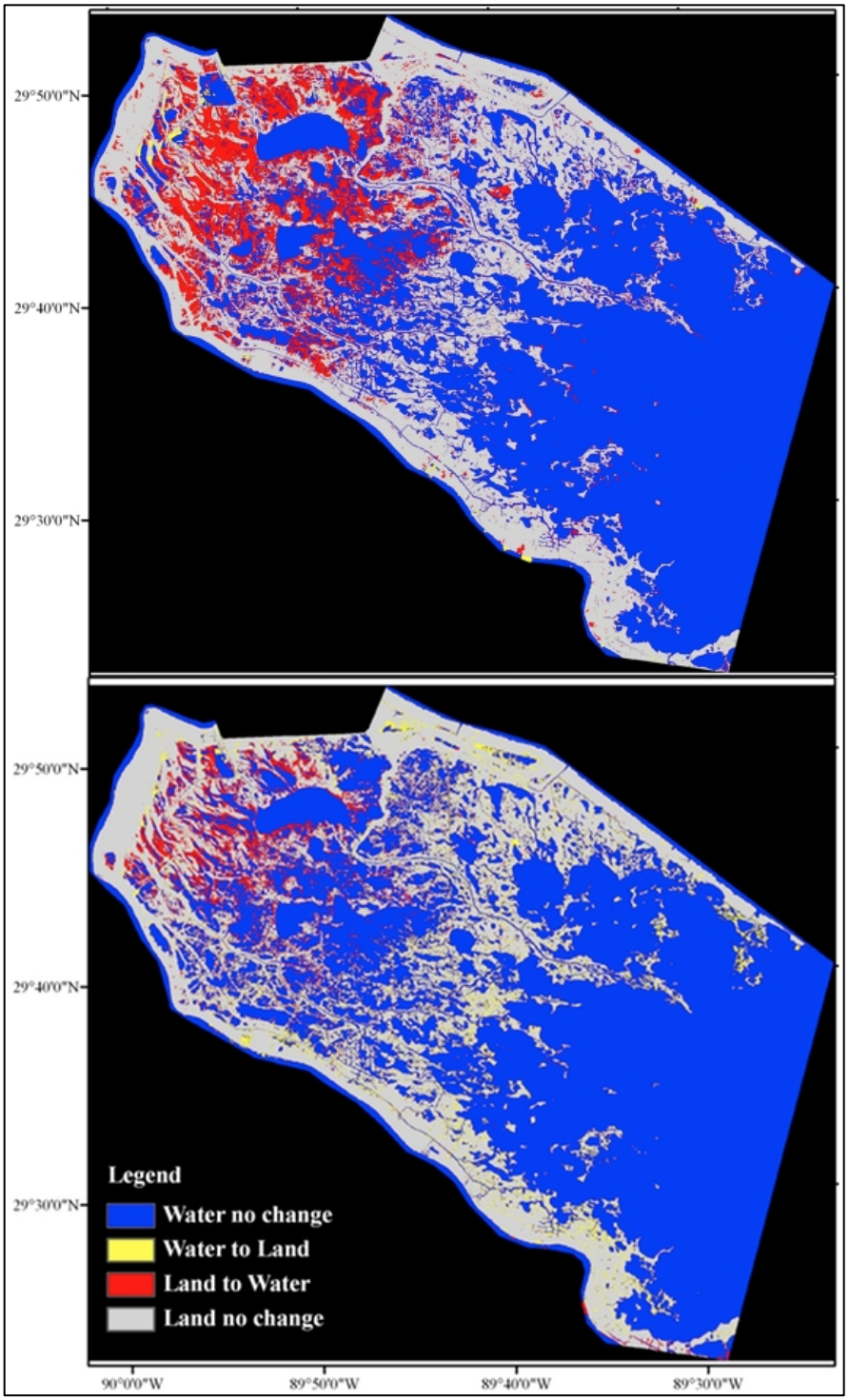

Figure 3.5 Change detection analysis for Breton Sound Estuary (c) 2004-2005 for Hurricanes Katrina and Rita (2005) (d) 2006-2008 for Hurricane Gustav

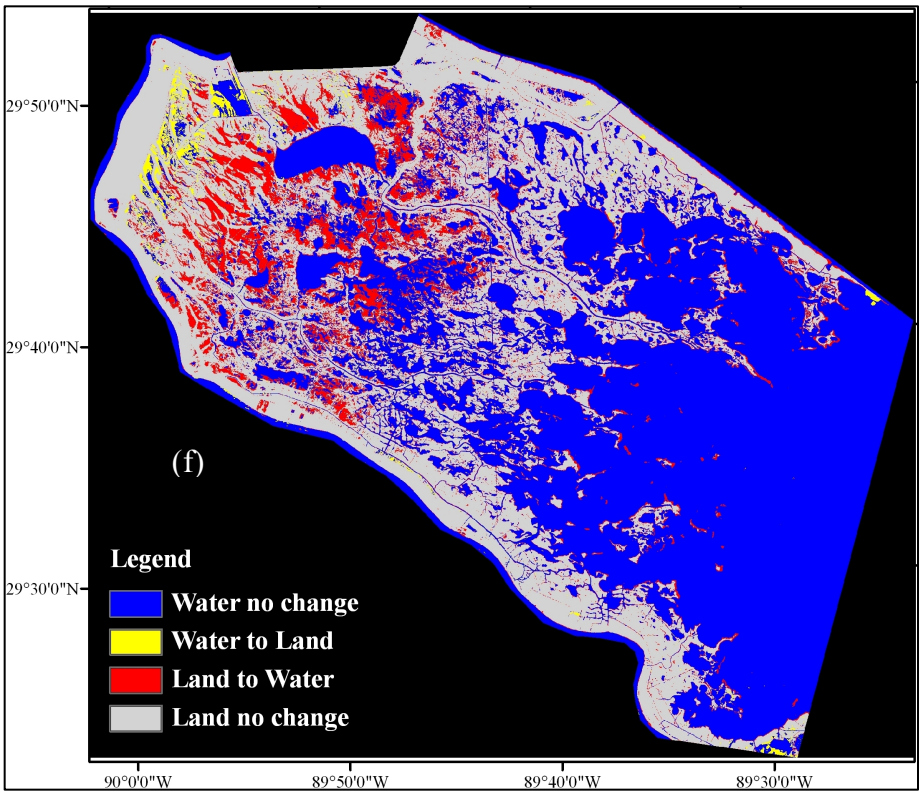

Figure 3.5 Change detection analysis for Breton Sound Estuary (f) long-term change between 1987 and 2010 images

The areas that were transformed from land to water do not necessarily imply a net land loss as the water to land area conversion must be considered for the analysis. Figure 3.6 depicts land to water conversion as a bar graph for the major hurricane events. Maximum land to water change occurred in 2005 due to Hurricane Katrina totaling 208 km^2. This was higher than the overall land to water conversion from 1987 to 2010 which was 201 km^2. Hurricane Gustav in 2008 resulted in a land to water transformation of 77 km^2, which was mostly observed in the northwestern portion of the diversion. Although, the land to water conversion was due to Gustav, there was no significant net land loss. This was due to the fact that the areas that were converted to water were compensated by water areas that became land in the central portion of the diversion (Figure 3.5 d, Figure 3.6).

Hurricane Lili in 2002 caused a land to water conversion of about 74 km^2. The Mississippi River flooding in 2011 resulted in a land area inundation of 107 km^2. An overall land change to water of 281 km^2 was observed over the 24 years from 1987-2011. This was different from the results from 1987-2010 due to the Mississippi River flooding in May 2011.

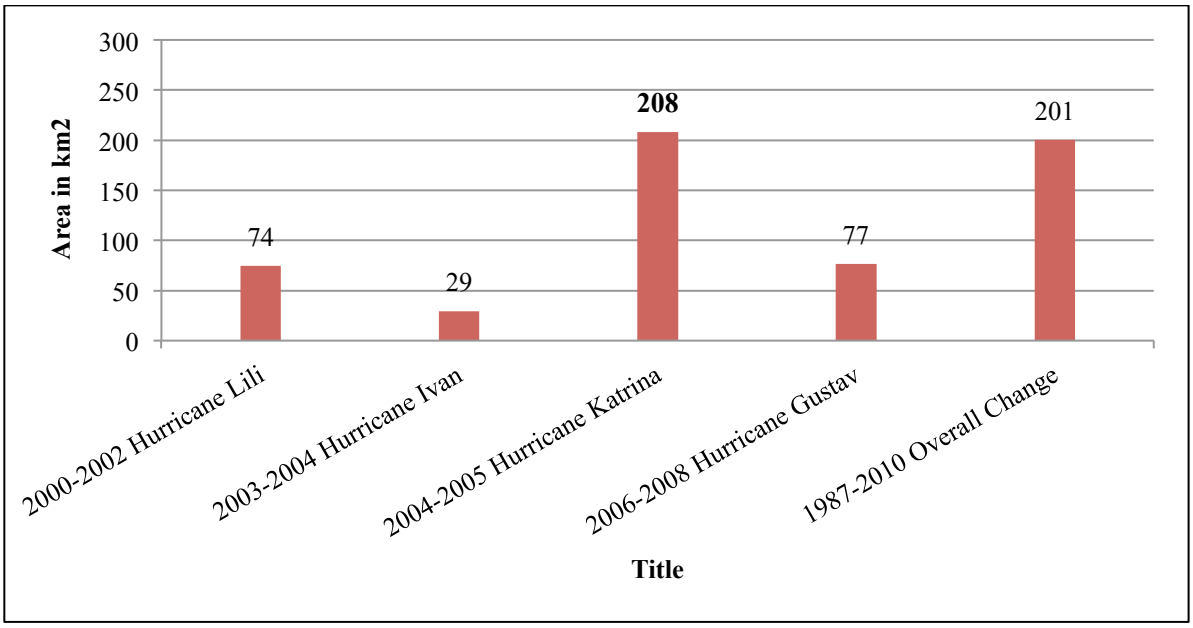

Figure 3.6 Land to water conversion observed in the Breton Sound Estuary due to the passage of major hurricanes from 1987 to 2010 in km^2

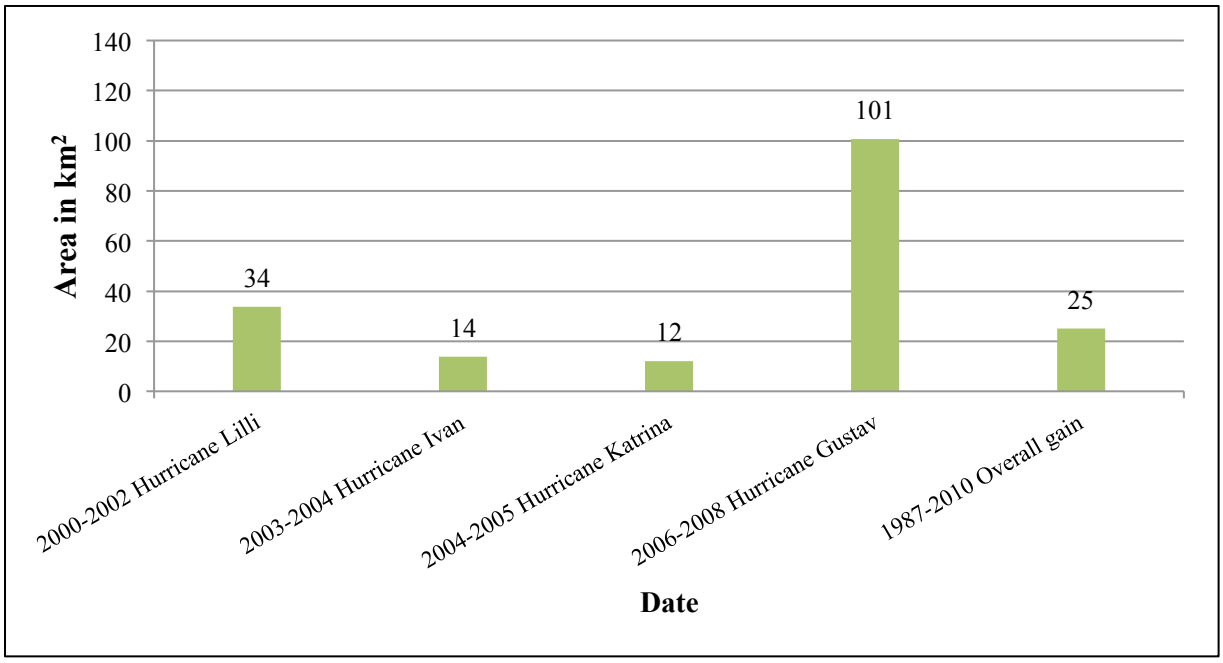

Figure 3.7 Water to land area conversion observed in the change detection analysis

The water to land conversion graphs in Figure 3.8 indicates that the maximum occurred after passage of Hurricane Gustav. This was attributed to the new marsh regions along with the barren/unvegetated land in the central portion of the estuary (Figure 3.6 d).

3.1.2. Field Trip on 11 November 2009

Ground truth of the Breton Sound Estuary was performed on 11 November 2009. The points visited during the field visit are shown in Figure 3.8. The regions that indicated "new land area" or few that indicated "no change in land area" in the change detection analysis were actually found to be marsh debris rolled up in huge mounds that have a signature of land in the satellite imagery. In these cases, "new land" areas were created from the marsh debris. Some of the water within channels in the diversion region was covered with floating vegetation that mostly consisted of duckweed and water hyacinth. The diversity of plant species that were identified at each of these field sites is presented in Table 3.1. The most predominant type of vegetation that was observed during the visit was *Panicum dichotomum florum*. This is commonly referred to as the fall panic grass, which is a freshwater marsh grass that grows in regions that have undergone stress (Stutzenbaker, 1996).

Figure 3.9 (a) shows an aerial view of the diversion and Figure 3.9 (b) is the southernmost point of Breton Sound Estuary called Mozambique Point. Several aerial photographs that were taken in the Breton Sound Estuary region indicated a very flooded and fragmented marsh environment (Figure 3.9 (c) and (d)). Field trips helped better understand the fragmented nature of the marsh environment and diversity of marsh plants.

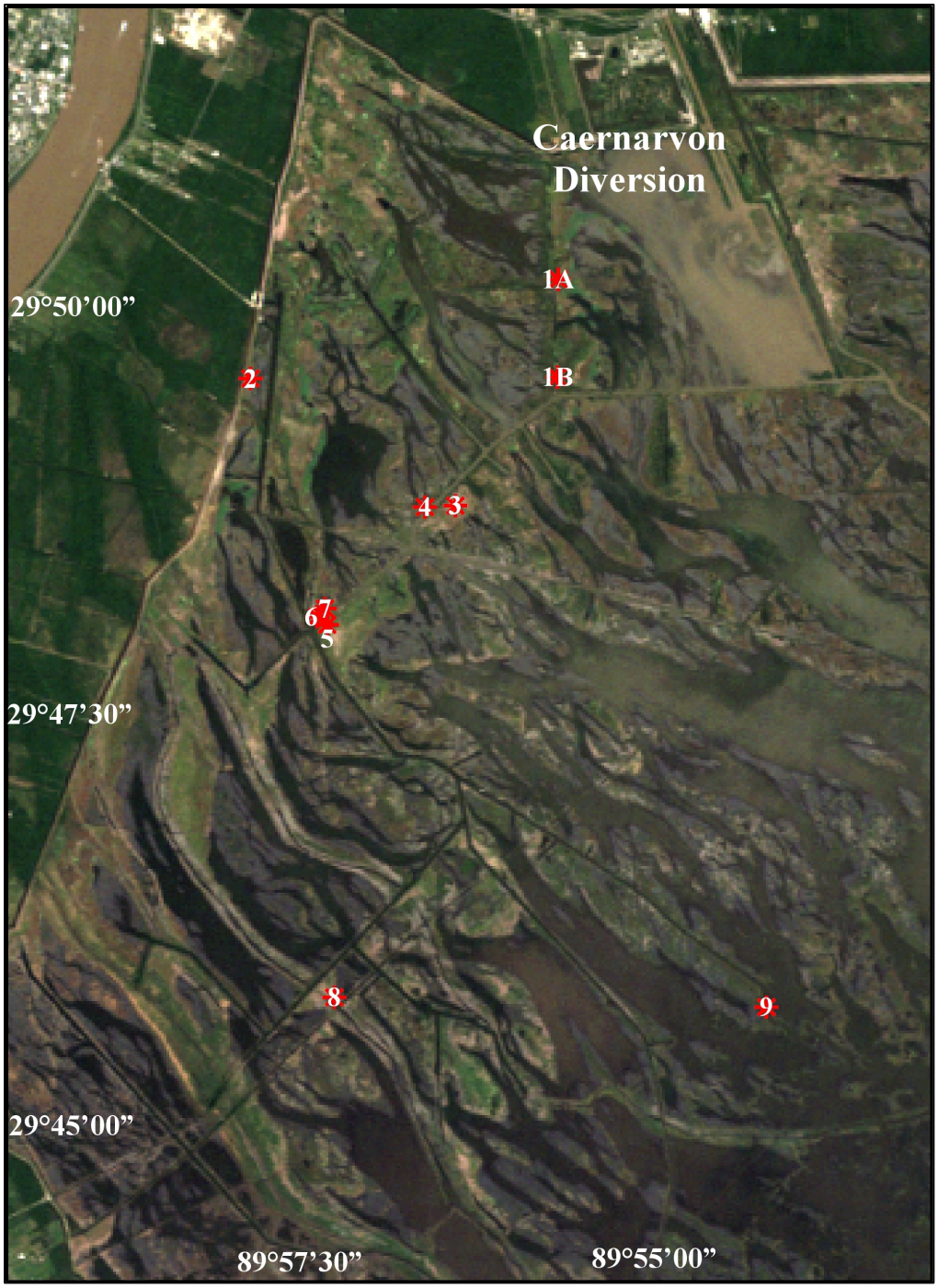

Figure 3.8 Field points considered for the ground truth on November 11, 2009 overlaid on "true color composite" imagery with 321 band combination where green indicates vegetation, brown is marsh/land areas, white indicates developed areas, shades of black is water and tan indicates river water

Table 3.1 Different plant species identified during the field trip on 11 November 2009 (plant species scientific name source: USDA, NRCS, 2011, Urbatsch, 2011)

Point ID	Latitude	Longitude	Vegetation types
1A	29.83° N	-89.92° W	*Cerratophyllum* (hornworts), *Caltha palustris*(marsh marigold), *Salix nigra* (black willow), *Eichhornia crassipes* (water hyacinth), *Panicum dichotomum florum* (fall panic grass), *Sagittaria lancitolia* (bulltongue arrowhead), *Salvinia*, *Najas guadalupensis* (southern waternymph), *Lemnaoideae*(duckweed), *Sacciolepis striata* (american cupscale)
1B	29.82° N	-89.93° W	*Ludwigia leptocarpa* (anglestem primrose-willow), *Lemnaoideae*(duckweed), *Salix nigra* (black willow), *Ludwigia peploides* (floating primrose-willow), *Hydrocotiles ranuncaloides* (floating marshpennywort), *Eichhornia crassipes* (water hyacinth), *Vigna luteola* (hairypod cowpea)
2	29.83° N	-89.96° W	*Caltha palustris* (marsh marigold), *Panicum dichotomum florum* (Fall panic grass), *Salix nigra* (black willow), *Acernegundo* (box elder), *Triadiaca sebifera* (chinese tallow tree), *Cynodon dactylon* (bermuda grass), *Vigna luteola* (hairypod cowpea), *Sesbania macrocarpa* (yellow bladderpod), *Celtis laevigata* (sugarberry), *Morus rubra* (red mulberry)
3	29.81° N	-89.94° W	*Alternanthera philoxeroides* (alligator weed), *Sacciolepus* (glenwood grass), *Polyganum* (knotweed), *Vigna luteola* (hairypod cowpea), *Salix nigra* (black willow) Hurricane built piles of organic matter
4	29.81° N	-89.94° W	*Panicum dichotomum florum* (fall panic grass), *Salix nigra* (black willow), *Baccharis halimifolia* (eastern baccharis), *Sesbania macrocarpa* (yellow bladderpod), *Sesbania drummondii* (rattlebush)
5	29.80° N	-89.95° W	*Panicum dichotomum florum* (fall panic grass), *Baccharis halimifolia* (eastern baccharis), *Salix nigra* (black willow), *Sesbania macrocarpa* (yellow bladderpod), *Ludwigia leptocarpa* (anglestem primrose-willow), *Vigna luteola* (hairypod cowpea), *Eichhornia crassipes* (water hyacinth), *Triadiaca sebifera* (chinese tallow tree), *Melia azedarach* (china berry tree), *Celtis lavigata* (sugarberry)
6	29.80° N	-89.95° W	*Panicum dichotomum florum* (Fall panic grass), young *Salix nigra* (Black willow), *Sesbania macrocarpa* (Yellow bladderpod)
7	29.80° N	-89.95° W	*Panicum dichotomum florum* (fall panic grass), *Baccharis halimifolia* (eastern baccharis), young *Salix nigra* (black willow) Table cont.

8	29.76° N	-89.95° W	*Celtis lavigata* (sugarberry), *Baccharis halimifolia* (eastern baccharis), *Triadiaca sebifera* (chinese tallow tree)
9	29.76° N	-89.90° W	*Panicum dichotomum florum* (fall panic grass)

Figure 3.9 (a) aerial photograph of the Breton Sound Estuary (b) aerial photograph of the Mozambique Point in Breton Sound Estuary, which is the southernmost tip of the diversion (c) and (d) aerial photographs of the flooded and fragmented marshes in the Breton Sound Estuary

3.1.3. Water Level Analysis

Water level data were analysed for four stations in the Breton Sound Estuary region. These data were mainly studied to assess the possibility of false positives in the fluctuations of land area changes that could be due to the fluctuations in water level (Morton et al, 2005). The water level digital data were on different time scales ranging from once every 6 minutes to hourly data. For

example, the Caernarvon Outfall station had data for every 15 minutes, Reggio Canal was hourly, Gardene was every 6 minutes for some years and hourly for the rest, Snake Island had data every thirty minutes. The daily means were calculated for each of the water level stations from 1997 to 2011 since every station had a different time interval. Figure 3.10 depicts the time series of daily mean of water levels from the four stations in meters. One meter was added to all the measurements, as some of the values were negative.

Figure 3.10 (a) is the daily mean plot for Caernarvon Outfall station. Note the water level peaks during Hurricanes Lili and Ivan (Figure 3.11 a). These water level peaks are not "real maximum" high water levels, as the stations were not functioning at the time of the storm leading to a gap in the time series. Therefore, the water level peaks identified are the highest water level attained before the station stopped functioning.

During the passage of Hurricane Katrina all the stations stopped functioning, thus there is a gap of ten days in the data during that period. In the case of Hurricane Gustav, the stations Caernarvon, Gardene, and Snake Island had a loss of data for ten days. Hurricane Gustav did not affect the Reggio Canal. Figure 3.10 (b) is the daily mean for Reggio Canal, which is geographically close to the previous station (Figure 2.1). The water level peaks for Hurricanes Lili, Ivan and Katrina were noticeable. The daily means at the Gardene station clearly indicates the high water levels during Hurricanes Lili, Ivan, Katrina and Gustav (Figure 3.10 c). Similarly, Figure 3.10 d is the daily mean for Snake Island station depicting the high water levels during all the four hurricanes.

Plots were generated for individual hurricanes to assess the high water level events with the water level for the respective time intervals (from every 6 minutes to every hour). For Hurricane Lili, plots were generated from October 1, 2002 to October 3, 2002. In case of

Hurricane Katrina, water levels were plotted from August 27 to August 29 2005, after which there was no data in all the stations. Hurricane Gustav was plotted from August 31 to September 2, 2008. Adding 1m adjusted the water levels so that there are no negative values.

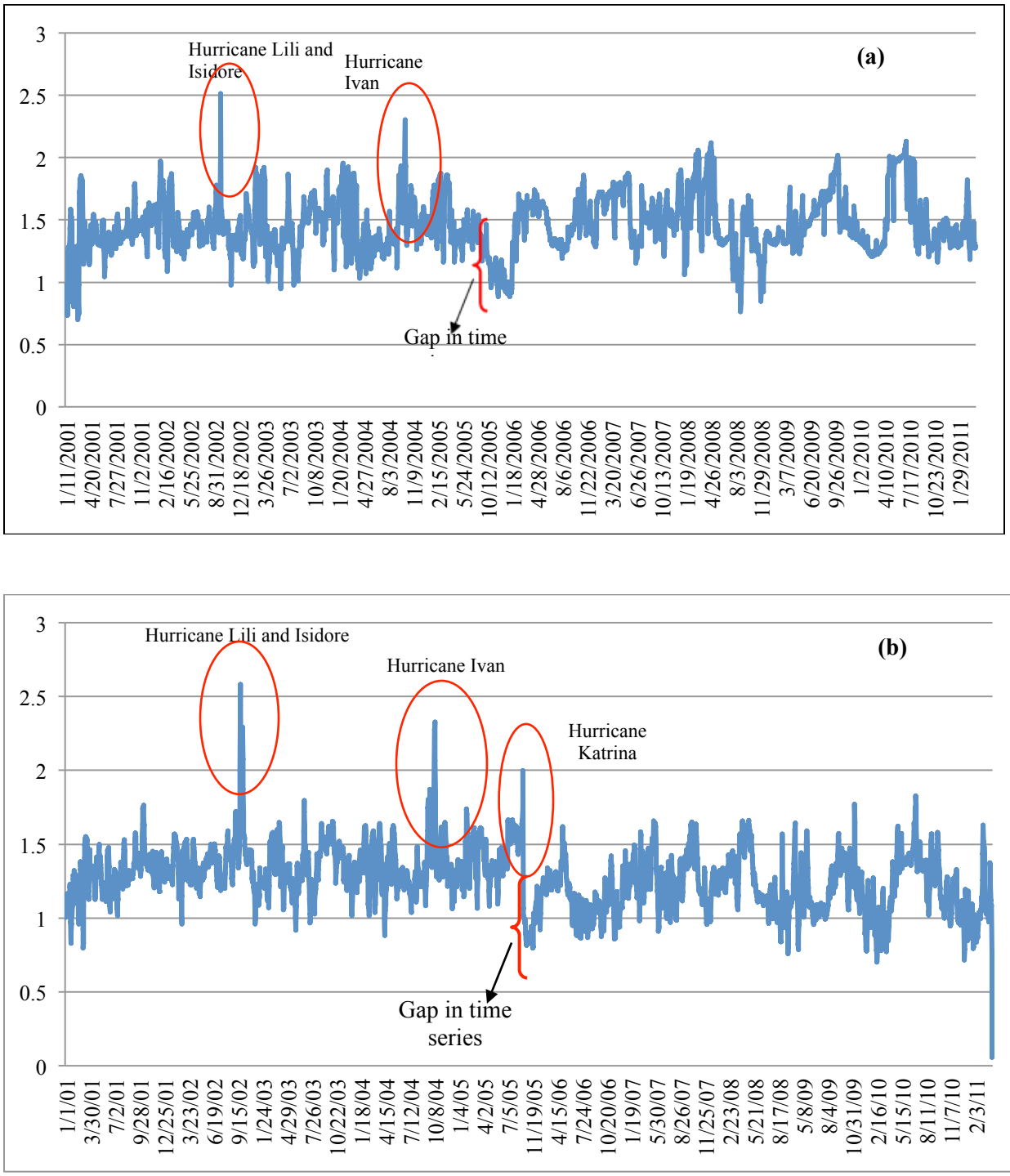

Figure 3.10 Water levels as daily mean in meters from 2001 to 2011 for (a) Caernarvon Outfall (b) Reggio Canal stations (locations are shown in Figure 1.1)

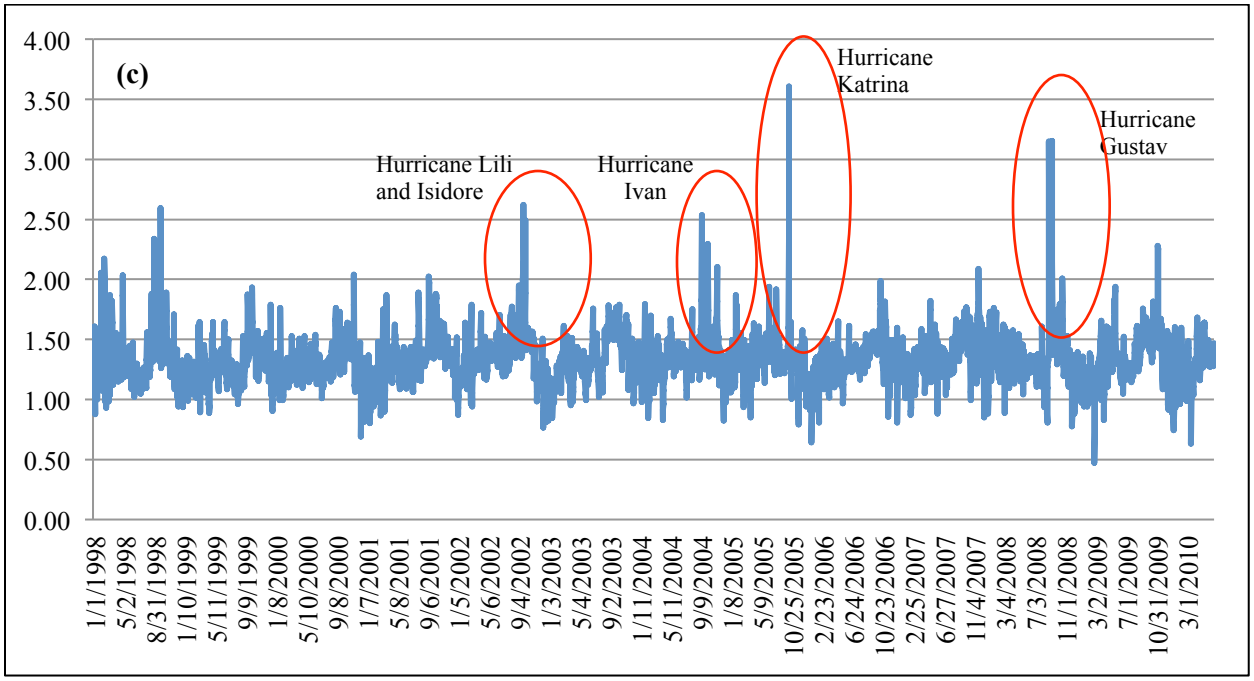

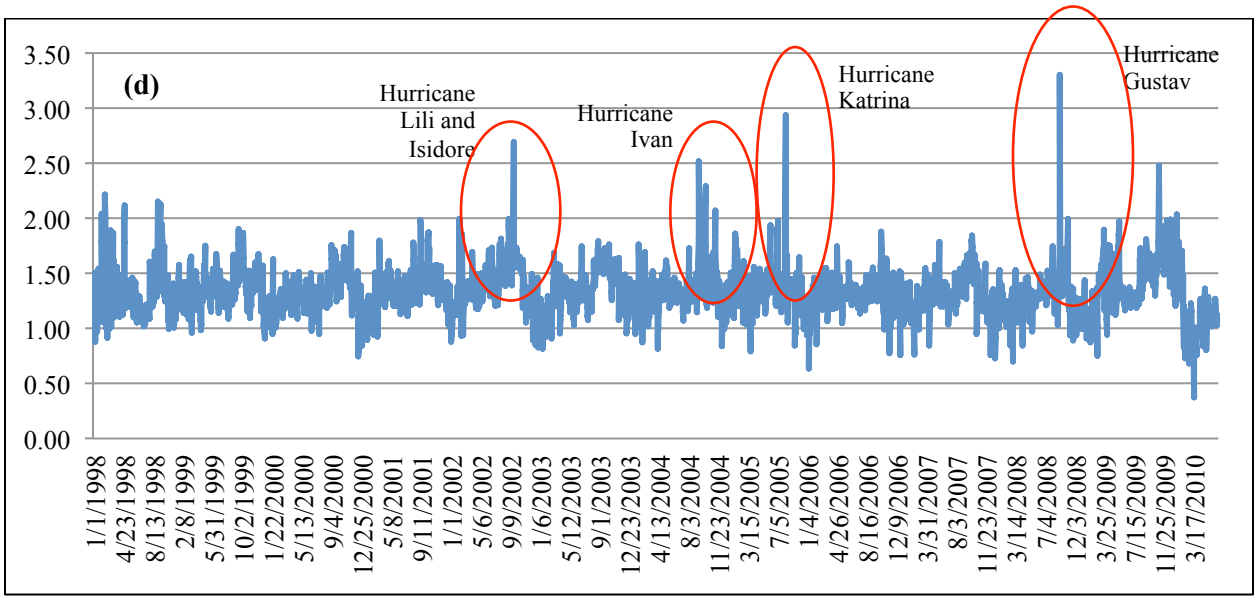

Figure 3.10 Water levels as daily mean in meters from 1998 to 2010 for (c) Gardene (d) Snake Island stations (locations are shown in Figure 1.1)

3.1.4. Regression Analysis

A regression analysis was performed to assess the relationship between the land area changes and the water level changes with land area as the dependent 'y' variable and water level as the independent 'x' variable. This was performed for all the water level stations.

Null Hypothesis:

The null hypothesis states that the slope is equal to zero indicating that there is no significant relationship between the independent and the dependant variable.

$$H_0: B_1 = 0$$

Alternate Hypothesis:

Slope is not equal to zero indicating that there is a significant relationship between the independent and the dependant variable.

$$H_0: B_1 \neq 0$$

Figure 3.11 shows water levels at the Caernarvon Outfall station and the land areas for all images. The regression analysis resulted in a *p value* of 0.52, which is greater than the confidence interval of 0.05. Thus, we fail to reject the null hypothesis and the slope is equal to zero. Therefore, the x and the y variables are not linearly related. The correlation analysis resulted in a correlation coefficient of 7%.

The regression analysis of the water level from Gardene station with the land areas in Breton Sound Estuary resulted in a *p value* of 0.25, which is greater than the confidence interval of 0.05 therefore, we fail to reject the null hypothesis and the slope is equal to zero. The water levels and the land areas are not linearly related (Figure 3.12). The correlation coefficient resulted in a value of 15%.

The regression analysis for the Reggio Canal station (Figure 3.13) resulted in a *p value* of 0.69, which is greater than the confidence interval of 0.05. Therefore, we fail to reject the null hypothesis and infer that the water level fluctuations from Reggio Canal are not linearly related to the land area changes. The correlation coefficient was 2%.

The regression analysis for the Snake Island station (Figure 3.14) resulted in a *p value* of 0.88, which is greater than the confidence interval of 0.05. Therefore, we fail to reject the null hypothesis and infer that the water level fluctuations from Snake Island are not linearly related to the land area changes. The correlation coefficient was 0.1%.

3.1.5. Tasseled Cap Analysis

Tasseled cap is similar a principal component analysis, which accumulates the information from the 6 Landsat bands into three bands (Vorovencii, 2007). Figure 3.15 indicates the tasseled cap analysis results for the 2004 and 2005 images depicting the changes due to Hurricane Katrina. The grey to white tones indicate higher values and darker tones indicate lower values in the three bands. The greenness band is the indicator for presence of vegetation and health. Similarly, the brightness band depicts the presence of base dryness. The wetness band is the indicator of water content.

The brightness band is a clear indicator for the presence or absence of vegetation from the 2004 and 2005 images respectively (Figure 3.15). Figure 3.16 is the RGB composite with the brightness, greenness and wetness bands of the TCAP analysis. The composite clearly indicates the regions of damaged marsh in the 2005 image after passage of Hurricanes Katrina and Rita. Healthy marsh was found to have a bright yellow color where as damaged marsh was orange and darker in color. Bright red colors in both the images are clouds and blue indicates water areas.

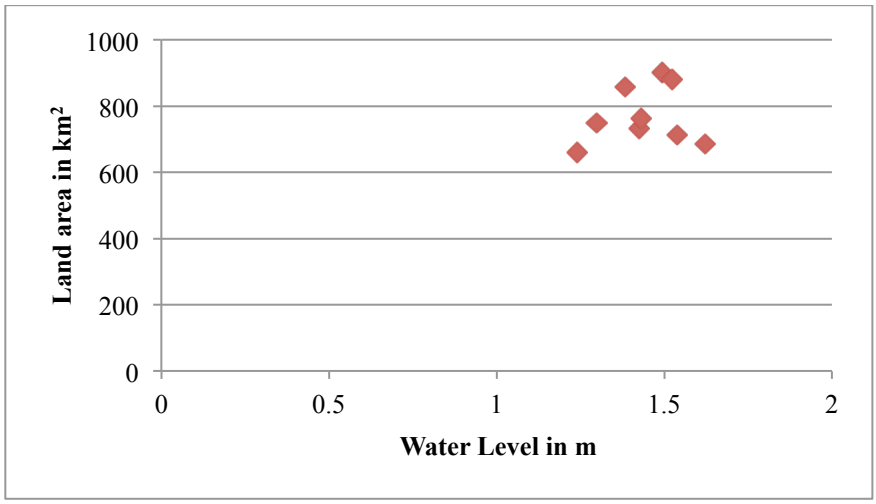

Figure 3.11 Water levels vs. Land Area for Caernarvon Outfall Station

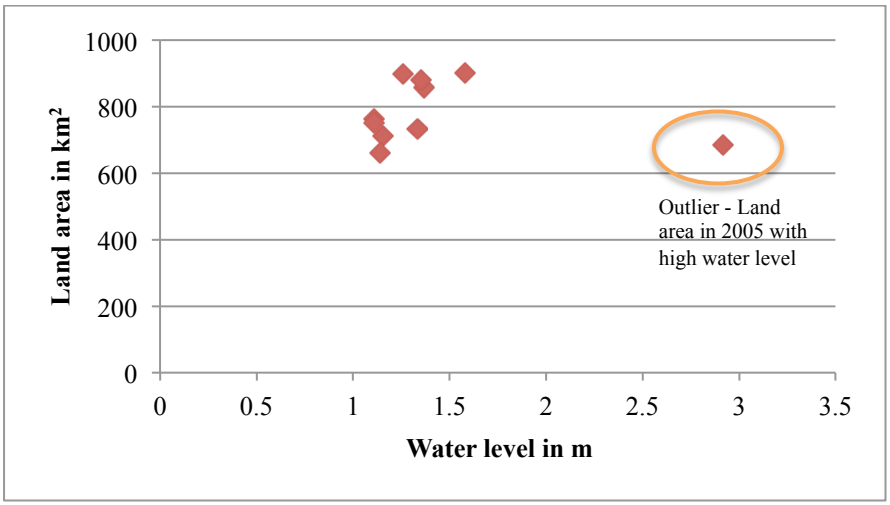

Figure 3.12 Water levels vs. Land Area graph for Gardene Station

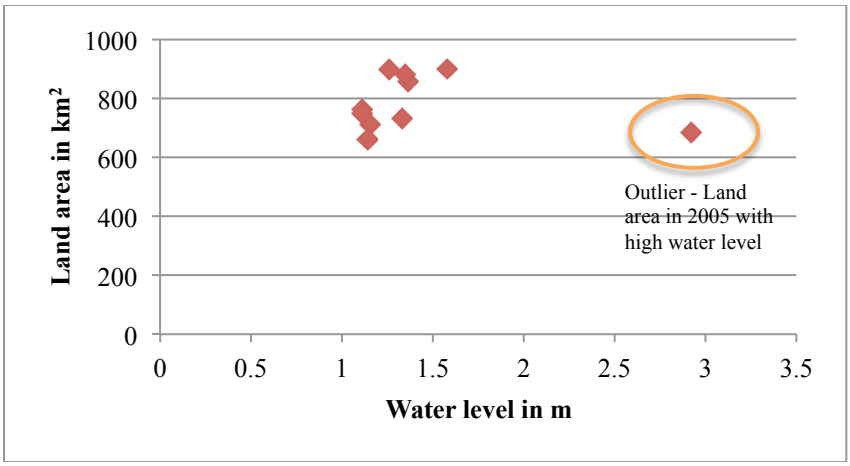

Figure 3.13 Water levels vs. Land Area graph for Reggio Canal Station

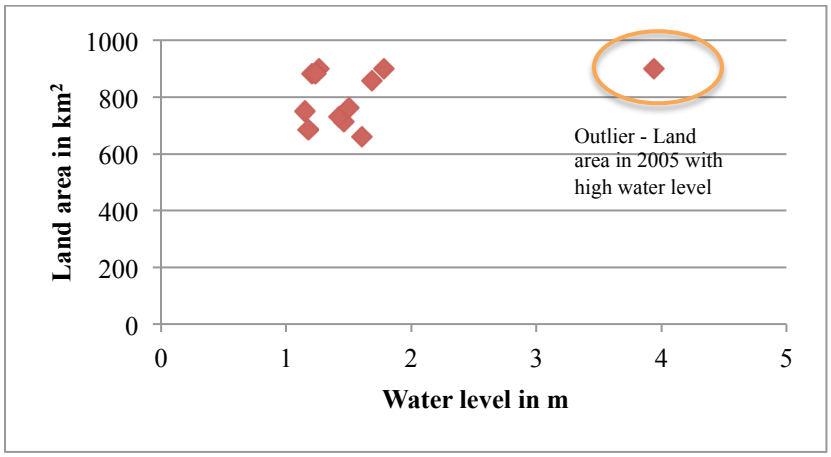

Figure 3.14 Water levels vs. Land Area graph for Snake Island Station

Change detection between the two brightness bands indicates the areas that were most affected by the hurricane (Figure 3.17). This is a valuable tool to visualize the areas of change. The result from the Change Vector Analysis (CVA) indicates the areas of maximum change, which can be used to identify persistent change over a period of time (Figure 3.18). However, the change direction cannot be identified using this technique.

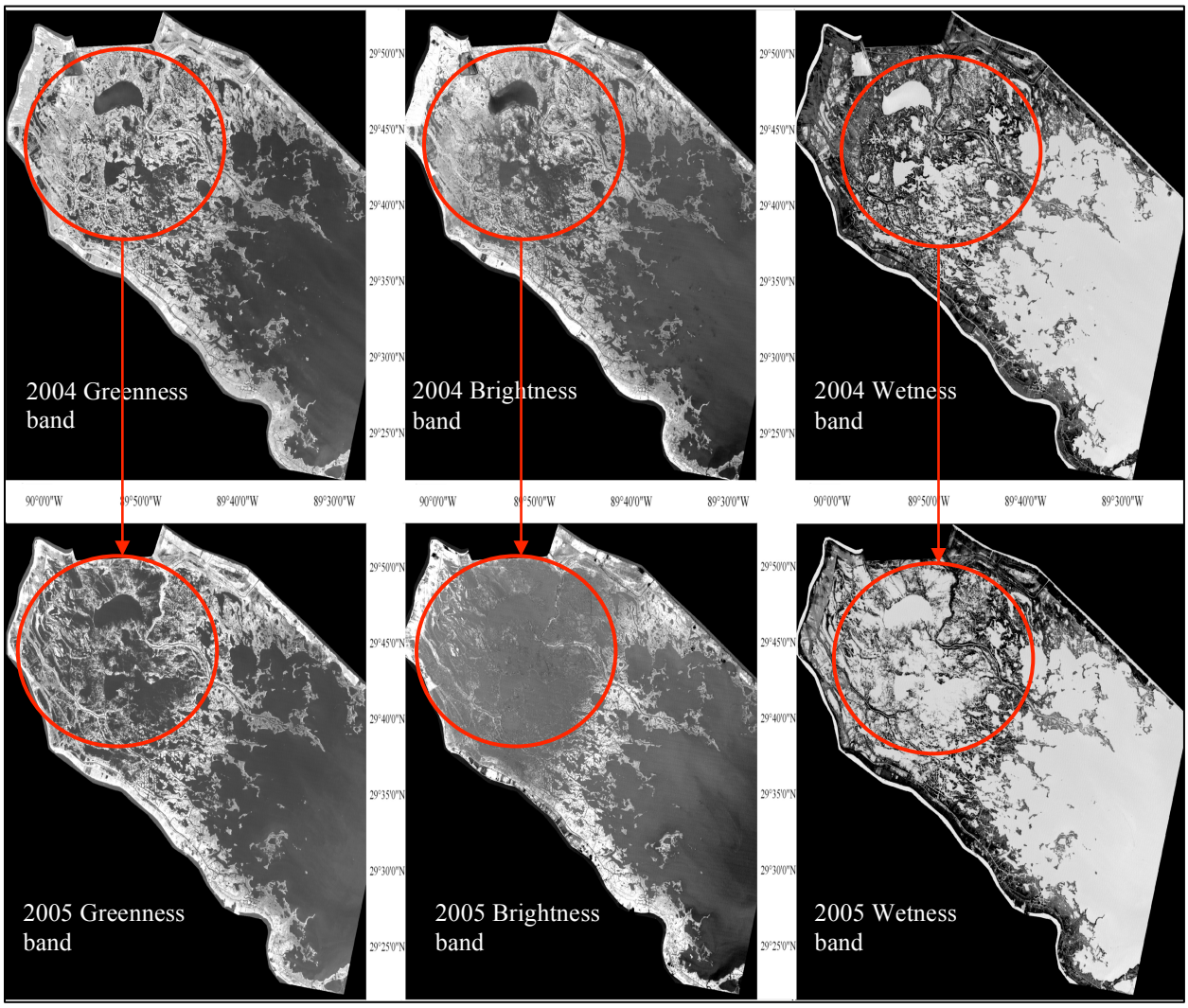

Figure 3.15 Tasseled cap Analysis image results with Greenness, Brightness and Wetness for Breton Sound Estuary Images 11/07/2004 and 10/09/2005 where the bright shades of grey indicate high values of greenness, brightness and wetness while darker shades of grey indicate low values or absence of features such as vegetation or water

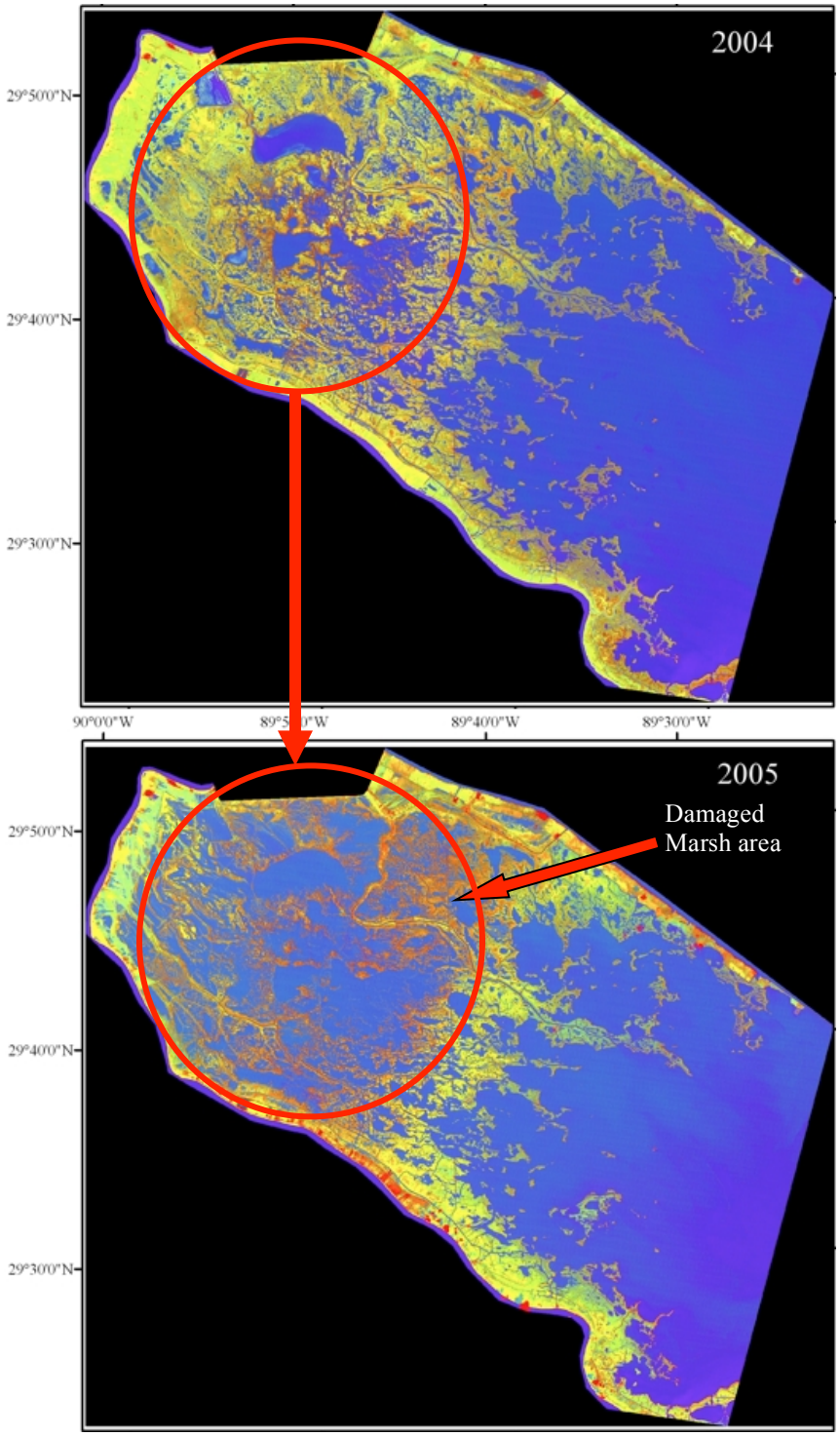

Figure 3.16 RGB composite of the three bands of TCAP analysis for 11/07/2004 and 10/09/2005 indicating the region of destroyed/damaged marsh after Hurricanes Katrina and Rita

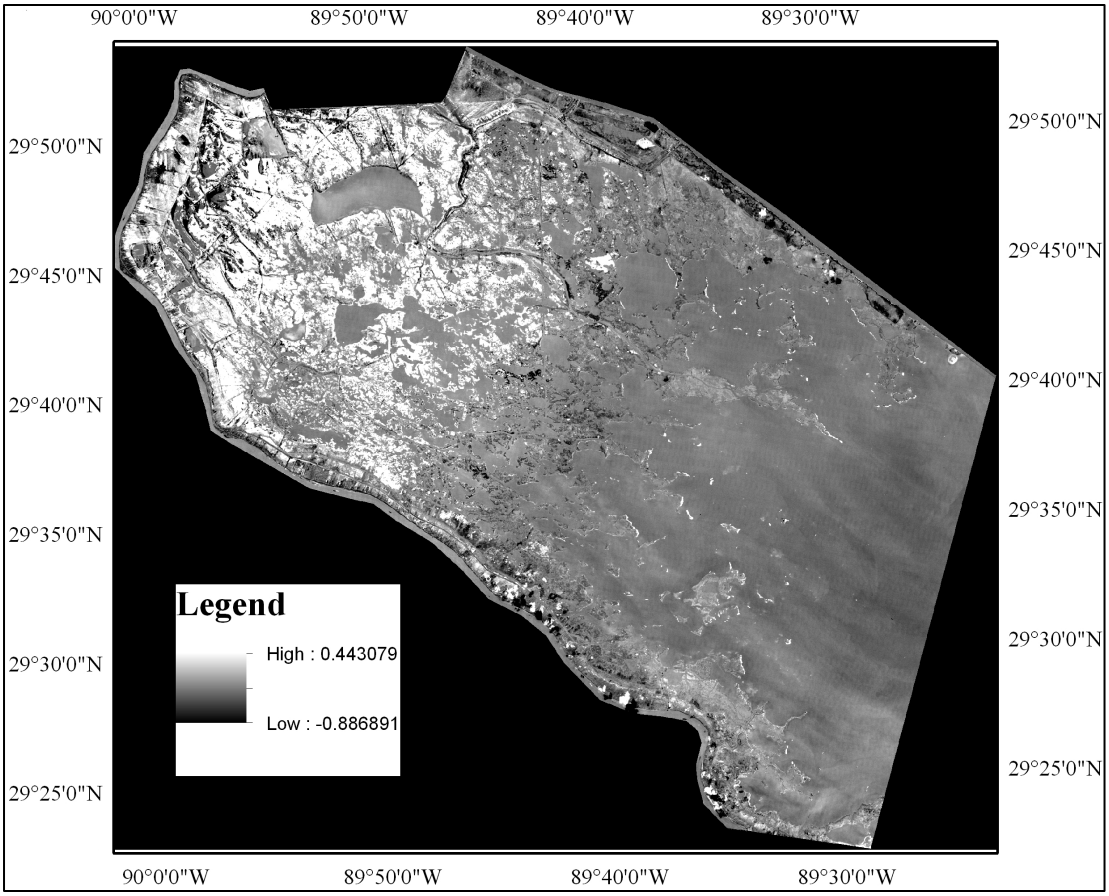

Figure 3.17 Tasseled cap change detection for Breton Sound Estuary between the brightness bands of 11/07/2004 and 10/09/2005 Images

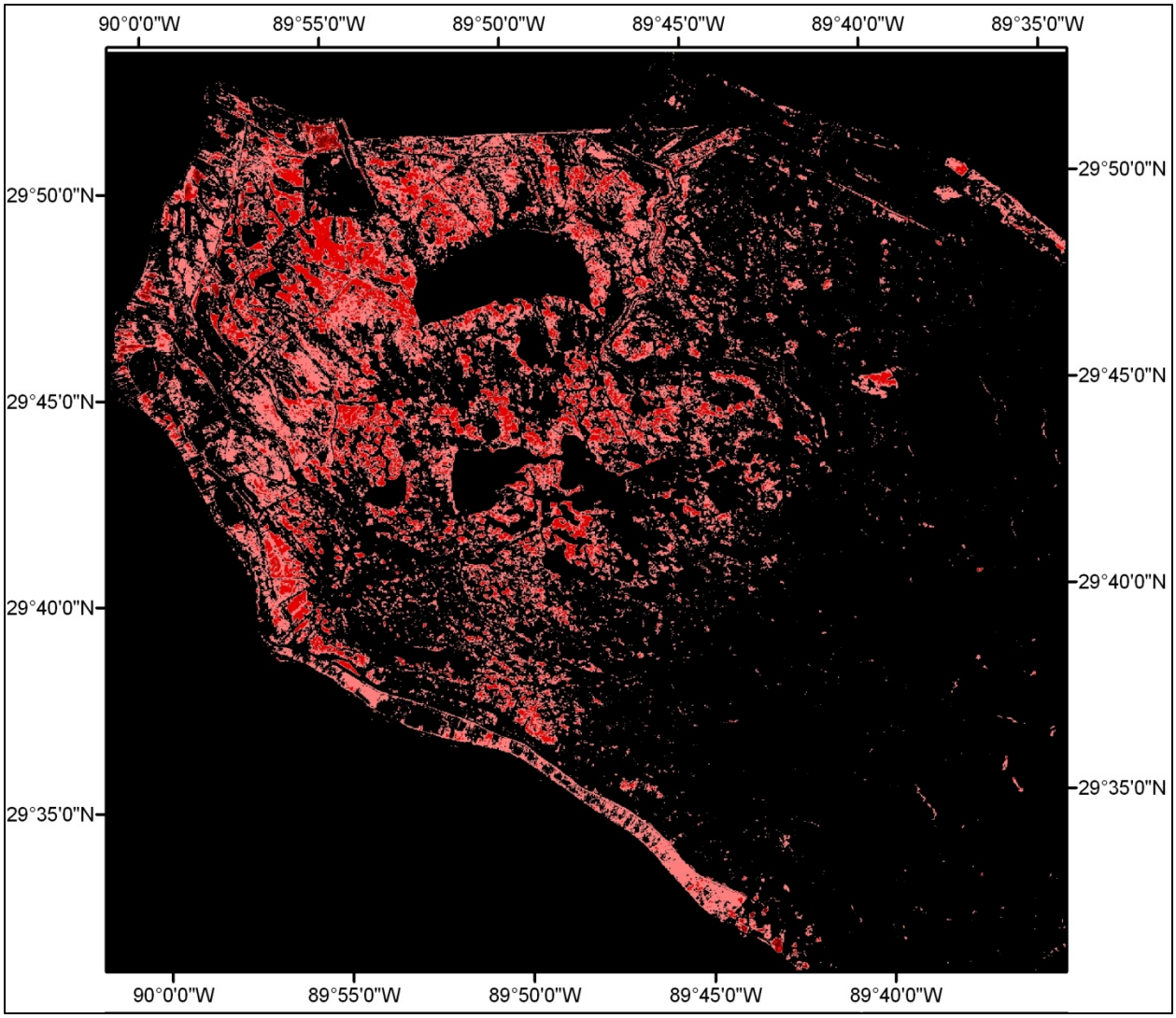

Figure 3.18 Maximum change areas detected using Change Vector analysis where the red color indicates areas of maximum change, darker red indicate greater change magnitude

3.2. Chandeleur Islands

All 13 images from 1997 to 2011 were classified using the Hybrid technique. In this classification the blue, cyan, red and brown colors represent water, beach, vegetation and mudflat, respectively (Figure 3.19). The results from the classification of the area into land and water over a period of thirteen years indicate that the maximum land loss occurred from Hurricane Georges in 1998 when a total of 41 km^2 (72%) land was lost (Figure 3.20). From 1998 to 2003 a period of land gain was identified amounting to 9 km^2. Hurricane Ivan hit these islands in 2004 and caused a land loss of 7 km^2. Hurricane Katrina in 2005 greatly impacted these islands reducing it to nothing but shoals and destroying the lighthouse in the northernmost tip of the islands. It caused a land loss of 12 km^2. By 2006, there was no change in the land area.

Hurricane Gustav in 2008 resulted in further land loss of 3 km^2 (50% of the remaining area). Immediately after the passage of Hurricane Gustav, the islands became almost non-existent due to erosion and this situation persisted through 2009. Some land gain was identified in February 2010, which further increased to a total of 6 km^2 by December 2010. This increase in land area was not due to natural processes but rather due to artificial beach nourishment by a combined measure of United States Wildlife and Fisheries services and British Petroleum (USWF, personal contact). The land that was gained towards the end of 2010 was found to decrease in June 2011(most recent image) by 50%. This decrease in land area may be attributable to the Mississippi River floods, which caused unusually high water levels.

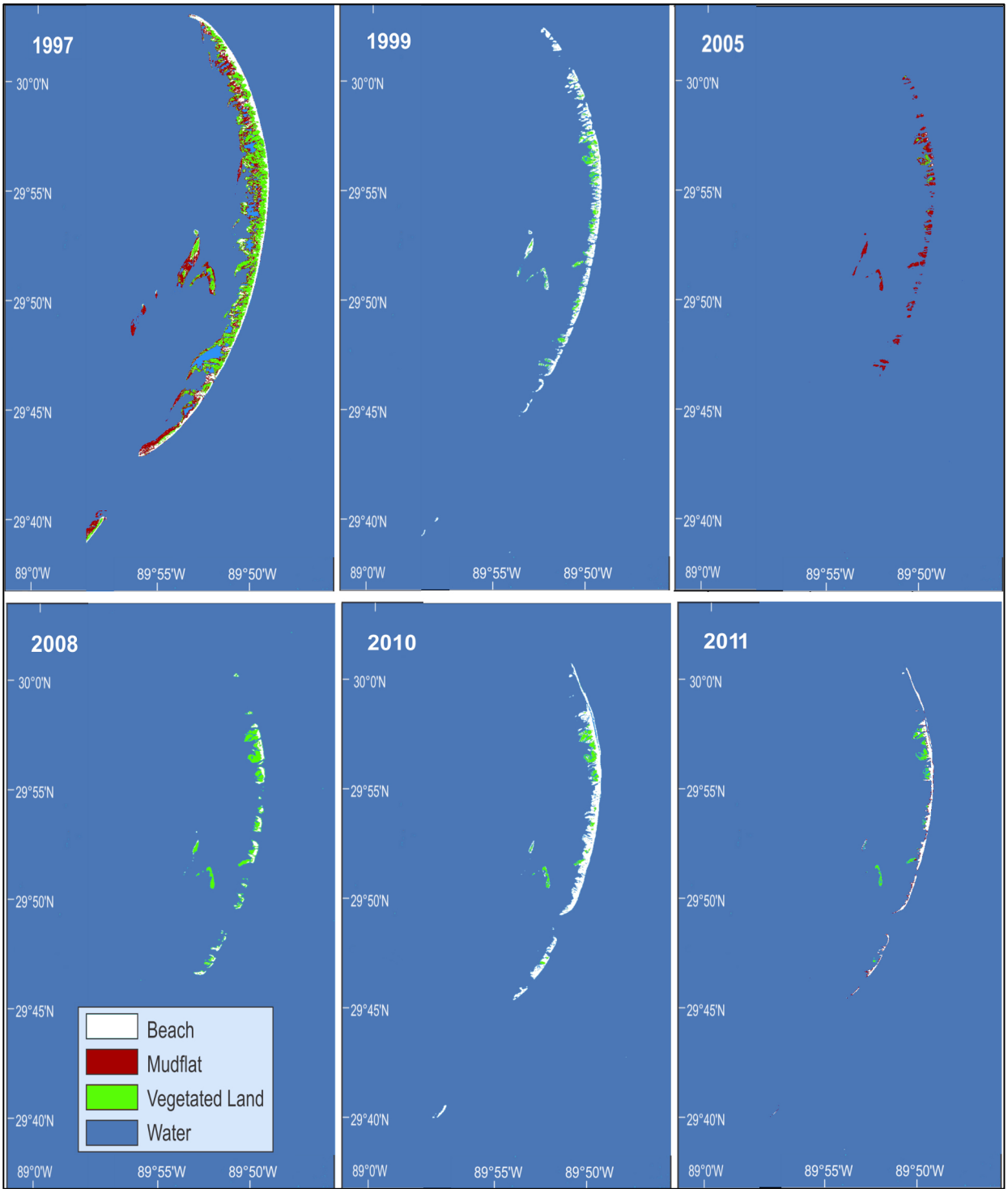

Figure 3.19 Classification outputs for Chandeleur Islands

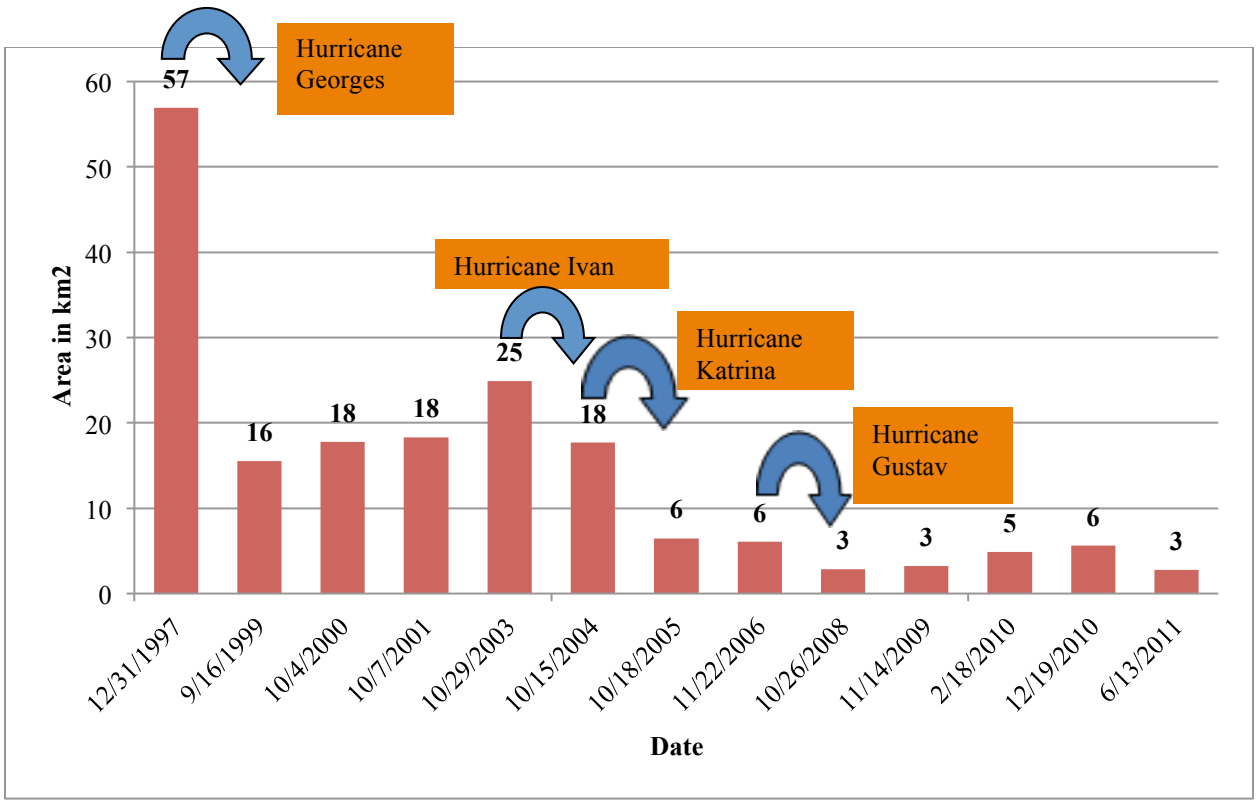

Figure 3.20 Land Area Changes in Chandeleur Islands from 1997 to 2011

The southern Chandeleur islands were more affected than the northern islands. Previous studies have shown that after the passage of every storm in the past century, these islands have been greatly affected and reduced in size (Kahn 1980, Stone et al 2004, Miner et al 2009, and Fearnly et al 2009). The image analysis demonstrated significant land gain after Hurricane Georges in 1998 until Hurricane Ivan in 2004. Land loss after Hurricane Ivan was increased by Hurricanes Katrina in 2005 and Gustav in 2008, during which time no land gain was documented. The recovery that has taken place ever since is negligible. Even though there have been no major hurricanes since 2009, the islands have regained very little land area.

Figure 3.21 Aerial photography of the Chandeleur Islands during field trip on June 04, 2011 (a) northern section of the islands (b) southern section of the islands (c) central islands (d) vegetated portion of the Chandeleur Islands

The loss of beach (Figure 3.22) and vegetated area (Figure 3.23) follows the same pattern as the total land area changes (Figure 3.20). Based on our classification results there was a drastic decrease in beach area after Hurricane Gustav by 10 km^2, whereas the maximum decrease in vegetated area was after Hurricane Georges by 19 km^2. Hurricane Katrina in 2005 further reduced the vegetated area by 7 km^2. There was no significant recovery in the vegetated area subsequently. The beach area increase in December 2010 was not due to natural growth (Figure 3.23). The field trip to Chandeleur Islands revealed that land gain in 2010 was due to artificial beach nourishment and building of artificial berms on the seaward side to prevent oiling of the coast from Deepwater Horizon oil spill in April-July 2010.

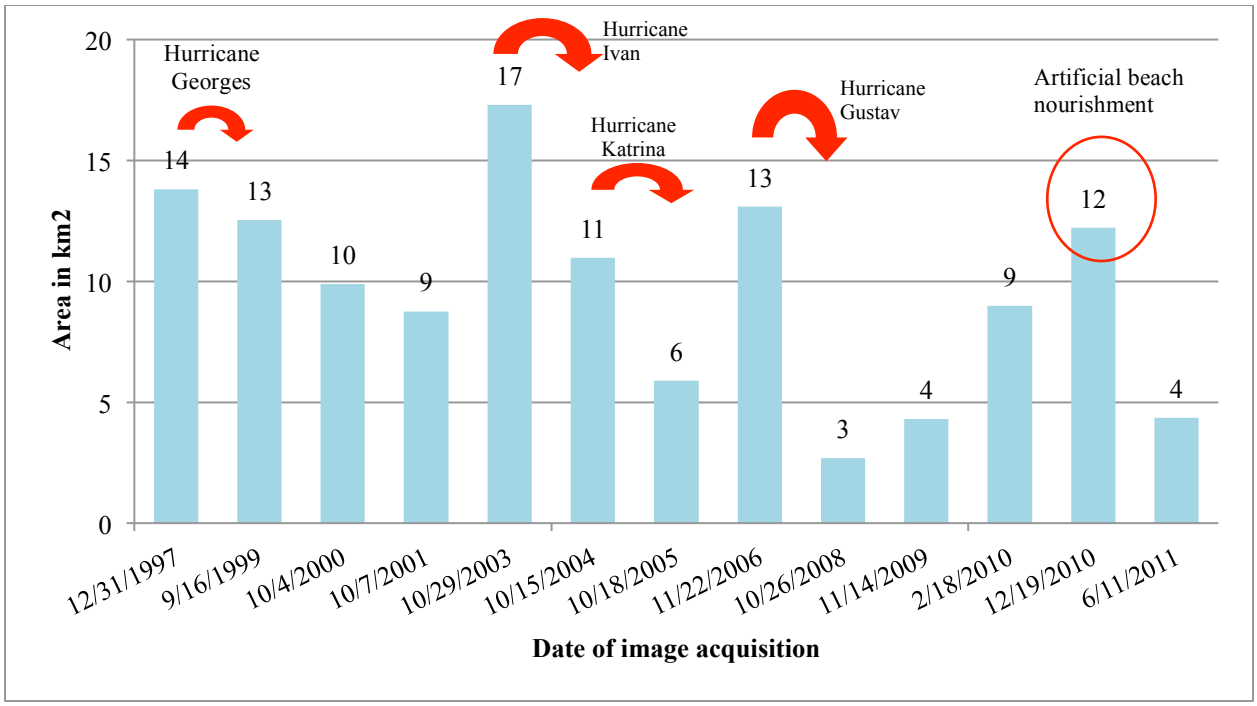

Figure 3.22 Beach area changes in Chandeleur Islands from 1997 to 2011

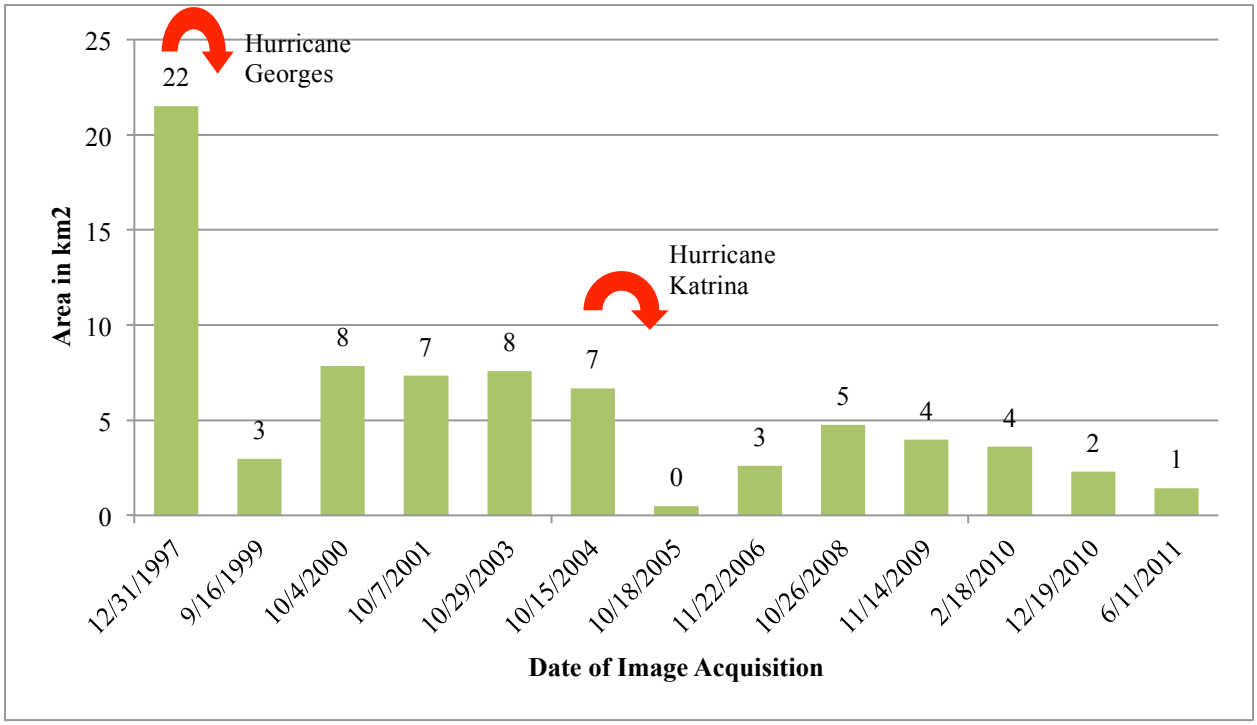

Figure 3.23 Vegetated area changes in Chandeleur Islands from 1997 to 2011

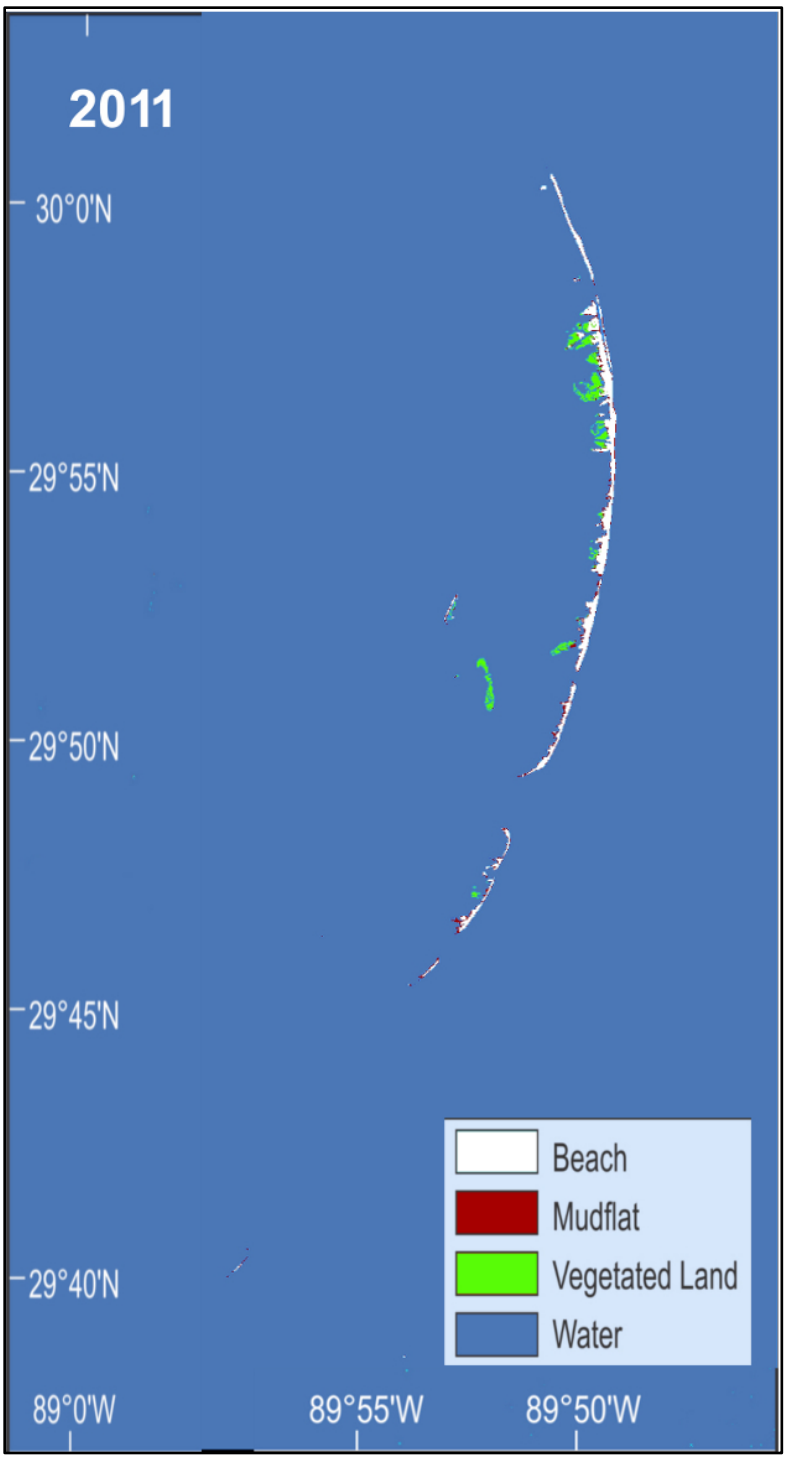

Figure 3.24 Classification image for 06-13-2011, which is the most recent condition of the Chandeleur Islands

3.2.1. Change Detection

The change detection analysis was an effective tool in identifying the changes that occurred after the passage of each hurricane. In Figure 3.25, the grey color indicates unchanged land area, blue indicates regions that were unchanged water areas, red indicates regions that were new water areas inundated by water and yellow indicates the regions with land gain. This analysis showed quantitatively the land loss that occurred after each hurricane event. Based on the results shown in Figure 3.26, Hurricane Georges had the maximum impact on these islands causing the greatest land to water conversion of about 42 km^2. The land loss caused by the other hurricanes added to the erosion from Hurricane Georges to a great extent reducing the islands to shoals. Figure 3.27 represents the long-term change detection from 1997 to 2010 indicating land area lost in red. There was no significant land gain seen in the southern Chandeleur Islands over the time series. Any water to land conversion noticed was confined to the northern portions (Figure 3.25).

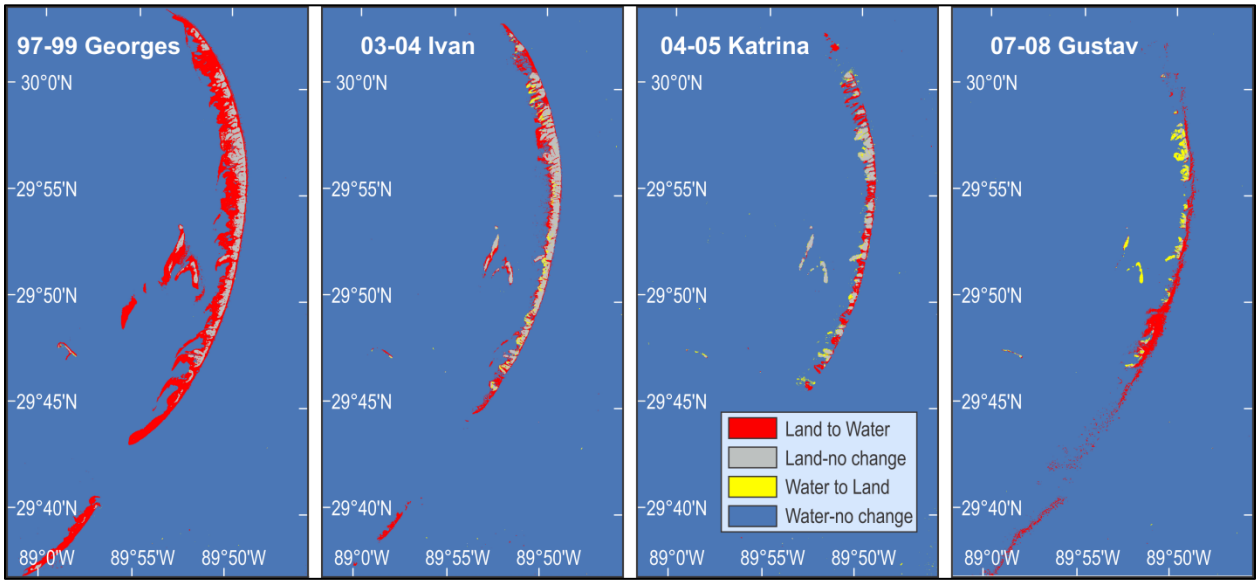

Figure 3.25 Change detection analysis for the Chandeleur Islands for major hurricane years before and after Hurricanes Georges, Ivan, Katrina and Gustav

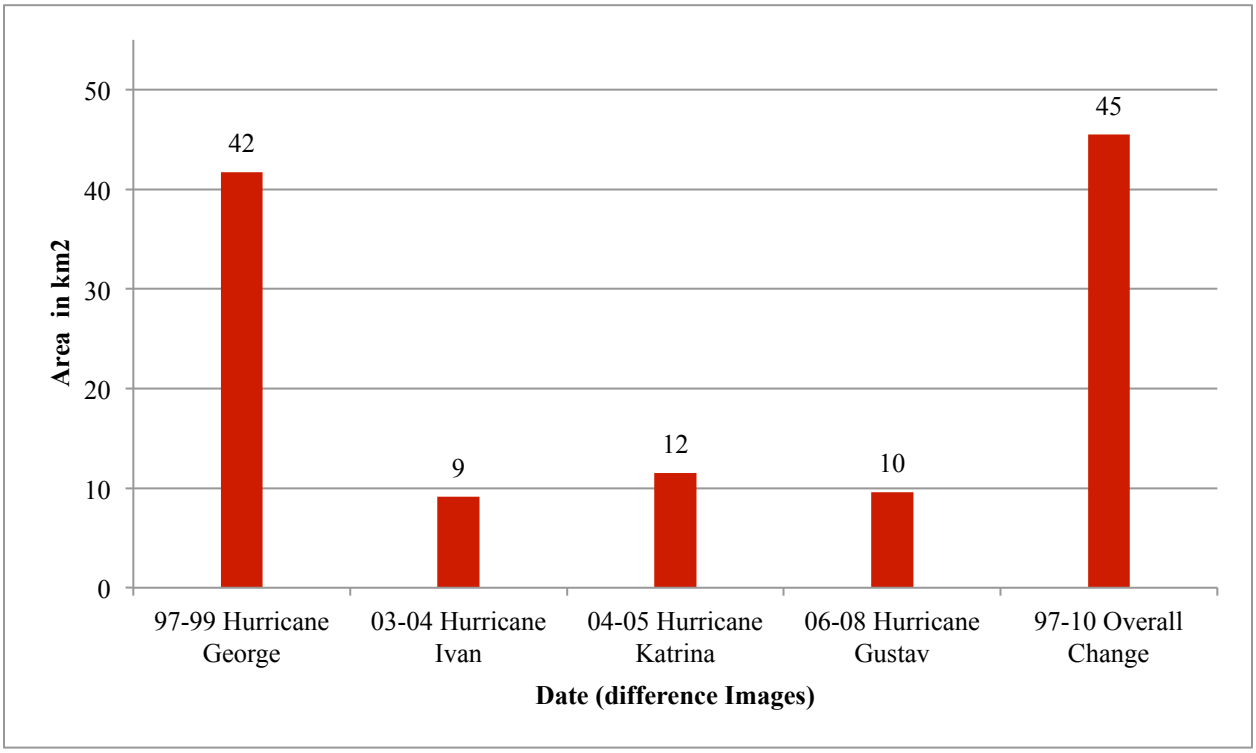

Figure 3.26 Land area converted to water in Chandeleur Islands

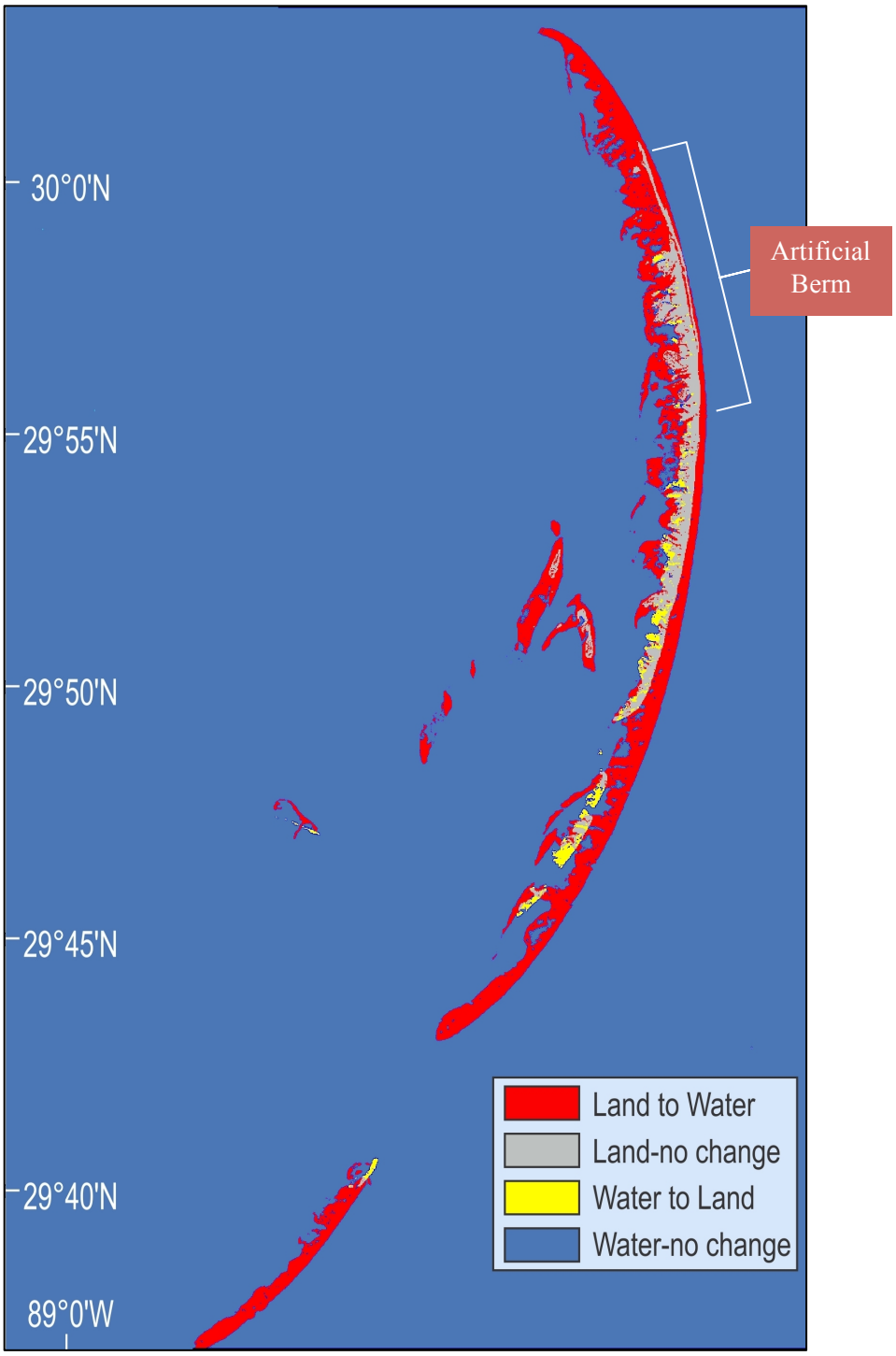

Figure 3.27 Long term change detection analysis for Chandeleur Islands from 1997 to 2010 indicating land area lost (red), unchanged land areas (grey) and land gain (yellow)

3.2.2. Field Trip to Chandeleur Islands on June 04, 2011

Figure 3.29 shows the aerial view of the Chandeleur Islands taken from a seaplane on June 04, 2011. The most important aspect of the field visit was that we were able to observe the artificial berm that was built on the east side of the northern islands to keep the oil from Deepwater Horizon oil spill from contaminating the islands. We found out from the USWF personnel that the berm was 9 miles long extending from the northern section to the southern section. The berm was built using sand that was dredged from offshore. Tropical storm Lee in 2011 greatly affected this berm due to erosion (USWF, personal contact). Several types of vegetation were identified on the northern parts of the Chandeleur Islands (Figure 3.29). Access to the islands are limited and controlled by USFW due to the large number of birds nesting there. However, there was very little vegetation remaining in our analysis of the southern islands.

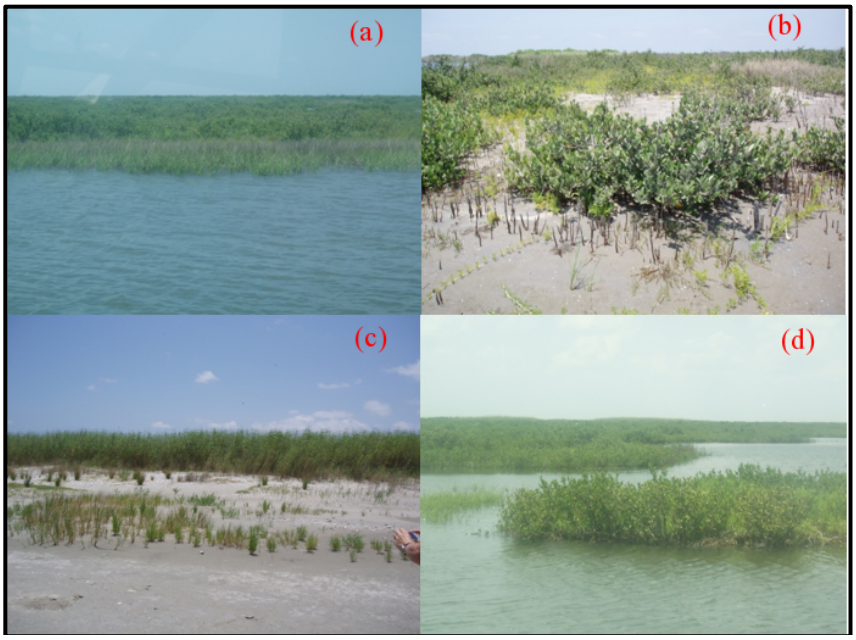

Figure 3.29 Types of vegetation in the Chandeleur Islands identified during the field trip on June 04, 2011 (a), (b) and (d) Black Mangroves (c) Phragmites

3.2.3. Regression Analysis

Based on the regression analysis between the water level from Snake Island and the land area from Chandeleur Islands the *p value* was 0.41, which is greater than the confidence interval of 0.05. Therefore, we fail to reject the null hypothesis and conclude that the slope is equal to zero, which denotes that the water level and land area were not linearly related (Figure 3.30). The correlation coefficient (R^2) value was 3% also indicating that the land area changes are entirely storm driven and not significantly affected by the water level fluctuations. Similarly, no relationship was found between land area and significant wave height (Figure 3.31). There was no correlation at an R^2 value of 0.006 with a slope of zero.

3.3. Accuracy Assessment

"Without an accuracy assessment, a classified map is just a pretty picture" (Cai et al 2011).

The accuracy assessment for the classification was performed using the Digital Orthophoto Quarter Quadrangles (DOQQ) from the Louisiana State University ATLAS website. The DOQQ were available for the years 1998, 2004, 2005 and 2010. Using the "Accuracy assessment" tool in ERDAS IMAGINE, 200 random points were generated for the classes using the "Stratified Random" method. This method of sampling ensures that all classes are represented in the accuracy assessment procedure, taking into account the proportion of the number of pixels in each class along with the total number of pixels in the image.

The output from the accuracy assessment procedure is the construction of an "error matrix" which includes the percentages of "User's accuracy", "Producer's accuracy" and "Overall classification accuracy".

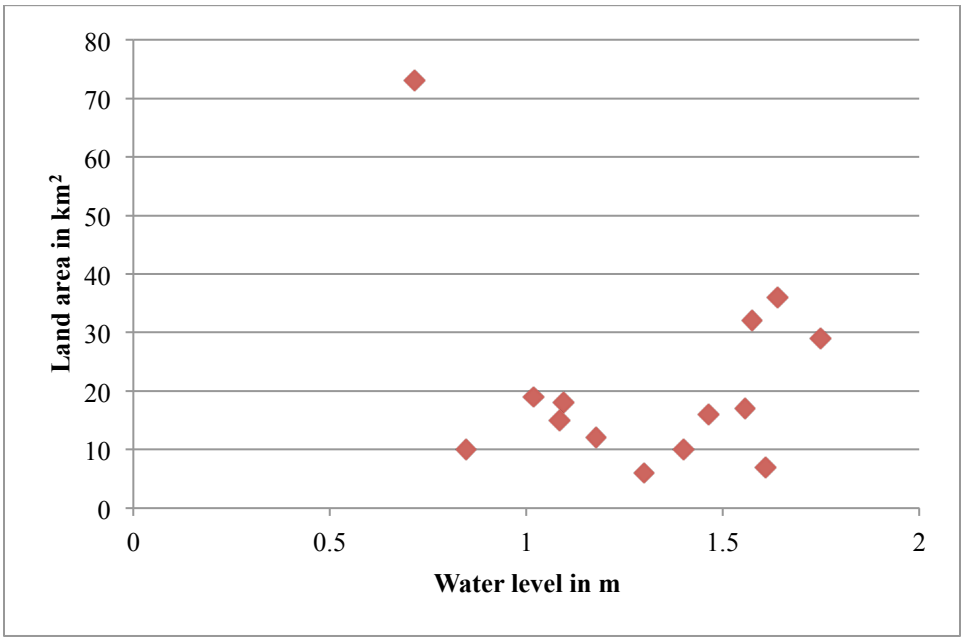

Figure 3.30 Water levels vs. land area plot for Chandeleur Islands over 14 years at the time of image acquisition

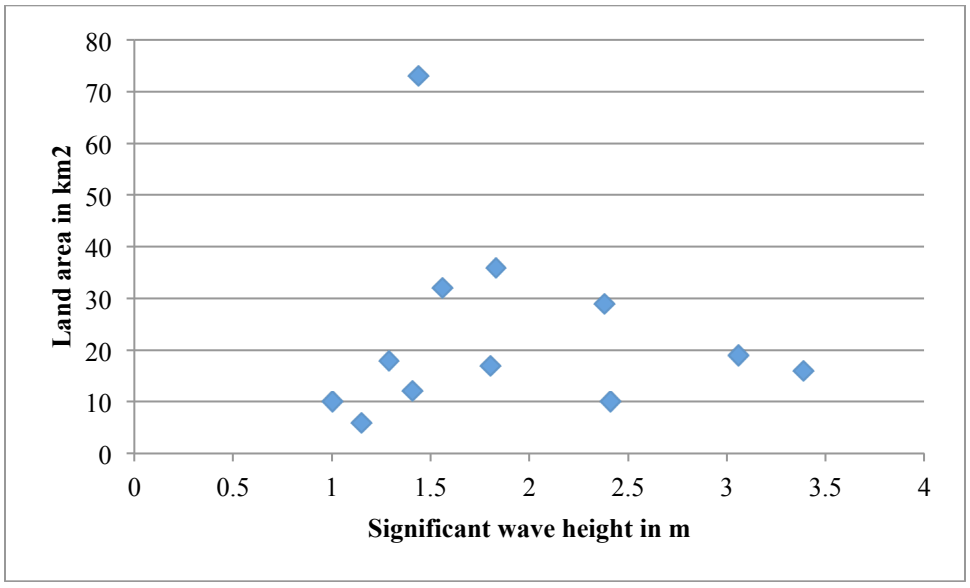

Figure 3.31 Significant wave heights vs. land area plot for Chandeleur Islands over 14 years at the time of image acquisition

User's accuracy is error due to "commission" which is the probability that pixels from a class were wrongly included in another class (e.g. 3 pixels from marsh class included erroneously in the water class). Producer's accuracy is error due to "omission" which is the probability that pixels from a class were omitted from a class, (e.g. 5 pixels were erroneously classified as forest area rather than marsh class) (Janssen and van der Wel, 1994 and Foody et al, 2002).

The User's accuracy is calculated by "dividing total number of pixels that were correctly classified in a class by total number of pixels in that class". Producer's accuracy is calculated by "dividing total number of pixels that were correctly classified in a class by the total number of training set pixels used for that class" (Lillesand and Kiefer, 1997)

3.3.1 Breton Sound Estuary

The accuracy assessment for the Breton Sound Estuary was performed using 200 stratified random points for three years 2004, 2005 and 2010. The results are tabulated in Table 3.2, Table 3.3 and Table 3.4. The overall accuracy of the classification for all the years were above 90%.

Table 3.2. Accuracy Assessment for 2004 Image Classification

Accuracy Totals - 2004		
Class Name	Producers Accuracy	Users Accuracy
Water	90.74%	99.32%
Forest	100.00%	100.00%
Marsh	98.91%	85.85%
Other Area	100.00%	80.00%
Overall Classification Accuracy = 92.68%		

Table 3.3. Accuracy Assessment for 2005 Image Classification

Accuracy Totals - 2005		
Class Name	Producers Accuracy	Users Accuracy
Water	95.00%	95.00%
Forest	66.67%	100%
Marsh	91.67%	84.62%
Other Area	100.00%	100.00%
Overall Classification Accuracy = 91.43%		

Table 3.4. Accuracy Assessment for 2010 Image Classification

Accuracy Totals - 2010		
Class Name	Producers Accuracy	Users Accuracy
Water	92.00%	95.32%
Forest	100.00%	100.00%
Marsh	98.74%	85.62%
Other Area	100.00%	100.00%
Overall Classification Accuracy = 94.35%		

3.3.2. Chandeleur Islands

The Accuracy assessment for the Chandeleur Islands also yielded an accuracy of over 90% for all the years. The accuracy assessment was performed using the DOQQ as the reference.

Table 3.5. Accuracy assessment report for Chandeleur Islands

Accuracy Totals - 2010		
Class Name	Producers Accuracy	Users Accuracy
Water	90.91%	100.00%
Vegetated land	90.91%	100%
Beach	90.00%	90.00%
Mudflat	100%	80.00%
Overall Classification Accuracy = 92.68%		

3.6. Correlation between the Land Loss in Caernarvon and Chandeleur Islands

A regression analysis was performed between the land losses in Breton Sound Estuary versus the land loss in Chandeleur Islands for the images from the same month of the same year. The y variable was the land area from Breton Sound Estuary and the x variable was the land area from the Chandeleur Islands. This resulted in a *p value* of 0.014 that is less than the confidence interval of 0.05. Therefore, we fail to reject the null hypothesis and conclude that they are linearly related. However, this statistical relationship does not imply that the land area changes in Breton Sound Estuary were affected by the land area changes in the Chandeleur Islands (Figure 3.32). The maximum land loss in Chandeleur Islands was due to Hurricane Georges in 1998 where as for Breton Sound Estuary the maximum land loss was due to Hurricane Katrina in 2005. The limited recovery for the both the study areas occurred at a different pace.

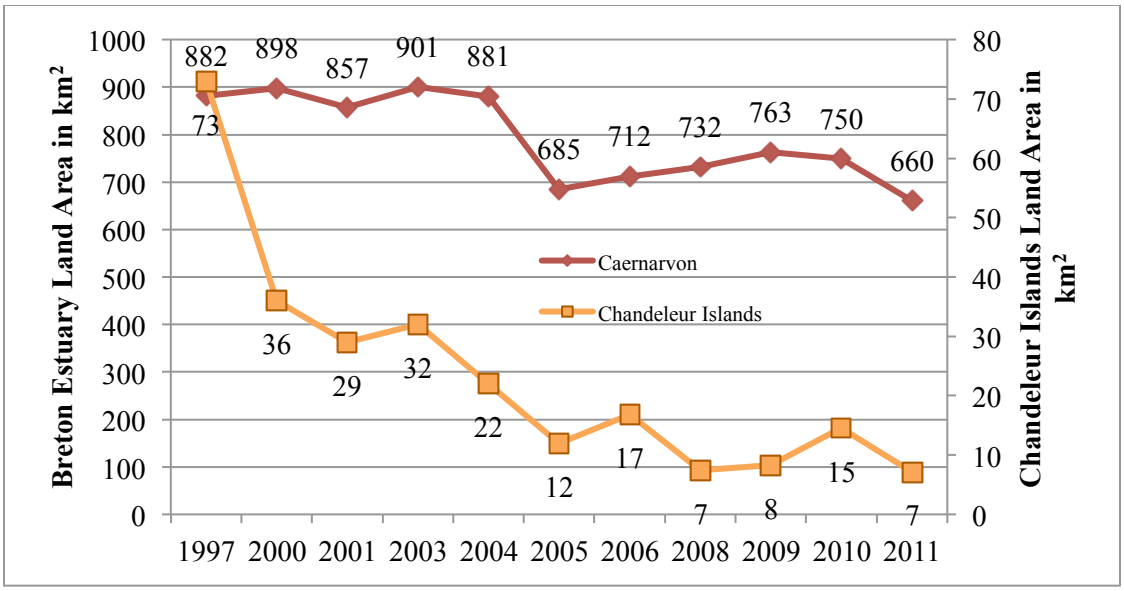

Figure 3.32 Areas of Breton Sound Estuary and Chandeleur Islands plotted on different axes to look at the changes for the same year

CHAPTER 4
DISCUSSION

4.1. Breton Sound Estuary

The Breton Sound Estuary is so spatially complex that mixed pixels were a frequent problem. The classification procedure proved to be problematic at times due to sub-pixel fragmentation, spatial resolution of the satellite data, presence of floating vegetation and mudflats. Nevertheless, by using band 5 (the middle infrared) and the band combinations 4,5,3 and 4,3,2, as a visual guide, satisfactory classification accuracy was obtained. The accuracy was checked with the DOQQ, which have a spatial resolution of 1 meter or less. The images that were chosen for this research were all cloud free and autumn imagery when vegetation is dormant and floating vegetation is minimal.

Storm surge information was necessary to understand the potential effect of the surge on land loss. The storm surge information was obtained from previous literature, based mainly on storm surge models such as the ADCIRC and observation of debris lines. Table 4.1 summarizes the storm data.

The results from the classification indicate that the land area changes in the Breton Sound Estuary can be divided into two phases i.e. before and after Hurricane Katrina in 2005 (Figure 3.3). The land area changes were almost stable until 2005 with minor fluctuations due to tropical storms. However, after Hurricane Katrina in August 2005, there was a drastic decrease in land area and the region has not been able to recover to its previous state since then. However from 2005 until 2010 there has been a measurable constant (albeit small) increase in land area.

Table 4.1 Major hurricanes and storms considered for the study (data from NOAA's National Hurricane Center, NHC)

Hurricane	Category at landfall	Track	Storm Surge at landfall / water level from water level stations
Andrew 1992	3	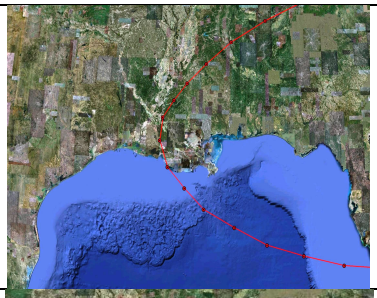	3 meters (Turner et al 2006)
Georges 1998	2	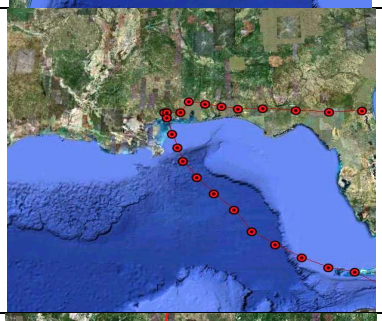	3 meters (NHC report, 1999) / 2.5 meters
Isidore 2002	Tropical Depression	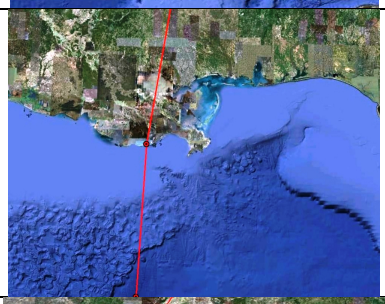	2.5 meters (NHC report, 2002) / 2.6 meters
Lili 2002	1	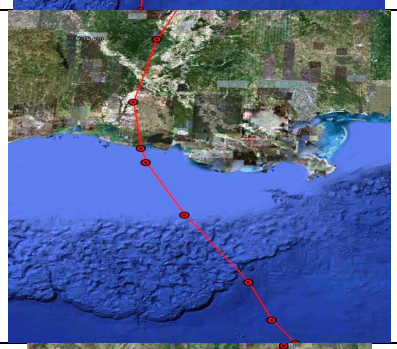	3.7 meters (NHC report, 2003) / 1.8 meters
Ivan 2004	3	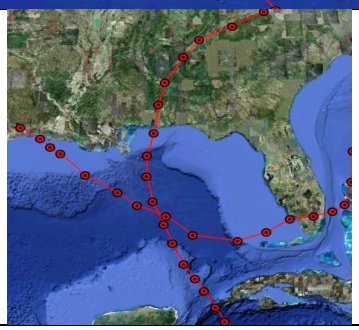	2 meters (NHC report, 2004) / 2.53 meters

Table cont.

Katrina 2005	3	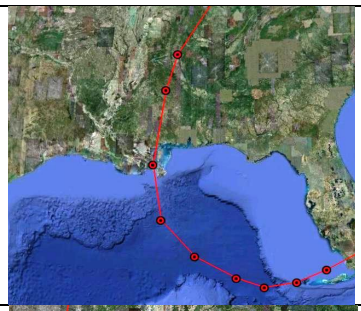	4 to 5 meters (Dietrich et al, 2009) / 4.9 meters (USACE, 2006)
Rita 2005	3	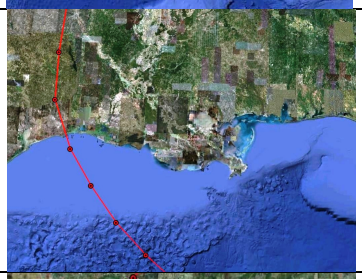	3.6 to 4 meters (NHC report, 2005)
Gustav 2008	2	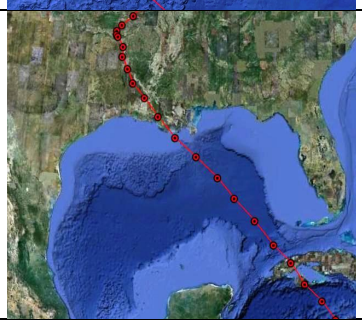	4 to 4.5 meters (Dietrich et al, 2011) / 3.9 meters (McGee et al, 2008)

Previous studies have documented significant land loss in the Breton Sound Estuary caused by the effect of hurricanes. Barras et al (2008) indicated that of the entire coastal Louisiana, the Breton Sound Estuary has suffered more than the other areas. Couvillion et al (2011) demonstrated similar results. Barras et al (2006) achieved similar results in the northern portion of the diversion where there was maximum land area to water conversion in 2005.

Turner et al (2006) indicated that Hurricanes Katrina and Rita in 2005 contributed greatly to the sedimentation of large amounts of inorganic materials in the Breton Sound Estuary region. They also suggested that hurricanes help distribute these sediments throughout the entire region, which would otherwise be concentrated at the mouth of the diversion. They concluded that hurricanes and other storm events contribute significantly to maintain the inorganic sediment

budget in a wetland system. In the course of our field observations, we observed organic marsh material in areas of new land after Hurricane Katrina.

Marsh area decreased by 94 km^2 due to the passage of Hurricane Andrew in 1992. The maximum marsh growth was detected in 2003 before Hurricane Ivan in 2004. Hurricane Katrina in 2005 caused the maximum marsh loss, which was about 173 km^2, which included all the types of marsh. The October 2005 TM image clearly indicates the health of the marsh as well. Most of the marsh area in the northern and the central portions of the diversion had a bluish appearance in the band 453 combination, which was also noticed in the Tasseled cap image of 2005 (Figure A.2). This indicates marshes that were unhealthy or dead. A loss of 92 km^2 was noticed in marsh area in the 2011 image, which could be attributed to high water during the Mississippi River flood. It is also interesting to note that the land area in 2006 increased by 27 km^2 but the marsh area decreased. This is possibly due to the rolling up of marsh debris during the storm surge (Figure 4.1). The area of unvegetated/barren land also increased in 2006. These were the regions that had no live vegetation on them but had the signature of land area, which was due to the marsh debris.

Barras (2007) estimated 562 km^2 of new water areas in coastal Louisiana after Hurricane Katrina, which was found to be the result of permanent water areas, marsh flooding and water level changes. He observed that the land gain in 2006 was due to "wrack deposition, rearrangement of existing marsh, floating vegetation misclassified and water level variations".

We were also able to identify several cases where there were burnt or recently burnt marsh in the images. However, due to lack of ground control and the relatively coarse spatial resolution of the imagery we did not classify the images into different types of marsh. During out

field trip in November 2009, we found that the majority of the marsh areas were covered with senescent fall panic grass.

Figure 4.1 Photographs of rolled up marsh debris in Breton Sound Estuary during a field trip in March 2009 (Nan Walker, personal contact)

The results obtained by Barras and others in their assessment of land area changes include the entire coast of Louisiana for Hurricanes Katrina, Rita and Gustav along with a long-term analysis. They utilized "thresholding" techniques with the infrared bands to obtain water areas. Couvillion et al, (2011) studied the status of land and water areas in coastal Louisiana from 1932 to 2010, utilized "thresholding" along with supervised and unsupervised classification for unclassified pixels, which is different from the hybrid technique used in this thesis. Fearnley et al, (2009) studied the shoreline changes of Chandeleur Islands over 100 years. They performed a vector analysis of satellite imagery, aerial photographs and topographic sheets data where this study involved raster analysis of the same type of satellite data (Landsat 5 TM). Furthermore, incorporation of Tasseled cap analysis validated the results obtained from the change detection analysis.

By obtaining the water level fluctuations for the entire time period we were able to quantify the relationships between land area changes and water level fluctuation by using the water level data at the time of image acquisition. Results from all the stations indicate that there is no linear relationship between the two. Therefore, we conclude that the land area changes observed are independent of the water level fluctuations (except in June 2011) and the changes are mainly due to the storm events. However, Hurricane Katrina was an outlier, which had high water level at the time of image acquisition that coincided with low land area.

We were able to identify the peaks in water level during some of the hurricane events. The different stations exhibited different high water level points for the hurricane events. For example, during Hurricane Katrina, the Caernarvon station showed as high a water level as the other stations before it stopped functioning. The highest water level was noticed at the Gardene station. Similarly, during Hurricane Lili, the Snake Island station showed the highest water level.

Snake Island and Gardene showed high water levels during Hurricane Gustav before they stopped working. Caernarvon station did not have that high of a water level during this hurricane. The variations in high water level points are due to the position of these stations. Gardene and Snake Island stations are at the northeastern and southeastern corners of the Diversion, respectively, closer to open gulf. Whereas the Caernarvon and Reggio stations are in the northwestern and southwestern corners respectively (Figure 2.1).

Tasseled cap analysis was an effective technique to observe the vegetation health using the greenness band. The change detection analysis using the TCAP image was performed for the year that had the maximum change in the entire time series, which was 2005. The Change Vector Analysis (CVA) proved to be a good tool for identifying the regions of maximum change and generating a mask for the pixels that did not undergo any change. Most of the change that was observed in the 2005 image analysis was identified to be land that was converted to water. This direction of change was found using a spatial intersection change detection function. These regions could be used to look for persistent change over the years. It was also noticed that regions with maximum change were in the northwestern parts of the Breton Sound Estuary close to the levee of the Mississippi River.

The results from the change detection analysis were plotted against the difference in the water levels at the time of image acquisition. Figure 4.2 indicates the comparison of water level changes from the Gardene station with land area to water conversion changes for major hurricane years. Negative values in the water level indicate higher water levels for the “after” image, for e.g. negative value in 2004-2005 indicate the water level in 2004 was lower than that of 2005. Similarly, figure 4.3 is the comparison analysis for the Snake Island station.

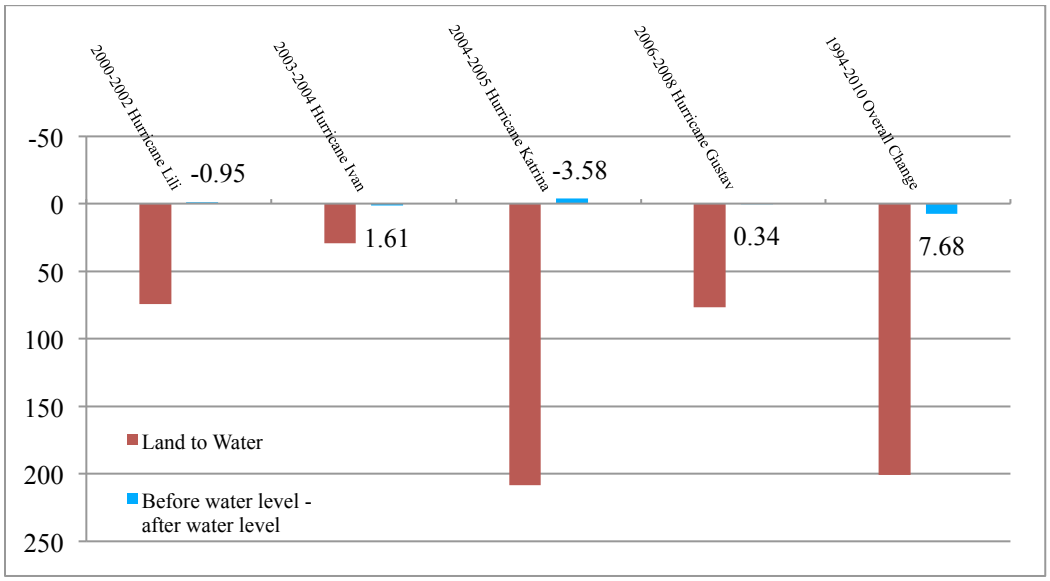

Figure 4.2 Comparison of water level changes in Gardene station with the "land to water" conversion changes in change detection procedure

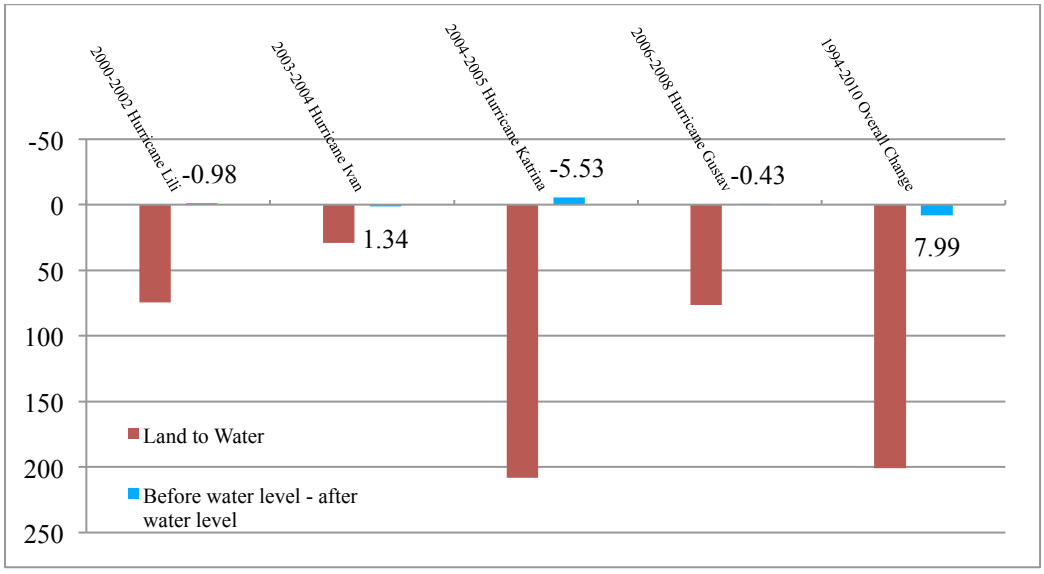

Figure 4.3 Comparison of water level changes in Snake Island station with the "land to water" conversion changes in change detection procedure

The analysis was performed only on these two stations because they were more representative of the water levels in the Breton Sound Estuary when compared to other two stations. With the exception of Hurricane Katrina in 2005, water level differences for the other years were not as great as the land area change, which provides additional evidence that they are not correlated.

4.2. Chandeleur Islands

The time series analysis of the Chandeleur Islands from 1997 to 2011 indicates that Hurricane Georges caused the maximum land loss in 1998 much more than that of Hurricane Katrina in 2005 (Figure 3.20, Figure 4.4 and Figure 4.5). The land area was reduced by 72%. The recovery was constant until 2004 after which Hurricane Katrina occurred in 2005. The recovery after 2005 was negligible. Hurricanes Katrina and Gustav affected the entire system of the islands and altered the land area greatly. The northern islands had considerably lesser impact when compared to the southern islands. This could be due to the presence of vegetation in these regions, which acts as anchors to hold the sediment intact. The pattern of long-shore sediment transport along with the presence/absence of sediment supply from offshore affects the building of land area (Stone et al 2004).

Miner et al (2009) indicated that most of the damage was concentrated in the southern portion of the islands. They explained this as a result of the presence of back-barrier marshes, which serve as a “Back Bone” of the system in the northern part preventing it from becoming completely eroded as the southern regions have. We achieved similar results to Miner et al (2009) from our classification and change detection results and verified some of the results during the field trip in June 2011 (Figure 3.21).

Figure 4.4 Photograph taken before the passage of Hurricane Georges in 1997 (Source: Coastal Research Laboratory- University of New Orleans, http://www.usgs.gov/solutions/northern_gulf.html)

Figure 4.5 Photograph taken after the passage of Hurricane Georges in 1998 (Source: Coastal Research Laboratory- University of New Orleans, http://www.usgs.gov/solutions/northern_gulf.html)

The longshore sediment transport of these islands was found to be of a bi-directional form originating from a center point towards both the north and south directions (Ellis and Stone, 2006). The Chandeleur Islands system has been shown to be sediment starved thus the recovery after storms takes longer (Kahn 1980, Stone et al 2004).

The change detection analysis is an effective tool to quantify the change after hurricane passage. Using the spatial intersection change detection technique we were able to effectively identify the direction of change i.e. land area converted to water, water converted to land etc. The overall change of land area to water from 1997 to 2010 was greater from that of 1997 to 2011 by 6 km^2. This could be attributed to high water levels at that time and the fact that June 2011 is not fall imagery. Change detection of land to water area conversion results were plotted with their respective changes in the water levels (Figure 4.6). Negative values in water level indicate higher water levels after the passage of the hurricane. Higher negative values and corresponding high change area indicates that they are related. Maximum change in land area was due to Hurricane Georges where as the maximum water level was measured for Hurricane Katrina indicating the water level fluctuations were not related to the land area changes.

Regression analysis between the water level and land area changes indicated that they are not related and the correlation coefficient was very small. Similar results were observed for significant wave heights indicating the wave heights had no relation with the land area changes.

4.4. Shoreline Change Analysis for Chandeleur Islands Using Vectors

Fearnly et al (2009) have studied the shoreline changes for the Chandeleur Islands from 1850 to 2005 using Toposheets, aerial photography and other higher resolution satellite imagery such as IKONOS and QUICKBIRD. They created vector layers on ArcGIS to evaluate the change in shoreline over the time series. A similar technique was utilized in this research to quantify the

changes in shoreline in terms of distance between the vectors generated from images (Figure 4.7). The two images considered for this analysis were December 1997 and August 2011. The change in shoreline displacement ranged from 161.1 m to 1742.3 m along the entire coast. The general trend was such that the shoreline has receded landward and the islands have moved westward from their position in 1997.

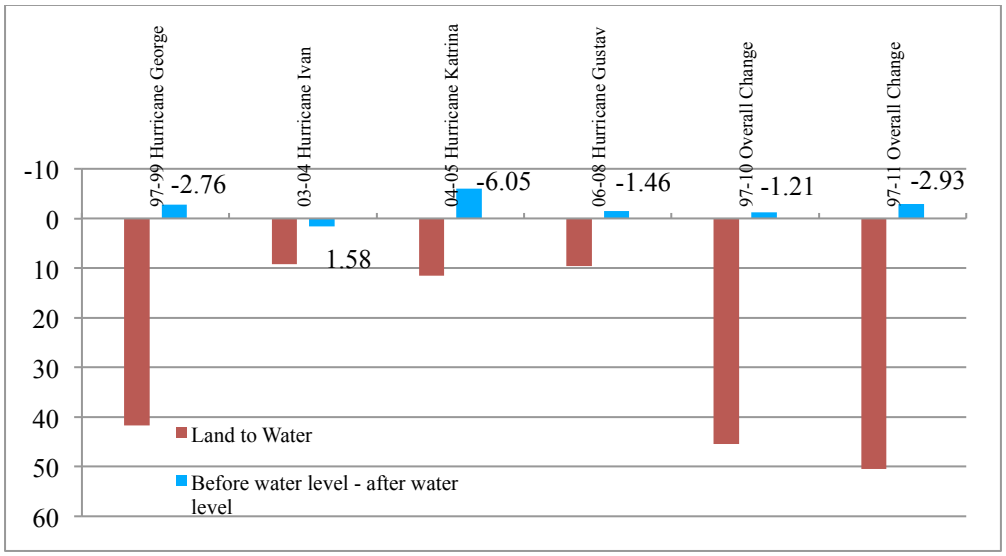

Figure 4.6 Comparison of water level changes in Snake Island station with the land to water conversion changes in change detection procedure

This analysis gave insight into the movement of the Chandeleur Islands demonstrating the transgressive nature of these islands. The artificial nourishment of these islands seems to have increased the land area in December 2010 but it was not apparent in June 2011. This suggests that the artificial nourishment to these islands did not persist. However, high water level during the Mississippi River flood could have been a factor in the June 2011 image.

Northern and southern portions of the island, since 1997, were eroded. The length of the northern section that was lost was 7.14 km and the length of the southern section that was lost was 15 km. Therefore it is evident that maximum loss occurred in the southern portion of the islands.

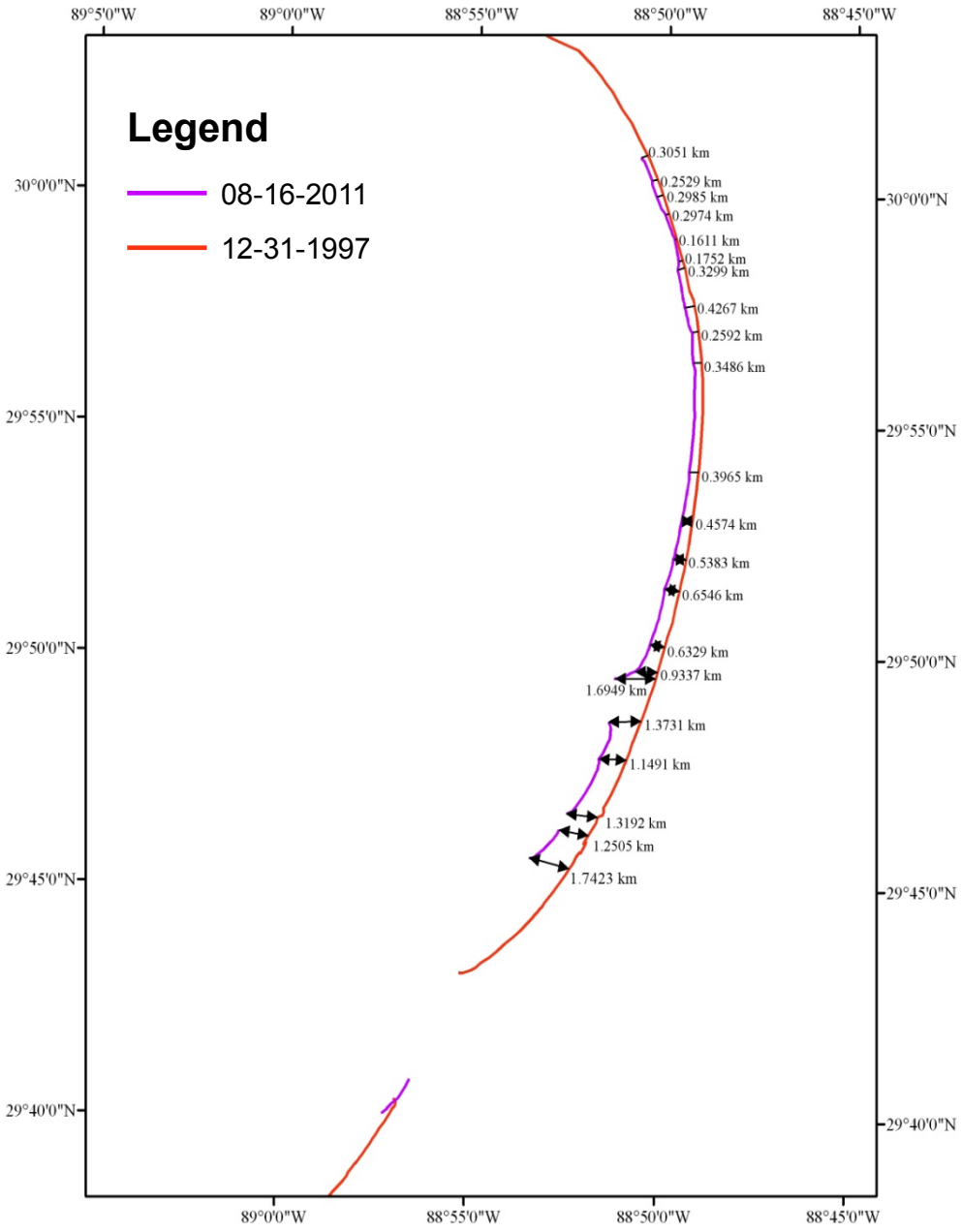

Figure 4.7 Shoreline Change Detection using Vectors for Chandeleur Islands

CHAPTER 5:
SUMMARY AND CONCLUSIONS

This study focuses on quantifying land and vegetation changes in the Breton Sound Estuary for the past 24 years (1987 to 2011) and in the Chandeleur Islands for the past 14 years (1997 to 2011). This was performed with the help of moderate-resolution satellite data (Landsat 5 TM) and image processing tools. Images were classified into land and water classes using a hybrid classification technique that incorporated both supervised and unsupervised classification algorithms. Classification accuracy was assessed using high-resolution infrared aerial photographs.

Change detection analysis was used to identify the regions with maximum change and the direction (loss or gain) of change. Change detection analysis was performed on the classified images to identify changes in land use types over a period of one year (before and after hurricane passage). Three techniques were used for change detection analysis, i.e. post-classification change detection matrix, tasseled cap image differencing, and Change Vector Analysis. The land area changes were compared to water level fluctuations from four stations located in the Breton Sound Estuary. Similar procedures were used for both study areas. The timing of major changes indicated fluctuations in land area could be attributed to hurricane/tropical storm passage. Even when storms did not make landfall near the Breton Estuary or the Chandeleur Islands, substantial decrease in land area was found. This reveals the vulnerable nature of these deltaic environments.

This research is unique when compared to past research conducted in these areas because it focuses on both Breton Sound Estuary and the Chandeleur Islands quantifying land/vegetation changes attributable to hurricane damage. The hybrid classification technique improved the

accuracy of classification when compared to other techniques previously used including thresholding, supervised classification and unsupervised classification. Water levels and significant wave heights were also considered for better understanding of the land loss causes and spatial patterns of change.

Based on the results the following conclusions were drawn:

5.1. Breton Sound Estuary

1) Major coastal land loss over the period of 24 years coincided closely in time to hurricanes and other tropical storms demonstrating their impact on erosion to land loss.

2) Maximum impact within this region was due to Hurricane Katrina (August 2005), which caused a land loss of 196 km^2 and marsh loss of 173 km^2. The recovery after Hurricane Katrina was very slow and was affected by subsequent storms.

3) Overall land area loss from 1987 to 2010 was 181 km^2 and marsh loss of 58 km^2. In the 24-year time series, marsh area loss coincided with the land area loss. However, marsh area increase and land area increase occurred at different times.

4) There was measurable growth in marsh area in three time segments from 1987 to 1991 (87 km2), 1992 to 2003 (111 km^2) and 2006 to 2009 (135 km2). This indicates marsh recovery between passages of hurricanes.

5) Change detection analysis indicated maximum land to water conversion occurred from 2004 to 2005 (208 km^2) attributable to Hurricane Katrina. Interestingly, this value was higher than the overall land to water conversion from 1987 to 2010 (201 km^2) indicating the intensity with which Hurricane Katrina damaged this region.

6) Change Vector Analysis revealed regions with maximum change magnitude. This coincided with the results obtained from spatial intersection technique.

7) Field trips revealed extensive fragmentation of marsh areas along with sub-pixel size variation in land and water classes.

5.2. Chandeleur Islands

1) The pattern of land loss was effectively quantified over a period of fourteen years. The most devastating hurricane to have impacted this island chain was Hurricane Georges in 1998, which led to major land loss of 72% (41 km^2) measured from December 1997 to October 1999.

2) Overall land loss from 1997 to 2011 was 54 km^2 (95%) indicating extreme and persistent damage caused by frequent hurricane passage in the past 14 years. Land areas that recovered between hurricanes were eroded due to subsequent hurricanes.

3) Two time segments of land area recovery were observed from September 1999 to October 2003 (9 km^2) and from November 2009 to December 2010 (3 km^2).

4) Hurricane Gustav significantly destroyed the beach area in 2008. Beach gain from 2008 to 2010 was 9 km^2 out of which 3 km^2 was from February 2010 to December 2010. This increase in beach area in 2010 is attributable to the artificial berm construction.

5) Shoreline change analysis indicated that the Chandeleur Islands have moved westward (landward) from 1997 to 2011 by a maximum of 1.7 km.

6) Seven kilometres of shoreline was lost in the northern tip and 15 km was lost in the southern tip over the 14 year time period.

5.3. Research Limitations

1) A major limitation for this research was the spatial resolution of the satellite data. Landsat 5 TM data has a coarse resolution of 30 m; a higher resolution data would give more accurate results. The individual marsh types could possibly be identified using higher resolution imagery. The quantitative mapping of land and water could have been significantly improved.

2) Ground control plays a major role in satellite remote sensing. Due to the lack of ground control we were unable to identify individual marsh species on the satellite data. This study could have been improved in the Breton Sound Estuary particularly by undertaking more ground truthing trips by aircraft in addition to boats. In case of using boats for ground truthing, some areas were inaccessible at the same time we were able to identify individual plant species. In case of using aircrafts, large portions of the study area were covered at the same time and inaccessible areas on the ground were flown over. However, individual marsh plant species could not be identified when using an aircraft for ground truthing. Therefore, it is necessary to utilize both for a comprehensive study.

3) Acquiring cloud free imagery for the same time of the year, in the same season every year was a challenge.

4) The floating vegetation, abundant within the Breton Estuary, was always a concern while classifying land and water as they masked water areas giving a less severe picture of changes that transpired.

5) The classification procedures tended to over-classify within particular classes thereby overestimating the area for that class.

5.4. Future Research Suggestions

1) This research could be improved using additional ground truth data

2) Improved spatial resolution of the satellite data could enable identifying types of marsh species.

3) Seasonal variations could be studied in more detail to understand changes due to vegetation and identify regions with persistent change.

BIBLIOGRAPHY

Allen, Y.C., Constant, G.C., and Couvillion, B.R., 2008. "Preliminary classification of water areas within the Atchafalaya Basin Floodway System by using Landsat imagery", *U.S. Geological Survey Open-File Report* 2008 –1320, 14 p.

Baker, C., Lawrence R.L., Montagne C., and Patten D., 2007. "Change Detection of Wetland Ecosystems Using Landsat Imagery and Change Vector Analysis." *Wetlands* 27.3: 610-19.

Barras, J., Beville, S., Britsch, D., Hartley, S., Hawes, S., Johnston, J., Kemp, P., Kinler, Q., Martucci, A., Porthouse, J., Reed, D., Roy, K., Sapkota, S., and Suhayda, J., 2003. "Historical and projected coastal Louisiana land changes: 1978-2050:" *USGS Open File Report 03*-334, 39 p. (Revised January 2004).

Barras, J.A., 2006. "Land area changes in coastal Louisiana after the 2005 hurricanes: a series of three maps" *USGS Open File Report 2006–1274 U.S. Geological Survey publication*. http://pubs.usgs. gov/of/2006/1274/. Accessed 7 December 2009.

Barras, J. A., 2007. "Satellite images and aerial photographs of the effects of Hurricanes Katrina and Rita on coastal Louisiana" *USGS Data Series 281 U.S. Geological Survey Publication* http://pubs.usgs.gov/ds/2007/281/. Accessed 7 December 2009.

Barras, J. A., 2007. "Land area changes in coastal Louisiana after Hurricanes Katrina and Rita" Pages 98 - 113 *in* G. S. Farris, G. J. Smith, M. P. Crane, C. R. Demas, L. L. Robbins, and D. L. Lavoie, editors. *Science and the storms: The USGS response to the hurricanes of 2005. U.S. Geological Survey Circular 1306* Available from http://pubs.usgs.gov/circ/1306/

Barras, J.A., Bernier, J., and Morton R., 2008. "Land area change in coastal Louisiana: A multidecadal perspective (from 1956 to 2006)" *USGS Scientific Investigations Map 3019, U.S. Geological Survey Publication* http://pubs.usgs.gov/sim/3019/. Accessed 7 December 2009.

Barras, J.A., 2009. "Land area change and overview of major hurricane impacts in coastal Louisiana, 2004-08" *U.S. Geological Survey Scientific Investigations Map 3080*, scale 1:250,000, 6 p. Pamphlet.

Bauer, M.E., Yuan, F., and Sawaya K.E., 2003. "Multi-Temporal Landsat Image Classification and Change Analysis of Land Cover in the Twin Cities (Minnesota) Metropolitan Area" *Second International Workshop on the Analysis of Multi-temporal Remote Sensing Images*.

Bernier, J. C., Morton, R. A., and Barras, J. A., 2006. "Constraining Rates and Trends of Historical Wetland Loss, Mississippi River Delta Plain, South-Central Louisiana." *Coastal Enviroment and Water Quality* 30: 371-82.

Bevin, J. L., and Kimberlain, T. B. 2008 "National Hurricane Center Report on Hurricane Gustav " available from <http://www.nhc.noaa.gov/pdf/TCR-AL072008_Gustav.pdf>.

Bourne, J., 2000. "Louisiana's Vanishing Wetlands: Going, Going..." *Science* 289.5486 (2000): 1860-63.

Bunya, S., Dietrich J.C., Westerink J.J., Ebersole B.A., Smith J.M., Atkinson J.H., Jensen R., Resio D.T., Luettich R.A., Dawson C., Cardone V.J., Cox A.T., Powell M.D., Westerink H.J., and Roberts H.J., 2010. "A High-Resolution Coupled Riverine Flow, Tide, Wind, Wind Wave and Storm Surge Model for Southern Louisiana and Mississippi: Part I - Model Development and Validation", *Monthly Weather Review,* 138(2): 345-377, DOI: 10.1175/2009MWR2906.1

Caffey, R. H., and Schexnayder, M., 2002. "Fisheries Implications of Freshwater Reintroductions" *Interpretive Topic Series on Coastal Wetland Restoration in Louisiana*, Coastal Wetland Planning, Protection, and Restoration Act (eds.), National Sea Grant Library No. LSU-G-02-003, 8p

Cai, G., Du, M., and Liu, Y., 2011. "Detection of Land Cover Change in Beijing from Tm Images." *Geoinformatics, 2011 19th International Conference on IEEE*: 1-6.

Chander, G., and Markham, B., 2003. "Revised Landsat-5 Tm Radiometric Calibration Procedures and Postcalibration Dynamic Ranges." *IEEE Transactions on Geoscience and Remote Sensing* 41.11: 2674- 77.

Chen, D.M., and Stow, D., 2002. "The Effect of Training Strategies on Supervised Classification at Different Spatial Resolutions." *Photogrammetric Engineering and Remote Sensing* 68.11: 1155-61.

Coleman, J.M., Huh, O.K., and Braud, D.W., 2008. "Wetland Loss in World Deltas." *Journal of Coastal Research* 24.1A: 1-14.

Collins, J.B., and Woodcock, C.E., 1995. "An Assessment of Several Linear Change Detection Techniques for Mapping Forest Mortality Using Multitemporal Landsat Tm Data." *Remote Sensing of the Environment* 56: 66-77.

Coppin, P., Jonckheere, I., Nackaerts, K., Muys, B., 2004. "Digital Change Detection Methods in Ecosystem Monitoring: A Review." *International Journal of Remote Sensing* 25.9: 1565-96.

Couvillion, B.R., Barras, J.A., Steyer, G.D., William, S., Fischer, M., Beck, H., Trahan, N., Griffin, B., and Heckman, D., 2011 "Land area change in coastal Louisiana from 1932 to

2010:" *U.S. Geological Survey Scientific Investigations Map 3164*, scale 1:265,000, 12 p. pamphlet

Crist, E.P., Laurin, R., and Cicone, R.C., 1986. "Vegetation soils information contained in transformed thematic mapper data" *Proceeding of IGARSS' 86 Symposium* 1465-70

Day, J.W., Shaffer, G.P., Britsch, L.D., Reed, D.J., Hawes, S.R., and Cahoon, D., 2000 "Pattern and Process of Land Loss in the Mississippi Delta: A Spatial and Temporal Analysis of Wetland Habitat Change." *Estuaries* 23.4: 425-38.

Day, J.W., Boesch, D.F., Clairain, E.J., Kemp, P.G., Laska, S.B., Mitsch, W.J., Orth, K., Mashriqui, H., Reed, D.J., Shabman, L., Simenstad, C.A., Streever, B.J., Twilley, R.R.,Watson, C.C., Wells, J.T., and Whigham, D.F., 2007. "Restoration of the Mississippi Delta: Lessons from Hurricanes Katrina and Rita." *Science* 315: 1679-84.

Day, J.W., Cable, J.E., Cowan, J.H., DeLaune, R., de Mutsert, K., Fry, B., Mashriqui, H., Justic, D., Kemp, P., Lane, R.R., Rick, J., Rick, S., Rozas, L.P., Snedden, G., Swenson, E., Twilley R.R., and Wissel, B., 2009. "The Impacts of Pulsed Reintroduction of River Water on a Mississippi Delta Coastal Basin." *Journal of Coastal Research* 54: 225-43.

Debusschere, K., Penland, S., Westphal, K., Handley, L., Michot, T., Reed, D., and Seal, R., 1990. "The Geomorphology of the Chandeleur Island Wetlands" *Gulf Coast Association of Geological Societies and Gulf Coast Section of SEPM (Society of Economics, Paleontologists, and Mineralogist) meeting, Lafayette, LA (USA)*.

Dietrich, J.C., Bunya, S., Westerink, J.J., Ebersole, B.A., Smith, J.M., Atkinson, J.H., Jensen, R., Resio, D.T., Luettich, R.A., Dawson, C., Cardone, V.J., Cox, A.T., Powell, M.D., Westerink, H.J., and Roberts, H.J., 2010. "A High-Resolution Coupled Riverine Flow, Tide, Wind, Wind Wave and Storm Surge Model for Southern Louisiana and Mississippi: Part II - Synoptic Description and Analysis of Hurricanes Katrina and Rita", *Monthly Weather Review,* 138(2): 378-404, DOI: 10.1175/2009MWR2907.1

Dietrich, J.C., Westerink, J.J., Kennedy, A.B., Smith, J.M., Jensen, R.E., Zijlema, M., Holthuijsen, L.H., Dawson, C., Luettich, R.A. Jr., Powell, M.D., Cardone, V.J., Cox, A.T., Stone, G.W., Pourtaheri, H., Hope, M.E., Tanaka, S., Westerink, L.G., Westerink, H.J., and Cobell, Z., 2011. "Hurricane Gustav (2008) Waves and Storm Surge: Hindcast, Synoptic Analysis and Validation in Southern Louisiana", *Monthly Weather Review,* 139:2488-2522, DOI: 10.1175/2011MWR3611.1

Edwards, B.L., and Namikas, S.L., 2011. "Changes in Shoreline Change Trends in Response to a Detached Breakwater Field at Grand Isle, Louisiana." *Journal of Coastal Research* 27.4: 698-705.

Edwards, A. J., Mumby, P. J., Green, E. P., and Clark, C. D., 1999. "Radiometric Correction of Satellite Images: When and Why Radiometric Correction is Necessary". In Edwards, A.

J., (Ed.), “Applications of Satellite and Airborne Image Data to Coastal Management. Coastal Region and Small Island Papers” (4 ed., pp. 185). Paris: UNESCO

Ellis, J., and Stone, W.G., 2006. “Numerical Simulation of net longshore sediment transport and granulometry of surficial sediments along Chandeleur Islands”, *Marine Geology*, 232, p.115-129

Fearnley, S. M., Miner, M. D., Kulp, M., Bohling, C., and Penland, S., 2009. "Hurricane Impact and Recovery Shoreline Change Analysis of the Chandeleur Islands, Louisiana, USA: 1855 to 2005." *Geo-Marine Letters* 29: 445-66.

Folk, R. L., and Ward, W. C., 1957. "Brazos River Bar: A Study in the Significance of Grain Size Parameters." *Journal of Sedimentary Petrology* 27.1: 3-26.

Forbes, C., Luettich, R.A., Mattocks, C., and Westerink, J.J., 2010. "A Retrospective Evaluation of the Storm Surge Produced by Hurricane Gustav (2008): Forecast and Hindcast Results". *Weather and Forecasting*, 25(December): 1577-1602, DOI: 10.1175/2010WAF2222416.1

Foody, G.M., 2002. "Status of Land Cover Classification Accuracy Assessment." *Remote Sensing of the Environment* 80: 185-201.

Frazier, P.S., and Page, K.J., 2000. "Water Body Detection and Delineation with Landsat Tm Data." *Photogrammetric Engineering and Remote Sensing* 66.12: 1461-67.

Fraser, R.S., Bahethi, O.P., and Abbas. A. H. Al., 1977. "The Effect of the Atmosphere on the Classification of Satelliteobservations to Identify Surface Features." *Remote Sensing of the Environment* 6: 229-49.

Guiney, J. L., 1999. “National Hurricane Center Report on Hurricane Georges” [online], Available from: http://www.nhc.noaa.gov/1998georges.html

Han, T., Wulder, M. A., White, J. C., Coops, N. C., Alvarez, M. F., and Butson, C., 2007. "An Efficient Protocol to Process Landsat Images for Change Detection with Tasselled Cap Transformation." *IEEE Transactions on Geoscience and Remote Sensing* 4.1: 147-51.

Howes, N.C., FitzGerald, D.M., Hughes, Z.J., Georgiou, I.Y., Kulp, M.A., Miner, M.D, Smith, J.M., and Barras, J.A., 2010. "Hurricane-Induced Failure of Low Salinity Wetlands." *Proceedings of North American Academy of Science* 107.32: 14014-19.

Huang, C., Wylie, B., Yang, L., Homer, C., and Zylstra, G., 2002. "Derivation of a Tasseled Cap Transformation Based on Landsat 7 at-Satellite Reflectance." *International Journal of Remote Sensing*, 23.8, 1741–1748, accessed from *U.S. Geological Survey Open File Report*.

Janssen, L.L.F., and Van der Wel, F.J.M., 1994. “Accuracy assessment of satellite derived land-cover data: a review” *Photogrammetric Engineering and Remote Sensing*, 60, 419 – 426

Jin, S., and Sader, S.A., 2005. "Comparison of Time Series Tasseled Cap Wetness and the Normalized Difference Moisture Index in Detecting Forest Disturbances." *Remote Sensing of the Environment* 94: 364-72.

Kahn, J.H., 1980. "The role of hurricanes in the long-term degradation of a barrier island chain: Chandeleur Island, Louisiana", *M.S. thesis (unpublished), Louisiana State University*, Baton Rouge, Louisiana, 99 pp.

Kahn, J. H., and Roberts H.H., 1982. "Variations in Storm Response along a Microtidal Transgressive Barrier-Island Arc", *Sedimentary Geology*, 33, p. 129-146.

Kawata, Y., Ohtani, A., Kusaka, T., and Ueno, S., 1990. "Classification Accuracy for the Mos-1 Messr Data before and after the Atmospheric Correction." *IEEE Transactions on Geoscience and Remote Sensing* 28.4: 755-60.

Knabb, R. D., Rhome, R. J., and Brown, P. D., 2006. "National Hurricane Center Report on Hurricane Katrina" [online] Available from: http://www.nhc.noaa.gov/pdf/TCR-AL122005_Katrina.pdf

Knabb, R. D., Brown, D. P., and Rhome, J. R., 2005. "Tropical Cyclone Report: Hurricane Rita", *National Hurricane Center Report* 2005

Koch, J., and Penland S., 2001. "Shoreline Characterization of the Geomorphological Impact of Hurricane Georges on the Chandeleur Islands: Southeast Louisiana." *Gulf Coast Association of Geological Societies Transactions* 51: 451-53.

Lane, R.R., Day, J.W., and Thibodeaux, D., 1999. "Water Quality Analysis of a Freshwater Diversion at Caernarvon, Louisiana." *Estuaries* 22.2A: 327-36.

Lavoie, D., Executive summary, in Lavoie, D., ed., 2009, "Sand resources, regional geology, and coastal processes of the Chandeleur Islands coastal system—an evaluation of the Breton National Wildlife Refuge": *U.S. Geological Survey Scientific Investigations Report*, 252, p. 1–6

Lillesand, T.M., and Kiefer, R.W., 1997. *Remote Sensing and Image Interpretation*. Ed. Harmon B., Provenzano M. 3 ed: John Wiley & Sons, Inc.

Lu, D., Mausel, P., Brondi´Z.E., Moran, E., 2003. "Change Detection Techniques." *International Journal of Remote Sensing* 25.12: 2365-407.

Macleod, R.D., and Congalton, R.G., 1998. "A Quantitative Comparison of Change-Detection Algorithms for Monitoring Eelgrass from Remotely Sensed Data." *Photogrammetric Engineering & Remote Sensing*, 64. 3: 207-216.

Marris, E., 2005. "The Vanishing Coast." *Science* 438: 908-09.

Mas, J.F., 1999. "Monitoring Land-Cover Changes: A Comparison of Change Detection Techniques." *International Journal of Remote Sensing* 20.1: 139-52.

McGee, B. D., Goree, B. B., Tollett, R. W., and Mason, R. R., 2008. Monitoring Inland Storm Surge and Flooding From Hurricane Gustav in Louisiana, September 2008. *USGS Open-File Report 2008–1373*. Retrieved from http://pubs.usgs.gov/of/2008/1373/

Millward, A.A., Piwowar, J.M., and Howrath, P.J., 2006. "Time series analysis of medium resolution multisensory satellite data for identifying landscape change." *Photogrammetric Engineering and Remote Sensing*, 72.6,: 653-663.

Miner, M.D., Kulp, M., Weathers, H.D., and Flocks, J., 2009. "Chapter D. Historical (1869–2007) sea floor evolution and sediment dynamics along the Chandeleur Islands, in Lavoie, D., ed., Sand resources, regional geology, and coastal processes of the Chandeleur Islands coastal system—an evaluation of the Breton National Wildlife Refuge." *U.S. Geological Survey Scientific Investigations Report* 2009–5252: 47–74.

Morton, R.A., Bernier, J.C., Barras, J.A., and Fernia, N.F., 2005. "Rapid subsidence and historical wetland loss in the Mississippi Delta Plain, likely causes and future implications." *U.S. Geological Survey Open-File Report* 2005-1216:124, *http://pubs.usgs.gov/of/2005/1216/*

Morimoto, T., Kumar, R., and Molion L.C.B., 1979. "Effect of the Atmosphere on the Classification of Landsat Data." *IEEE Symposium on Machine Processing of Remotely Sensed Data*.

Munyati, C., 2000. "Wetland Change Detection on the Kafue Flats, Zambia, by Classification of a Multitemporal Remote Sensing Image Dataset." *International Journal of Remote Sensing* 21.9: 1787-806.

NOAA. National Hurricane Center, "Hurricane Isidore Tropical Cyclone Report", 2002 <http://www.nhc.noaa.gov/2002isidore.shtml>

NOAA. National Hurricane Center, "Lili Prelimnary Report". 2003. <http://web.archive.org/web/20030417141302/www.srh.noaa.gov/lch/tropical/lili/lili_psh.htm>

Parmenter, A. W., Hansen, A., Kennedy, R.E., Cohen, W., Langner, U., Lawrence, R., Maxwell, B., Gallant, A., and Aspinall, R., 2003. "Land Use and Land Cover Change in the Greater Yellowstone Ecosystem: 1975–1995." *Ecological Applications* 13.3: 687-703.

Penland, S., Boyd, R., and Suter, R.J., 1988. "Transgressive depositional systems of the Mississippi Delta plain; a model for barrier shoreline and shelf sand development." *Journal of Sedimentary Research*, 58.6: 932-949.

Potter, J. F., 1974. "Haze and sun angle effects on automatic classification of satellite data-simulation and correction", *Proc. Soc. Photo-Optical Instrumention Engineers*, 51:73-83.

Quinn, J.W., 2001. “Landsat Band Combinations”. <http://web.pdx.edu/~emch/ip1/bandcombinations.html>

Ramsey, E., and Rangoonwala, A., 2006. "Canopy Reflectance Related to Marsh Dieback Onset and Progression in Coastal Louisiana." *Photogrammetric Engineering and Remote Sensing* 72.6: 641-52.

Rappaport, Ed., 2002. National Hurricane Center, “Hurricane Andrew Tropical Cyclone Report”, <http://www.nhc.noaa.gov/1992andrew.html>

Louisiana Department of Natural Resources, 2006. *Caernarvon Freshwater Diversion Project*.

Roberts, H.H., 1997. “Dynamic changes of the Holocene Mississippi river delta plain: The delta cycle.” *Journal Coastal Research* 13.3: 605-627.

Sable, S.E., and Villarrubia, C., 2011. “Analysis of Fisheries-Independent Data for Evaluation of Species Distribution Responses to the Caernarvon Freshwater Diversion”.

Sallenger, A.H., Jr., Wright, C.W., Howd, P., Doran, K., and Guy, K., 2009. Chapter B. Extreme coastal changes on the Chandeleur Islands, Louisiana, during and after Hurricane Katrina, in Lavoie, D., ed., Sand resources, regional geology, and coastal processes of the Chandeleur Islands coastal system—an evaluation of the Breton National Wildlife Refuge: U.S. Geological Survey Scientific Investigations Report, 5252, p. 27–36

Song, C., Woodcock, C.E., Seto, K. C., Lenny, P.M., Macomber, S.A., 2001. "Classification and Change Detection Using Landsat Tm Data: When and How to Correct Atmospheric Effects?" *Remote Sensing of the Environment* 75: 230-44.

Song, C., and Woodcock, C.E. 2003. "Monitoring Forest Succession with Multitemporal Landsat Images: Factors of Uncertainty." *IEEE Transactions on Geoscience and Remote Sensing* 41.11: 2557-67.

Stewart, S. R., 2005. National Hurricane Center Report on Hurricane Ivan [online] Available from: http://www.nhc.noaa.gov/2004ivan.shtml

Stokstad, E., 2005 "Louisiana's Wetlands Struggle for Survival." *Science* 310.5752: 1264-66.

Stone, G.W., Liu, B., Pepper, D.A., and Wang, P., 2004. "The Importance of Extratropical and Tropical Cyclones on the Short-Term Evolution of Barrier Islands Along the Northern Gulf of Mexico, USA." *Marine Geology* 210: 63-78.

Stone, G.W., Zhang, X., and Sheremet, A., 2005. “The Role of Barrier Islands, Muddy Shelf and Reefs in Mitigating the Wave Field Along Coastal Louisiana, *Journal of Coastal Research 44*: 40-55

Stutzenbaker, C.D., 1999. *Aquatic and Wetland Plants of the Western Gulf Coast* George Zappler, Texas Parks and Wildlife Division.

Turner, R.E., Baustian, J.J., Swenson, E.M., and Spicer, J.S., 2006. "Wetland Sedimentation from Hurricanes Katrina and Rita." *Science* 314: 449-52.

Turner, R.E. 2009. "Doubt and the Values of an Ignorance-Based World View for Restoration: Coastal Louisiana Wetlands." *Estuaries and Coasts* 32: 1054-68.

Turner, R. E., 2011. "Beneath the Salt Marsh Canopy: Loss of Soil Strength with Increasing Nutrient Loads." *Estuaries and Coasts* 34: 1084-93.

US.Army.Corp.of.Engineers, 2006. "Interagency Performance Evaluation Taskforce Report, 2006: Performance Evaluation of the New Orleans and Southeast Louisiana Hurricane Protection System, Draft Final Report of the Interagency Performance Evaluation Task Force". *U.S. Army Corps of Engineers, Volume 1- Executive Summary and Overview*, June 1, 2006

US.Army.Corp.of.Engineers, 2008. "Performance Evaluation of the New Orleans and Southeast Louisiana Hurricane Protection System".

USDA, NRCS., 2011. "The PLANTS Database (http://plants.usda.gov), National Plant Data Team", Greensboro, NC 27401-4901 USA.

Urbatsch, L., 2011. "Lsu Herbarium". http://www.herbarium.lsu.edu/.

Vorovencii, I. 2007. "Use of the "Tasseled Cap" Transformation for the Interpretation of Satellite Images." *Cadastral Journal Rev CAD*.

Walker, N. D., and Hammack A.B., 2000. Impacts of winter storms on circulation and sediment transport: Atchafalaya–Vermillion Bay Region, Louisiana, U.S.A., J. Coastal Res., 16, 996–1010.

Walker, N.D., and Rabalais, N.N., 2006. Relationships among satellite chlorophyll *a*, river inputs, and hypoxia on the Louisiana continental shelf, Gulf of Mexico. Estuaries and Coasts 29:1081-1093

Wu, G., Leeuw, J. De., Skidmore, A. K., Liu, Y., and Prins H. H. T., 2008. "Performance of Landsat Tm in Ship Detection in Turbid Waters." *International Journal of Applied Earth Observation and Geoinformation*.

Westerink, J.J., R.A. Luettich, Jr., J.C. Feyen, J.H. Atkinson, C. Dawson, M.D. Powell, J.P. Dunion, H.J. Roberts, E.J. Kubatko, H. Pourtaheri, 2008. "A Basin- to Channel- Scale Unstructured Grid Hurricane Storm Surge Model as Implemented for Southern Louisiana", *Monthly Weather Review*, 136:833-864, DOI: 10.1175/2007MWR1946.1

Williams, S.J., 2009. Chapter C. Past, present, and future sea level rise and effects on coasts under changing global climate, in Lavoie, D., ed., Sand resources, regional geology, and coastal processes of the Chandeleur Islands coastal system—an evaluation of the Breton

National Wildlife Refuge: U.S. Geological Survey Scientific Investigations Report, 5252, p. 37–46

APPENDIX I:

MODEL FOR REFLECTANCE CALCULATION

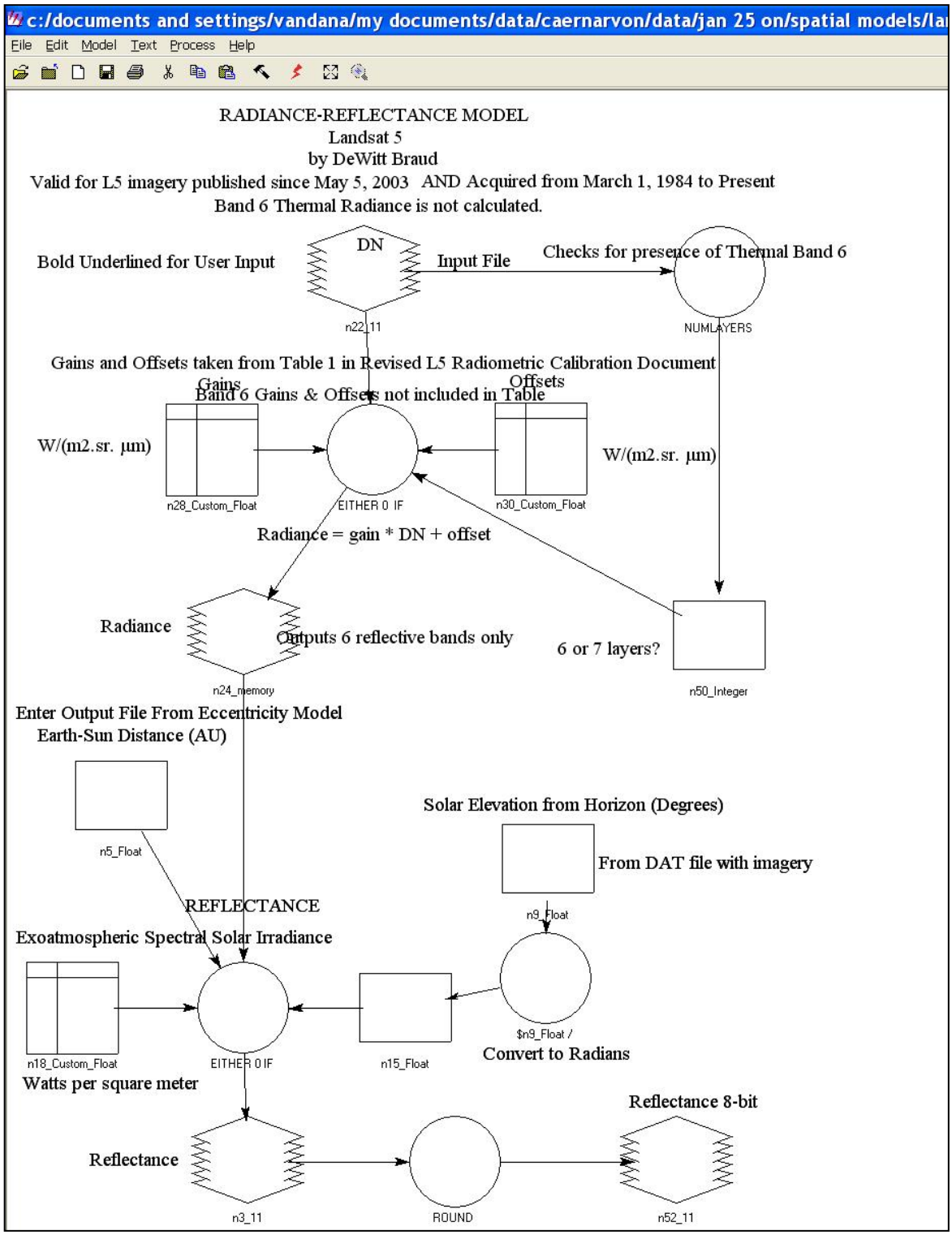

CALCULATION OF ECCENTRICITY TO BE USED IN THE REFLECTANCE MODEL

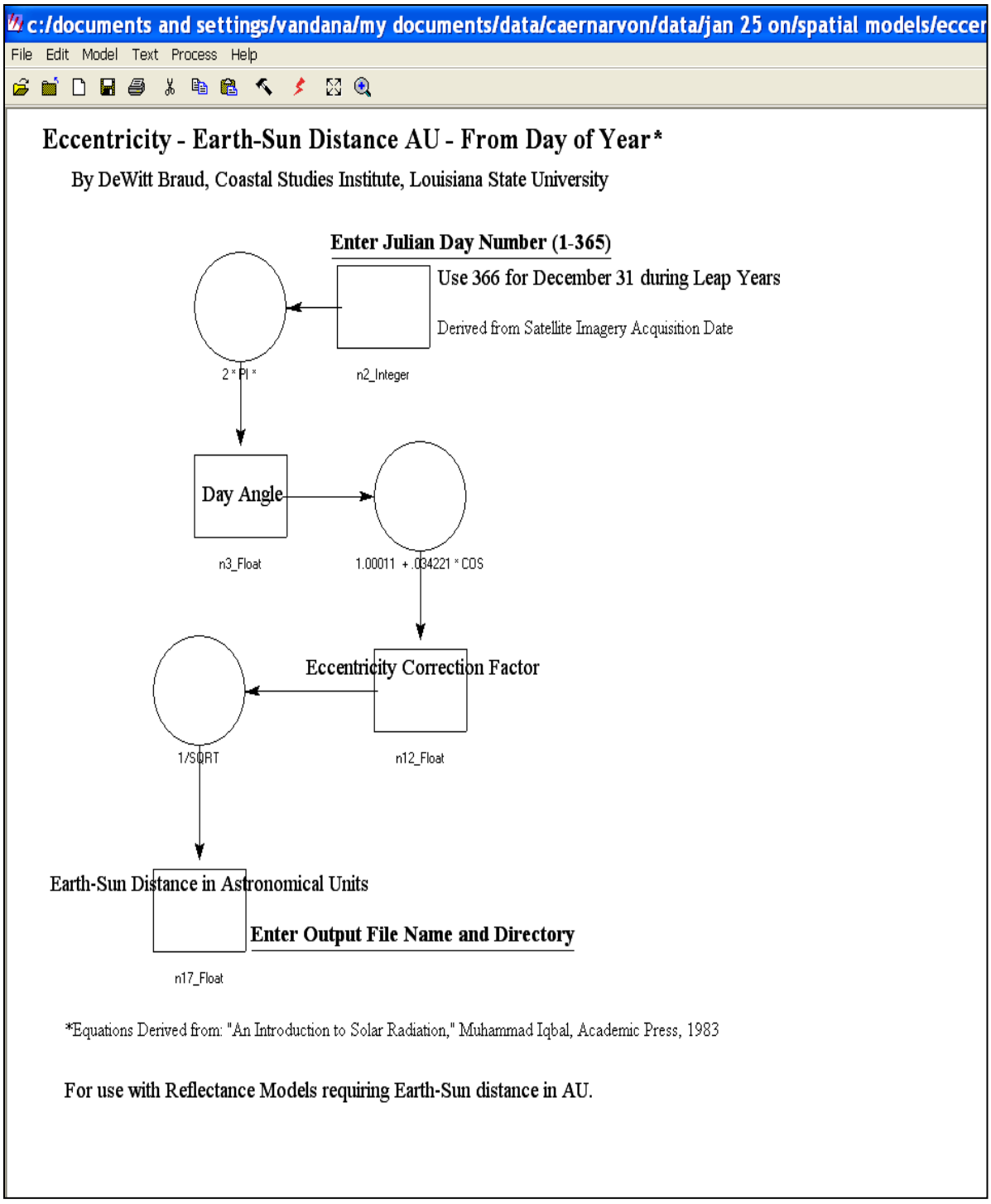

APPENDIX II

MODEL FOR TCAP CALCULATION

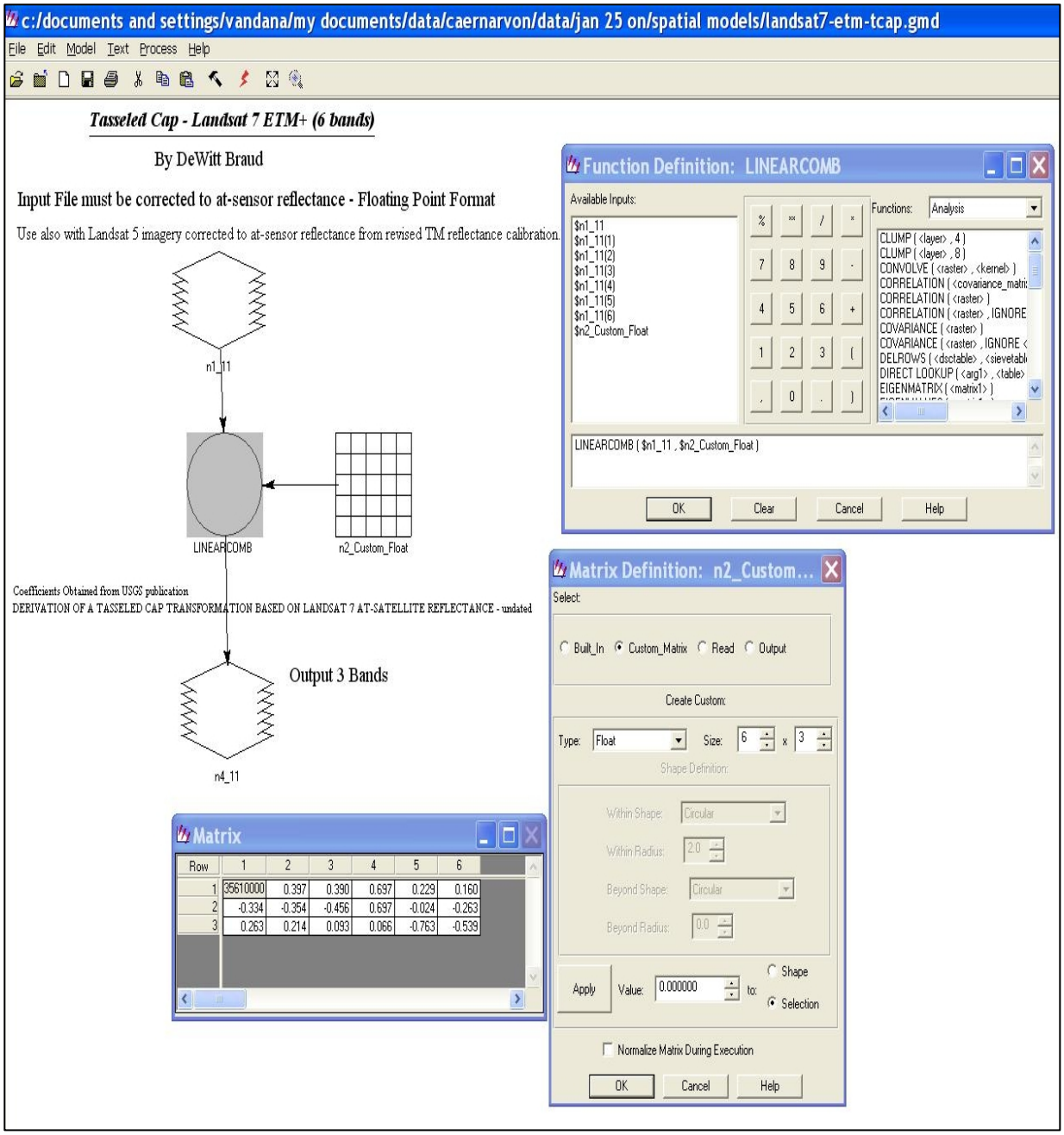

APPENDIX III
SELECT SATELLITE IMAGES

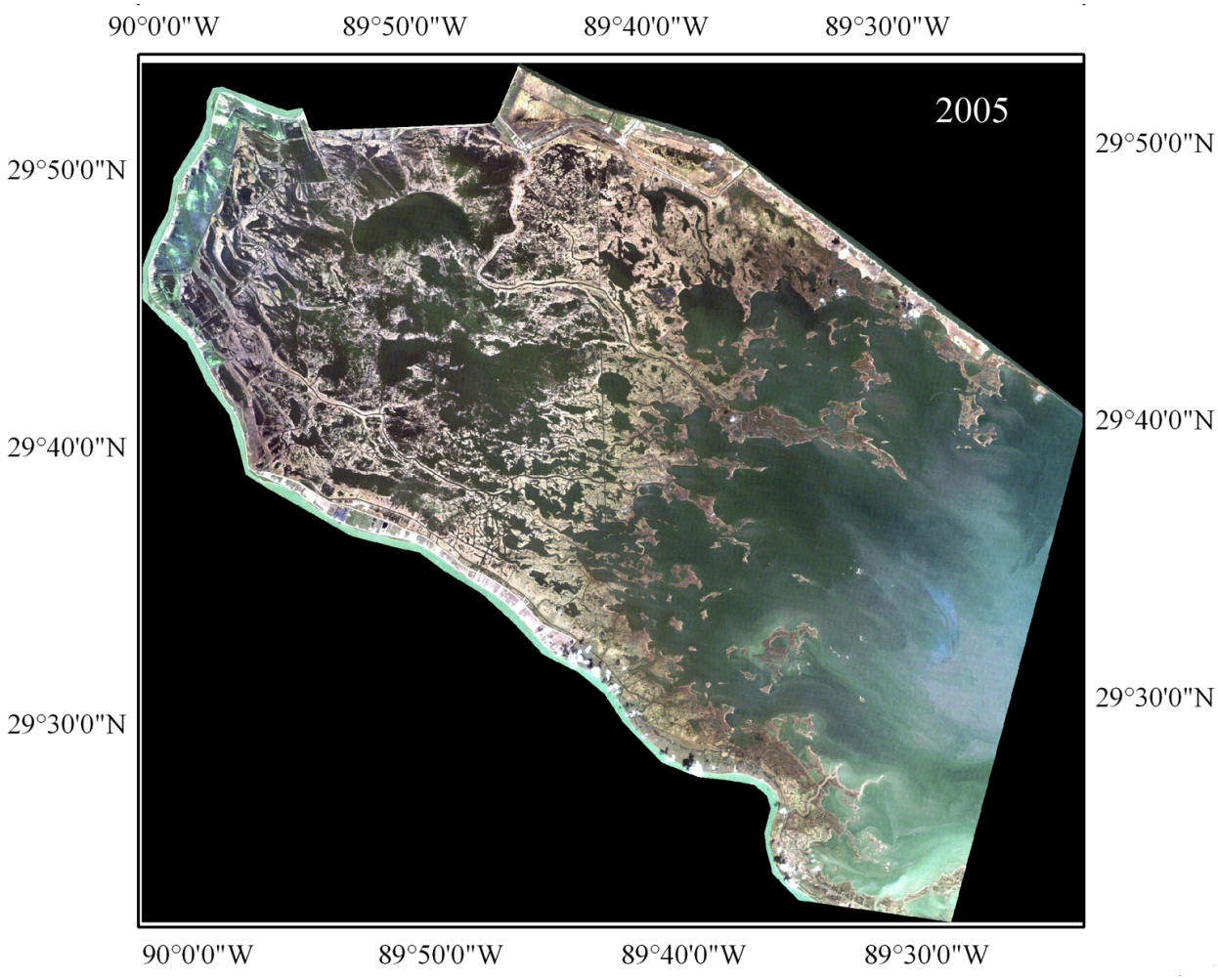

Figure A.1 True color composite (bands 3, 2 and 1 in RGB) of 10/09/2005

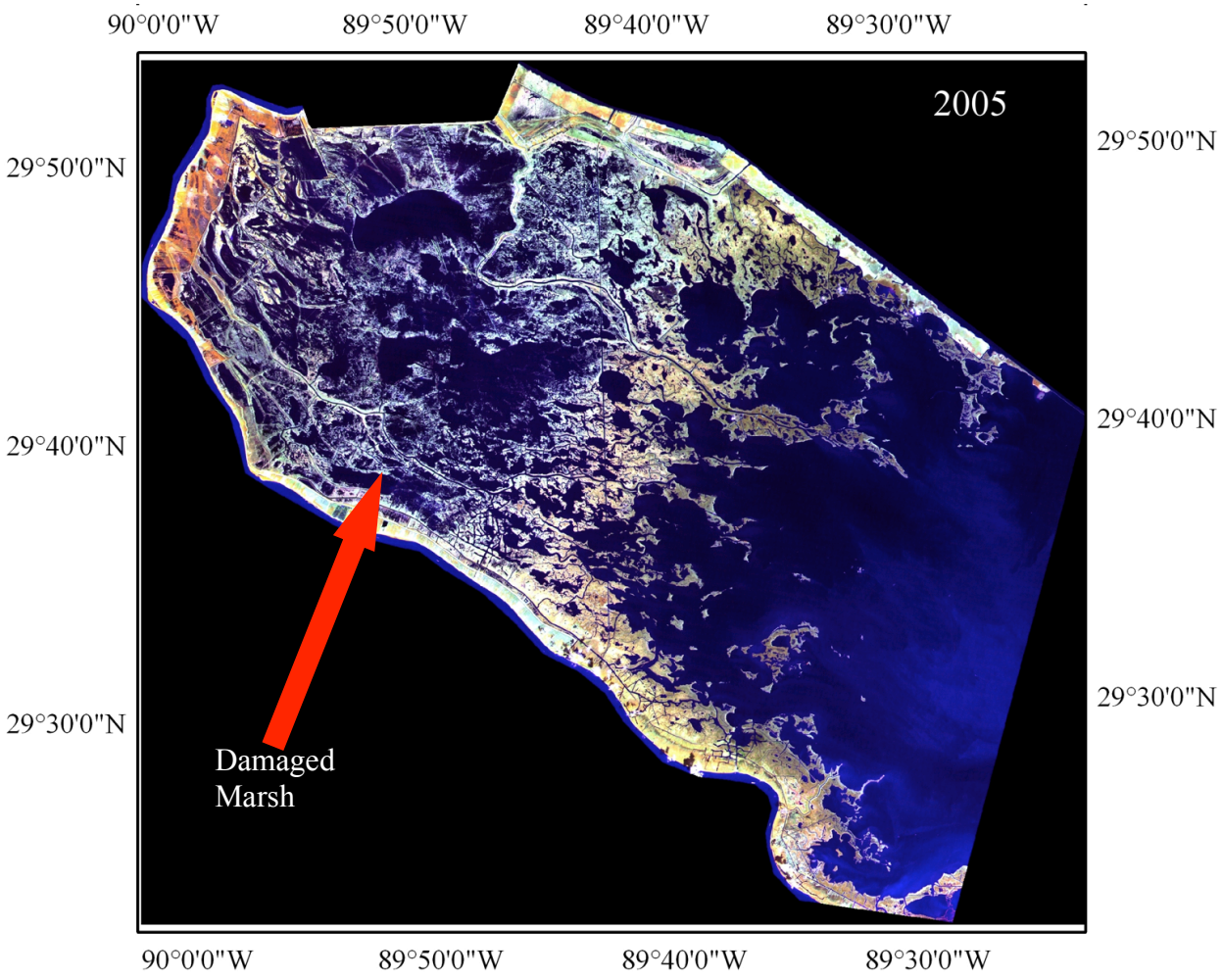

Figure A.2 Bands 4, 5 and 3 in RGB composite for 10/09/2005

Figure A.3 True color composite (bands 3, 2 and 1 in RGB) of 10/01/2008

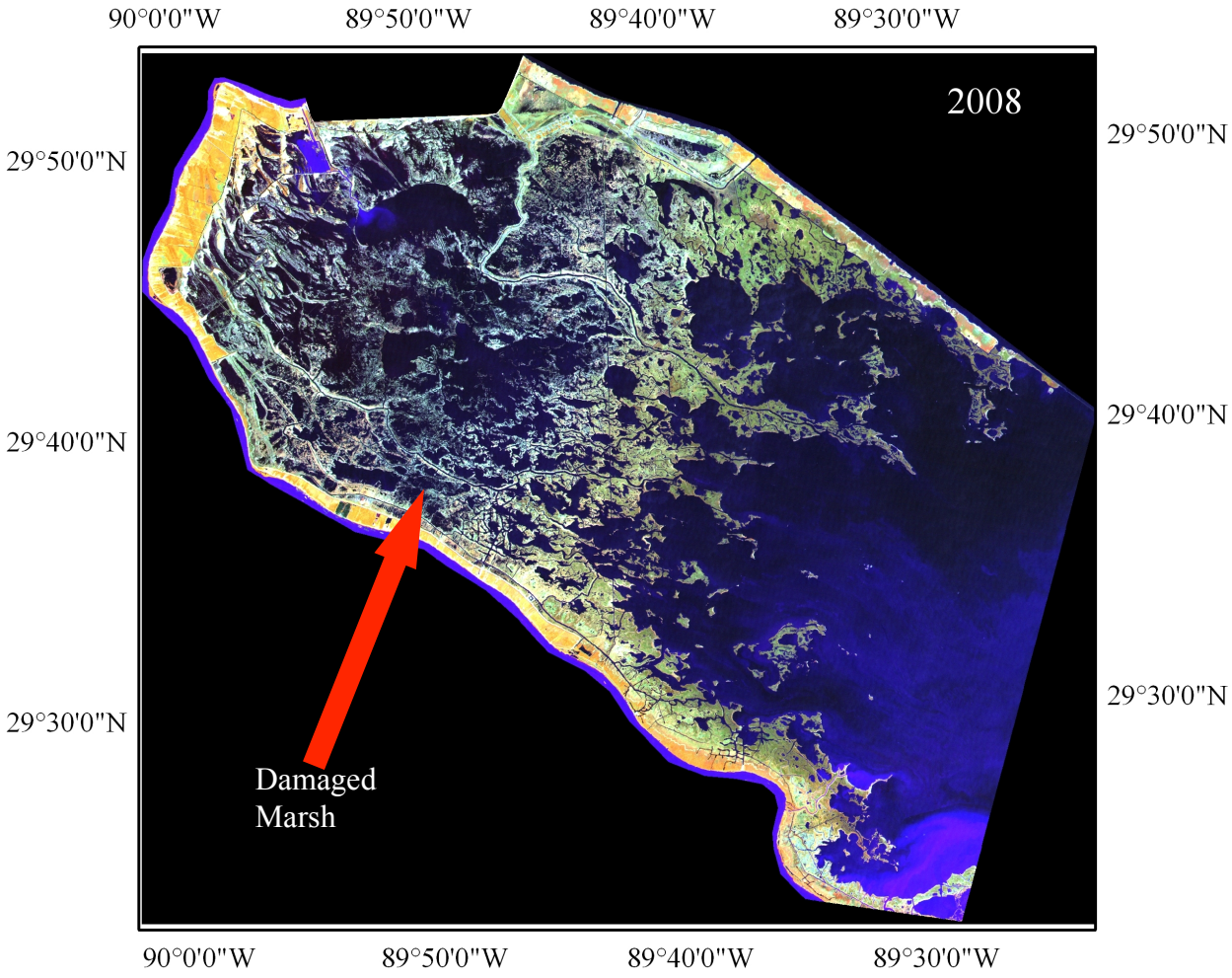

Figure A.4 Bands 4, 5 and 3 in RGB composite for 10/01/2008

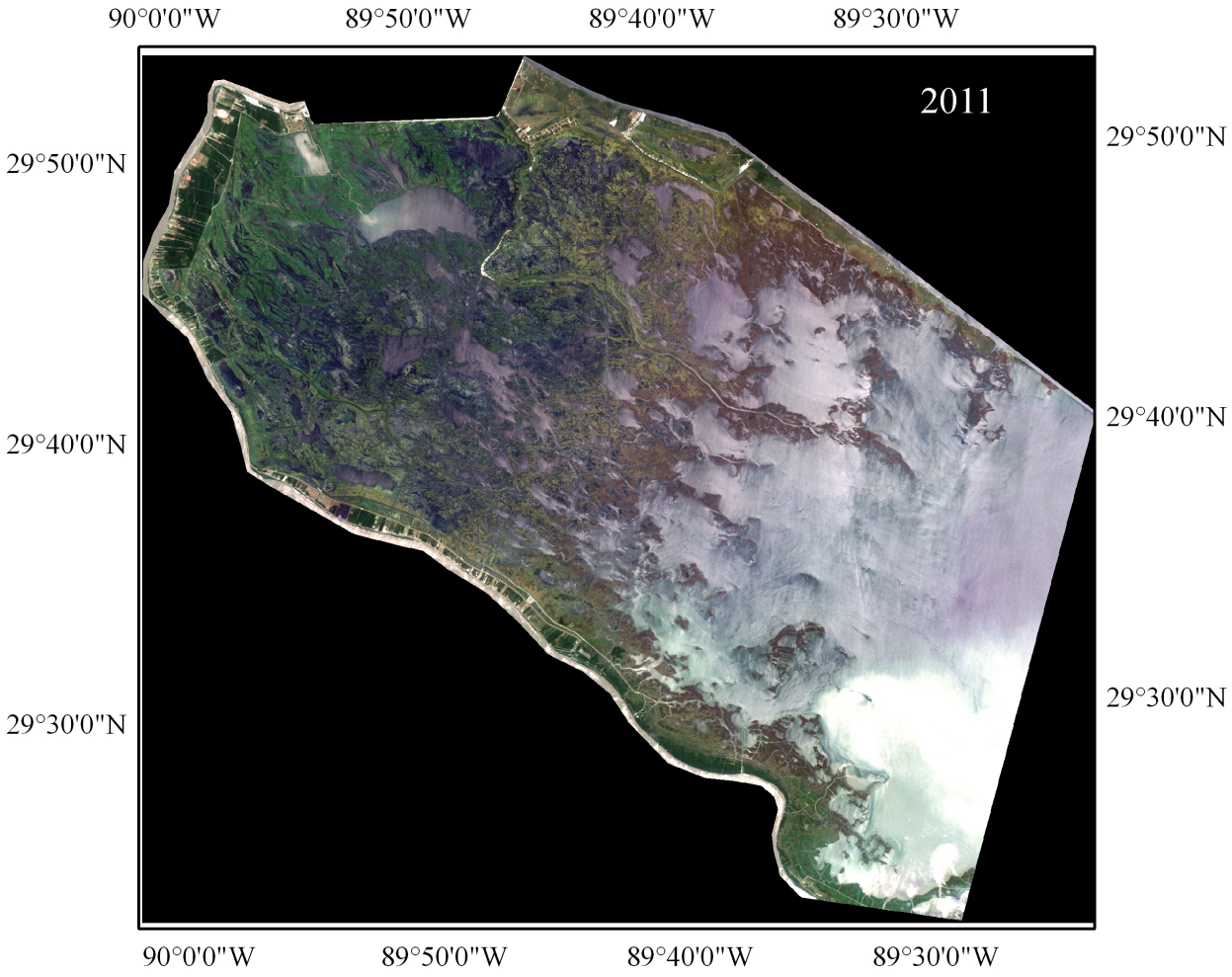

Figure A.5 True color composite (bands 3, 2 and 1 in RGB) of 06/04/2011

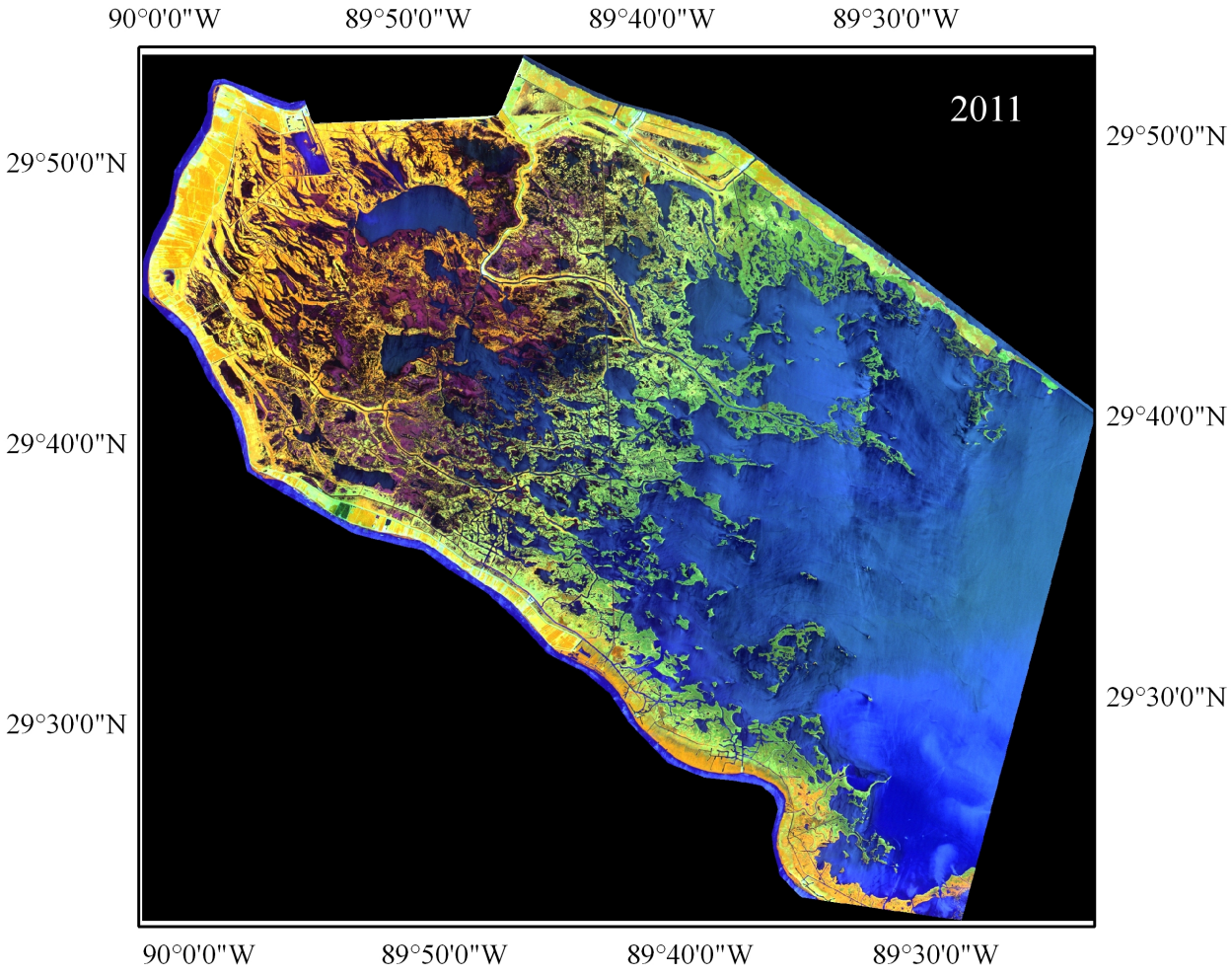

Figure A.6 Bands 4, 5 and 3 in RGB composite for 06/04/2011

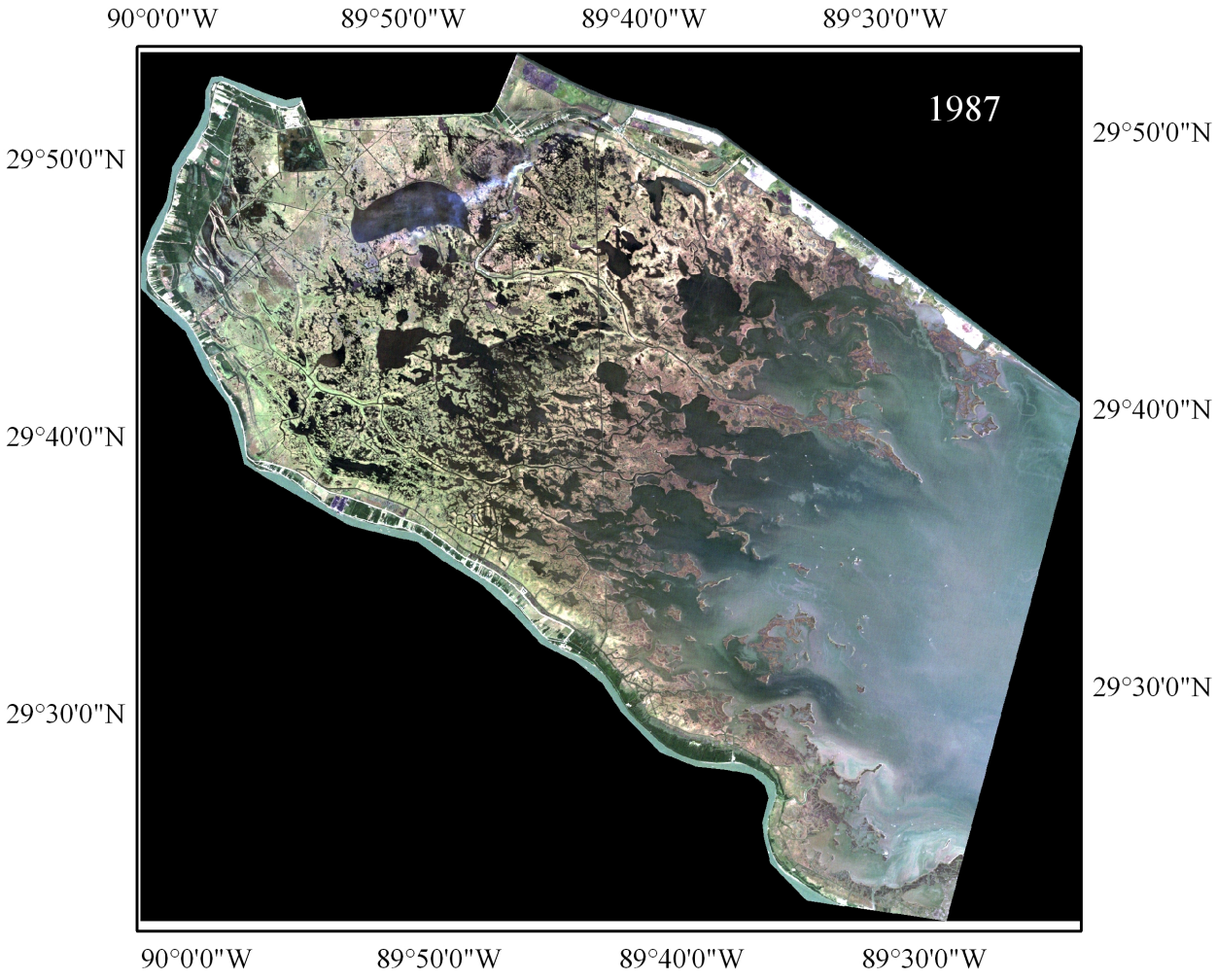

Figure A.7 True color composite (bands 3, 2 and 1 in RGB) of 10/08/1987

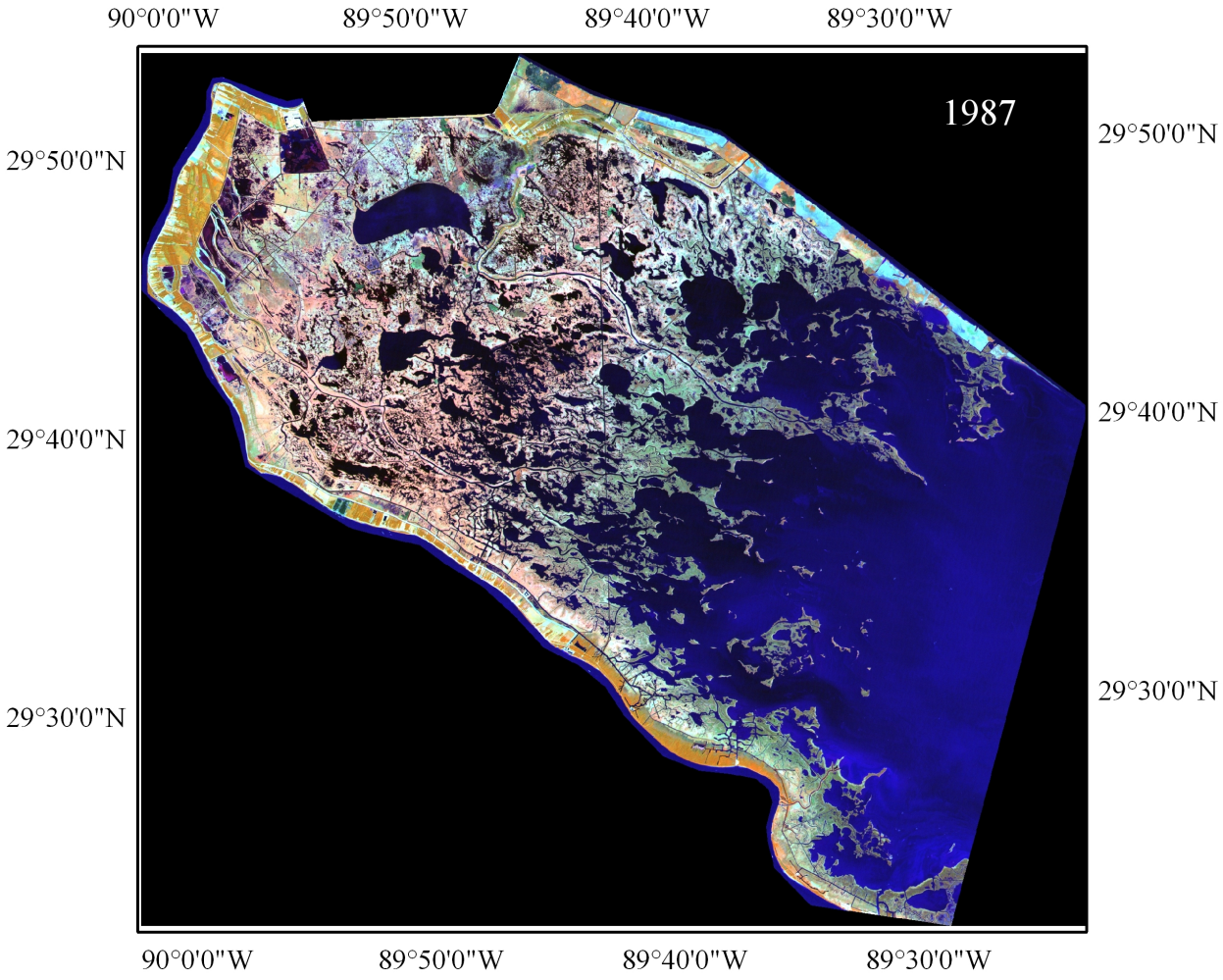

Figure A.8 Bands 4, 5 and 3 in RGB composite for 10/08/1987

APPENDIX IV:
GRAIN SIZE ANALYSIS

The results from the grain size analysis are tabulated in Table A.1. The grain size indicates that the Chandeleur Islands beach is made of very fine and symmetrical by the dunes and the nearshore berm. The very fine nature of the sediments by the vegetation in the dunes possibly indicates Aeolian deposits. The grain size increased and the beach appeared coarser as we progressed to the seaward side and the berm. The sorting of the grains ranged from very well sorted to moderately sorted. The sand on the berm (Sample 5) was the same texture as the sand from the far side of the beach (Sample 1). The sand on the berm was artificially added and its source was sediments dredged offshore.

Table A.1. Grain Size Analysis Results for the 5 sample sites in the transect on Chandeleur Islands

Sample	Mean	Description	Sorting	Skewness	Kurtosis
Sample 1	2.758	Fine Sand	Very well	Symmetrical	Leptokuritic
Sample 2	2.716	Fine Sand	Very well	Skewed	Platykuritic
Sample 3	2.556	Fine Sand	Well	Strongly coarse skewed	Extremely Leptokuritic
Sample 4	2.547	Fine Sand	Moderate	Coarse skewed	Mesokuritic
Sample 5	2.607	Fine Sand	Very well	Symmetrical	Very Leptokuritic

Figure A.9 is the output from the grain size analysis based on calculations from Folk and Ward, 1957. The figure indicates the number of grains in percentage on y-axis with the grain size in phi on x-axis.

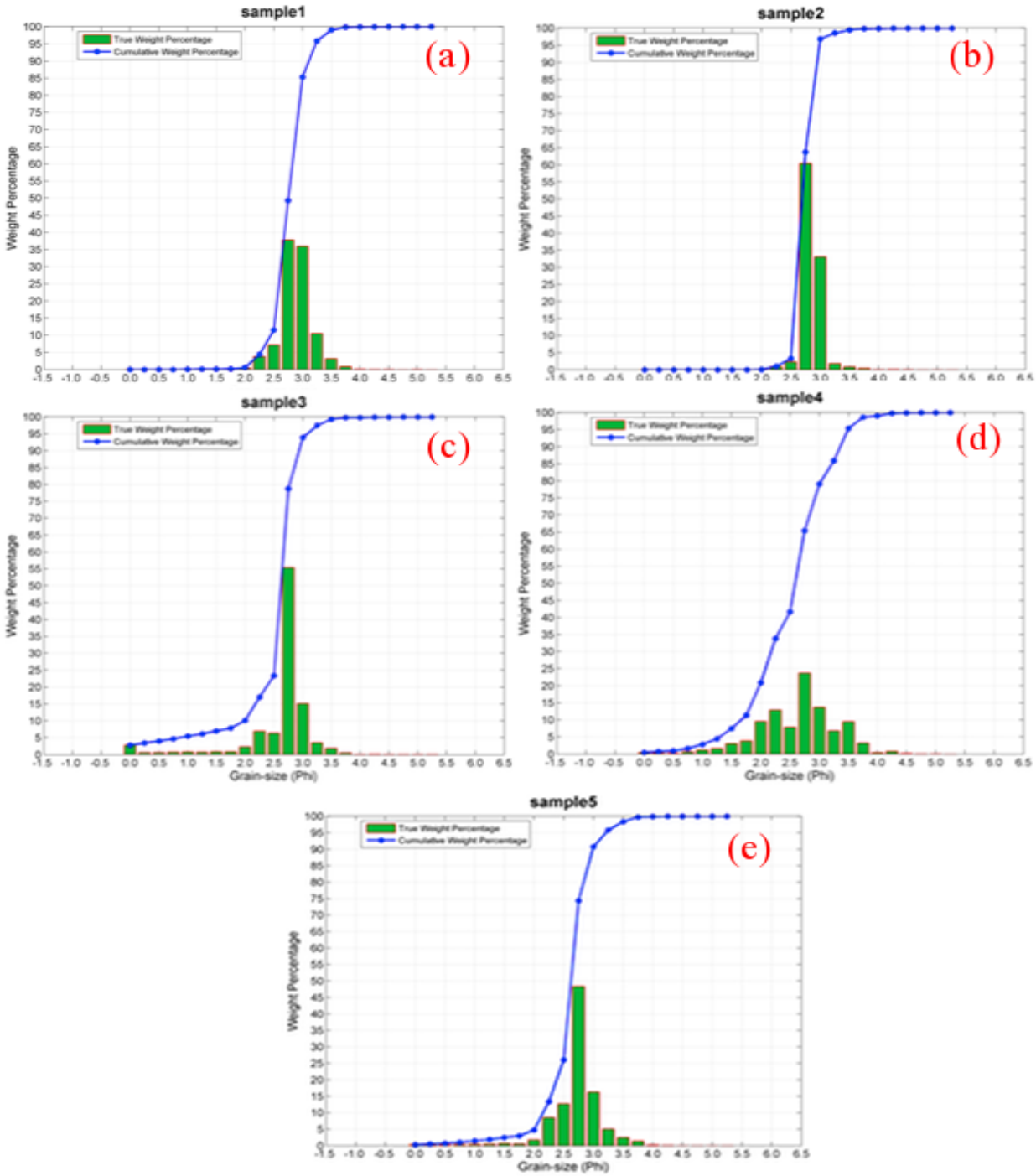

Figure A.9 Grain Size Analysis Output for (a) Sample 1 (b) Sample 2 (c) Sample 3 (d) Sample 4 (e) Sample 5

APPPENDIX V:

MATLAB CODE FOR WATER AND WAVE DATA ANALYSIS

```
load 98_waveheight.dat;

data=wave;

z=data(:,5);

time=(1:length(z))/24;

figure;

plot(time,z);

title('Wave height Station 42067 Jan 1998-Dec

1998','FontWeight','bold');

xlabel('Number of Days');

ylabel('Water level in Feet');

[b,a]=butter(6,0.05);

f=filtfilt(b,a,z);

figure;

plot(time,z);

hold on;

plot(time,f,'r','LineWidth',3);

title('Low pass filter for wave height Jan 1998-Dec

1998','FontWeight','bold');

xlabel('Number of Days'); ylabel('Water level in Feet');
```

VITA

Vandana Varshini Raghunathan grew up in Chennai, Tamilnadu India. She completed her Bachelor of Engineering degree in Geo Informatics from College of Engineering, Anna University, Guindy, India, in June 2008. She was working at the Institute of Remote Sensing, Anna University, as a research associate until June 2009. She then got the opportunity to pursue her Master of Science in Oceanography and Coastal Science degree at Louisiana State University in fall 2009.